Universidade do Porto
Faculdade de Engenharia
Departamento de Engenharia Electrotécnica e de Computadores

Dissertação de Mestrado

Automatic extraction of the size of myocardial infarction in an experimental murine model

Tiago Esteves (meb09026)

Orientador: Doutor Pedro Quelhas
Co-orientadora: Doutora Perpétua Pinto-do-Ó

Trabalho apresentado no âmbito do Mestrado em Engenharia Biomédica, como requisito parcial para obtenção do grau de Mestre em Engenharia Biomédica.

Julho de 2011

Acknowledgements

I would like to thank Professor Pedro Quelhas, my advisor, for his academic guidance in my Biomedical Engineering master studies. His friendship, continuous help, guidance and support help me overcome the problems and enrich my knowledge and skills.

Thanks to Dr. Perpétua Pinto-do-Ó, my coadviser, Mariana Valente and Diana S. Nascimento, for their time and expertise and for providing the images and infarct size results used to validate the work developed during my masters.

Thanks to my friends, classmates and to the lab members and staff I have worked with at Instituto de Engenharia Biomédica (INEB) for their friendship and periods of relaxation.

I am deeply grateful to my family for their help and encouragement in all the years of study and for their support and unconditional love.

Lastly, but certainly not in order of importance, I wish to express special acknowledgement to Raquel for her love, presence and continuous encouragement.

"The work presented in this manuscript was developed in collaboration with Mariana Valente, Diana S. Nascimento and Dr. Perpétua Pinto-do-Ó (Stem Cell Biology Team), from the INEB's NEWTherapies Group and was peformed within the scope of the project PTDC-SAU-OSM-68473/2006, co-funded by the Fundação para a Ciência e a Tecnologia (FCT), FEDER and Programa POFC/QREN."

Resumo

Modelos experimentais do enfarte do miocárdio baseados em roedores têm sido amplamente utilizados em pesquisas biomédicas para o estudo de alterações moleculares, celulares e histológicas após o enfarte.

Além disso, esses modelos têm sido recentemente aplicados para aceder ao potencial terapêutico de células candidatas a uma função de reparação funcional de lesão do músculo cardíaco. Estes estudos são fundamentados na indução de um enfarte, da aplicação de uma terapeutica em certos casos e subsequente análise do nível de enfarte final em ambos os casos. O nível de enfarte, definido como a percentagem do ventrículo esquerdo afectado pela oclusão da artéria coronária, é geralmente calculado em secções transversais marcados com tricrómico de Masson. O músculo do miocárdio lesado é substituído por fibras de colagénio, que podem ser visualizadas com cor azul logo após sete dias da ocorrência do enfarte. O valor final do nível de enfarte é uma média dos valores obtidos para todas as secções transversais do ventrículo esquerdo. Este parâmetro deve ser estimado através da identificação dos tecidos lesados e normais em cada secção. No entanto, uma vez que é um procedimento manual, é uma tarefa demorada, árdua e susceptível de ter um resultado diferente entre observadores. Deste modo, nós apresentamos abordagens automáticas, supervisionadas ou não, para realizar a segmentação e identificação dos tecidos que são então utilizados para obter uma medição do nível de enfarte. A validação experimental é feita comparando as abordagens propostas com a anotação manual e um erro total não superior a 8% é relatado em todos os casos.

Com base na técnica de segmentação supervisionada testada foi desenvolvido um programa para a avaliação do nível de enfarte chamado MIQuant. O MIQuant é uma ferramenta supervisionada de fácil utilização que permite a medição do nível de enfarte numa única secção do coração ou em várias secções, com base na técnica de segmentação region-growing. O valor médio final do nível de enfarte e os respectivos valores intermédios são obtidos pelo programa e podem ser guardados em formato de arquivo excel.

Palavras-chave: Avaliação do nível de enfarte, segmentação de imagem.

Abstract

Experimental rodent models of myocardial infarction (MI) have been extensively used in biomedical research to study molecular, cellular and histological alterations following induced heart ischemia.

These models have continuously been employed to test the potential of newly developed therapeutic approaches for the functional restoration of heart function. Such studies are based on myocardial infarction induction by permanent ligation of a main branch of the left coronary artery followed by some sort of therapeutic intervention. The power of the latter to significantly improve the heart condition is then inferred by analyzing the size of the infarcted tissue as compared to the infarcted non-intervened animals. The infarct size, defined as the percentage of the left ventricle (LV) affected by coronary artery occlusion, is typically calculated on transverse sections stained with Masson´s Trichrome. The lost myocardium is replaced by collagen fibers that can be visualized in blue following histological staining of the infarcted tissue, as early as 7 days post-MI. The final value of infarct size is an average of the obtained values for all representative transverse sections of the LV. This parameter is estimated by manually delineating the infarcted and normal tissue regions in the LV of the dissected heart. However, this is a time-consuming, arduous and prone to bias process. Herein, we introduce automatic supervised and unsupervised approaches to perform image segmentation which is then used to obtain the infarct size measurement. Experimental validation is performed comparing the proposed approaches with manual annotation and a total error not exceeding 8% is reported in all cases.

Based on the supervised segmentation technique tested we developed a tool for evaluation of experimental MI which was named MIQuant. The MIQuant is a user-friendly supervised tool that enables the infarct size measurement in a single cross-section or in multiple sections, based on region growing segmentation technique. The final average value of infarct size and the respective intermediate values are obtained and can be saved in an excel file-format for further data processing.

Keywords: Infarct size evaluation, image segmentation.

List of Figures

List of Tables

Contents

1. Introduction

Acute myocardial infarction is one of the major causes of premature morbidity and mortality worldwide. It results from the occlusion of coronary arteries and the establishment of tissue ischemia which can lead to heart failure. To study the lesions caused by this health problem and test the efficiency of potential therapeutic interventions, biomedical researchers conduct in vivo experimentation in which acute and/or chronic-like MI is induced. This is performed by the permanent ligation of a main branch of the left coronary artery in the mouse that leads to severe ischemia and thus to myocardial infarction. Through these assays it is possible to reproduce several of the pathological events that develop within the frame of a heart infarction condition in Man. In these assays myocardial infarction size, which is defined as the percentage of the left ventricle affected by the coronary occlusion, is one parameter measured obtained by the analysis of the dissected heart stained with Masson's Trichrome, a histological stain that enables the identification of collagen deposition, a hallmark of established infarction [8, 29].

Myocardial infarction (MI) size in animal model assays is estimated by identifying the infarcted and the normal heart tissue regions in the left ventricle of the animal´s heart. In this evaluation task researchers must delineate the contour of the infarcted area and of the left ventricle. The right ventricle region is ignored in this evaluation analysis since it is not affected by myocardial infarction induced in these animal assays [29]. Currently the infarct size analysis is a fully manual task performed by biologists, making it a time-consuming and arduous task, which is prone to subjective bias. The latter is a driving force for the development of automatic approaches for the analysis of myocardial infarction size in animal assays. To automatically perform such analysis it is necessary to select both healthy and infarcted tissue regions. The task of automatic tissue classification in medical and biology digital image processing is tackled by using automatic digital image segmentation approaches.

There are multiple techniques in image segmentation that have been applied to the analysis of cardiac tissue. For example, Chenyang Xu et al. described the segmentation of the LV of a human heart using deformable models [36, 37]. An initial contour is defined that evolves until a final segmentation is achieved. Mustafa Alattar et al. proposed the use of region growing method applied in the segmentation of the LV in cardiac MRI scans [1]. In this case a criterion for merging regions or pixels is selected and initial positions are established. Ghassan Hamarneh et al. presented MR cardiac images segmented with watershed transform, dealing with oversegmentation by applying k-means clustering to assign regions according to a measure of similarity [15].

Other techniques have also been applied for the segmentation of medical images of other body regions or tissues. Neeraj Sharma et al. described the segmentation of CT abdomen images using a multiple threshold segmentation technique to separate different regions in the images [28]. Watershed transform is also used in segmentation of high-magnification images of vesicles in a liver cell [3]. This is a region based segmentation that considers the images as a topographic surface and by considering an immersion simulation from each regional minimum

defines different regions. Another technique used in medical images segmentation is the mean-shift algorithm. It defines regions by grouping the points which converge to the same color mode in an image. Abdomen CT images have been segmented using this technique where different regions are defined [32]. The use of anatomical models has also been employed by Matthew Brown et al. for the segmentation of chest CT images [5]. Anatomical models provide constrains that guide the segmentation process. This modeling can also be extended to the task of segmenting the cross sections of the heart.

With respect to user intervention image segmentation techniques can be separated into supervised and unsupervised. In the first case the user needs to define initial parameters for each image, like an initial contour or seed point for the start of the segmentation. Unsupervised segmentation on other hand requires validation of initial parameters, after which the algorithm segments all input images.

For the automatic evaluation of the infarct size in animal model assays we tested both unsupervised and supervised techniques. Within the supervised approaches we tested the use of parametric active contours and region growing segmentation. Parametric active contours were tested to find the contour which is closer to the boundary of the object of interest. In this technique the user must define the initial contour and based on energy functions the contour evolves to the boundary of the target object, which can be the normal tissue, the infarcted tissue or the LV lumen of the cross-sections of the heart. Parametric active contours were also tested based on the gradient vector flow [37]. This novel approach has an external energy map that best attract the contour to the desired boundary, overcoming convergence and initialization issues. Finally, within the supervised techniques, the use of region growing was also tested. This technique examines neighboring pixels of initial points and determines whether the pixel neighbors should be added to the region according to some criterion.

Within the unsupervised techniques, we tested otsu automatic thresholding, watershed, k-means and mean-shift for the segmentation of the tissues of the heart. Otsu thresholding technique selects an adequate threshold for the gray level in order to separate objects from their background. This threshold is used to convert an intensity image into a binary one. Watershed technique was also tested to the segmentation task. Watershed technique is based on immersion simulation. The input image is considered as a topographic surface which is flooded by water starting from regional minima. The final segmented regions arising from the various regional minima are called catchment basins. All pixels associated with the same catchment basin are assigned to the same label. Given the watershed segmentation we decided if each segmented region corresponds to normal or infarcted tissue based on color properties. K-means was also tested to perform the segmentation of the heart tissue. This technique assigns cluster labels to data points with similar properties (color) from the entire image. After obtaining the segmentation result we identify each segmented cluster from its average color. Mean-shift is a clustering technique which evaluates both pixel spatial coordinate and pixel color space. It was also used for segment the cross-sections of the heart tissue. This technique needs the definition of the radius of the kernel used. As in the k-means clustering technique we selected three clusters and if more than three clusters are obtained we increase the radius of the kernel and repeat the

segmentation process.

The heart cross-section images show both right and left ventricle. However, for the evaluation of infarct size only the LV is considered. Before any segmentation process the right ventricle (RV) is manually delineated and not considered in the infarct size evaluation.

We also tested an anatomical model adaptation approach using expectation maximization. We defined an anatomical model similar to the structure of the heart that has the possibility to adapt to the tissue in analysis. The anatomical model consists in one major ellipse with two small ellipses inside and the size and position relations between them. Using the expectation maximization algorithm we iteratively improved the parameters that describe the ellipses until they best fit to the heart tissue. Given the result of the adaptation of the anatomical model we identified the normal and infarcted tissue by analyzing the tissue color. By performing infarct size estimation through anatomical model adaptation we do not need to manually delineate the RV since it is possible to automatically identify each tissue region and evaluate the infarct size only in the LV.

Given the segmentation results we can then estimate the infarct size. This estimation can be measured by different methods: *area* and *midline length* measurements. The *area method* is based on the ratio between the infarcted tissue area and the LV tissue area. The *midline length* measurement is based on the ratio between the distance from the midline that passes through the infarcted tissue and the midline which crosses through all the tissue of the LV. The segmentation of the tissue and identification of these specific regions in the images allows the evaluation of the infarction size by both methods.

The results of infarct size obtained with the segmentation of the heart tissue performed by the different approaches were in close agreement with manual results. Comparing the approaches tested with manual results the differences in infarct size were not higher than 8%. Within the unsupervised segmentation approaches, the watershed technique produced better results, with the differences not higher than 3%. The differences from the supervised approach used were at most 5%. Using an anatomical model for tissue segmentation produced results with differences below 8%. Although the performance of unsupervised approaches was better than supervised methods, biomedical researchers prefer the possibility to control the segmentation results in relation to fully automatic approaches. This led to the creation of a software application based on supervised techniques.

Based on the tested approaches we developed software for infarct size evaluation named MIQuant. It allows the segmentation of the tissue and provides results of the infarct size evaluation. The software is controlled by users and is based on region growing segmentation. Within supervised techniques, region growing proved to be the fastest and easy to interact with, providing the best results in comparison with manual results. The developed software is currently under evaluation at the Institute of Biomedical Engineering by the Stem Cell Biology Team (NEWTherapies Group) where the myocardial injury animal models are developed.

1.1 Contributions

Several supervised and unsupervised techniques are applied and tested to perform the segmentation of the heart images and get the infarct size, in particular:

- Supervised segmentation methods, which includes active contours, gradient vector flow and region growing.
- Unsupervised segmentation methods, as threshold segmentation, watershed segmentation, k-means and mean shift segmentations.
- Unsupervised tissue segmentation through model adaptation.
- Automatic methods for evaluate the infarct extension based on those performed manually.

Comparisons between methods are presented and discussed and a semi-automatic tool based on the supervised technique with better performance is also presented to perform the analysis of infarct size with the supervision of a biomedical researcher.

1.2 Resulting publications and communication

The work presented in this manuscript has also been published in peer-reviewed conference proceedings and been submitted for publication in related journals:

Automatic and semi-automatic analysis of the extension of myocardial infarction in an experimental murine model. Tiago Esteves, Mariana Valente, Diana S Nascimento, Perpétua Pinto-do-Ó, Pedro Quelhas. **Proceedings of IbPRIA, LNCS 6669**, pages 151-158, 2011. Included in appendix A [13].

Semi-automatic extraction of the level of infarction in mouse hearts. T. Esteves, P. Pinto-do Ó, and P. Quelhas. **RecPad**, pages 1-2, 2010. Included in appendix C [11].

Automated myocardial infarction analysis in an experimental model using image segmentation and model adaptation. Tiago Esteves, Diana S. Nascimento, Mariana Valente, Perpétua Pinto-do-Ó and Pedro Quelhas. **Pattern Recognition**, special issue, 2011 (Under Revision). Abstract included in appendix E [12].

MIQuant - semi-automated quantification of myocardial infarction size in preclinical models of ischemia. Diana S. Nascimento*, Mariana Valente*, Tiago Esteves, Maria Fátima Pina, Joana Guedes, Pedro Quelhas and Perpétua Pinto-do-Ó. Submitted. *equal contribution **PLoS ONE**, 2011 (Under Revision) [20].

Some of the published work was accepted for oral presentation:

5^{th} Iberian Conference on Pattern Recognition and Image Analysis (IbPRIA 2011) held at the Las Palmas de Gran Canaria. *Automatic and semi-automatic analysis of the extension of myocardial infarction in an experimental murine model*. Tiago Esteves, Mariana Valente, Diana S Nascimento, Perpétua Pinto-do-Ó, Pedro Quelhas. Included in appendix B.

XII Congresso Técnico de Anatomia Patológica, Centro Multimeios de Espinho, Espinho, Portugal. *MIQuant - towards standardization of cardiac regenerative therapies experimental assessment*. Nascimento DS, Valente M, Esteves T, Pina MF, Guedes JG, Freire A, Quelhas P and Pinto-do-Ó P. Included in appendix I.

Some of the published work was accepted for poster presentation:

RecPad 2010, Vila Real, Portugal. *Semi-automatic extraction of the level of infarction in mouse hearts*. T. Esteves, P. Pinto-do Ó, and P. Quelhas. Included in appendix D.

Second I3S Scientific Retreat IBMC | INEB | IPATIMUP together in Science , Axis Vermar, Póvoa do Varzim, Portugal. *Analysis of the extension of myocardial infarction in an experimental murine model*. Tiago Esteves, Mariana Valente, Diana S. Nascimento, Perpétua Pinto-do-Ó and Pedro Quelhas. Included in appendix F.

Second I3S Scientific Retreat IBMC | INEB | IPATIMUP together in Science , Axis Vermar, Póvoa do Varzim, Portugal. *MIQuant - towards standardization of cardiac regenerative therapies experimental assessment*. Nascimento D.S., Valente M., Esteves T., Freire A., Quelhas P. and Pinto-do-Ó P.. Included in appendix G.

6^{th} International Meeting of the Portuguese Society for stem Cells and Cell Therapies (SPCE-TC), Biocant, Cantanhede, Portugal. *MIQuant - towards standardization of cardiac regenerative therapies experimental assessment*. Nascimento D.S., Valente M., Esteves T., Freire A., Quelhas P. and Pinto-do-Ó P.. Included in appendix G.

1^{st} Advanced Summer School Interrogations at the Biointerface - *Cancer/Regeneration Interface* INEB | IPATIMUP | IBEC, Porto, Portugal. *MIQuant - towards standardization of cardiac regenerative therapies experimental assessment*. Nascimento D.S., Valente M., Esteves T., Guedes J.G., Freire A., Pina M.F., Quelhas P. and Pinto-do-Ó P.. Included in appendix H.

Spring Biointerfaces Lab Meeting, Porto, Portugal. *MIQuant - towards standardization of cardiac regenerative therapies experimental assessment*. Nascimento D.S., Valente M., Esteves T., Guedes J.G., Freire A., Pina M.F., Quelhas P. and Pinto-do-Ó P.. Included in appendix H.

1.3 Outline of the dissertation

The next chapter introduces the anatomic analysis of the mouse heart used in this study and the process of induction of MI as well as the determination of the infarct size.

Chapter 3 deals with automatic analysis of infarct size and the pre-processing techniques applied to the images. Several segmentation techniques are explained, applied to the images and results are presented.

In Chapter 4 a supervised tool for obtain the infarct size is presented and an anatomical model is introduced and described in detail. The methodology applied to automatically measure the infarct size is also explained.

Finally, Chapter 5 is reserved for some conclusions of this dissertation.

2. Myocardial Infarction Assays

Acute myocardial infarction is a major public health problem, resulting mainly from the occlusion of coronary arteries, due to the build-up of arteriosclerotic plaques, and the establishment of tissue ischemia eventually leading to end-stage heart failure. In order to reproduce several of the human-associated pathological events and study the lesions caused, permanent ligation of a main branch of the left coronary artery is performed in animal models, including the rat and the mouse. This surgical procedure allows the implementation of pre-clinical models of disease which are a pre-requisite for testing cell/drug-therapies before proceeding into clinical trials [8]. The tissue extension of the induced MI, which is defined as the percentage of the LV affected by coronary occlusion, is a critical parameter to evaluate the effect of any applied therapy at the experimental setting. The analysis of the tissue is based on microscopy images, in which both normal and infarcted tissue need to be identified.

For a better understanding of the MI induction assay analysis it is critical to briefly revise the relevant anatomy of the heart as well as the infarction inducing procedure. Additionally, it is very important to understand the current means of infarct size evaluation.

2.1 Why the Mouse?

Preclinical models of myocardial ischemia have been reported in several large animal species, including dogs and goats. The model that most closely resembles the response seen in humans is the pig ameroid model. This has been used in a variety of therapeutic studies. However, the logistics and practical demands of porcine surgical facilities severely limit the extent of such studies, precluding the use of this model for larger scale screening studies of novel therapeutic approaches [8].

Therefore, a rodent model of acute MI was developed in mice [17, 8, 22]. The step of the wild mouse to the worldwide most-used laboratory animal was principally caused by the usefulness of this species for different interests [17, 8, 19, 22, 10]. Historically, mice have been used in biomedical research since the 16th century, when Robert Hooke investigated the biological consequences of increasing air pressure. In the 19th century several fanciers in Europe, the United States and Asia were breeding and exchanging in particular pet mice and rats (rarely other rodents like hamsters, guinea pigs, etc.) showing a variety of coat color or behavioral mutations [10].

A booming use of mice has been reported since the 20th century in many areas of biomedical research. Thus, mice have been playing an instrumental role in several scientific fields, such as genetics, physiology, immunology, metabolism, pathology, oncology or cardiovascular diseases [10].

The use of the laboratory mouse as a model for cardiovascular research poses several relevant challenges. Its small size demands precise surgical skills, as well as specialized equipment

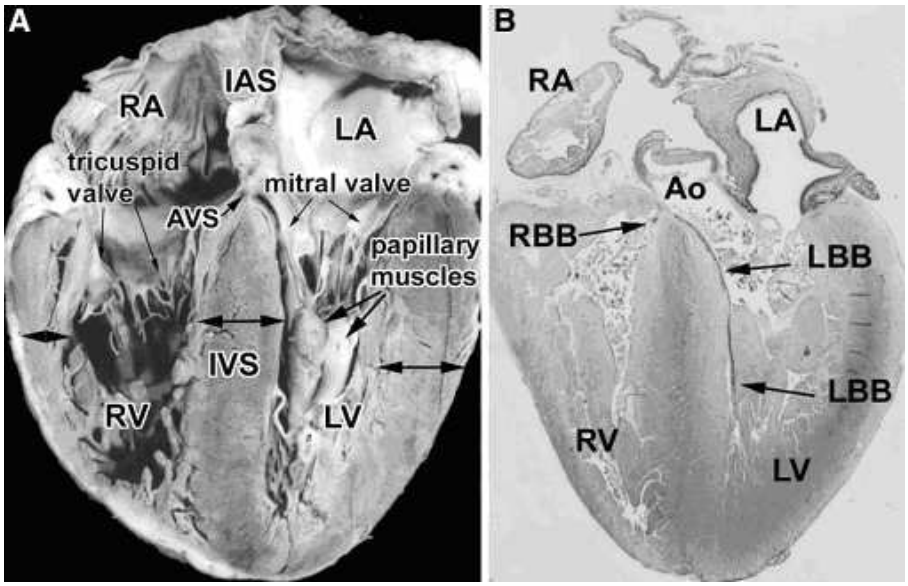

Figure 2.1 Anatomy of the postnatal human heart. A: a postnatal human heart in 4-chamber view: B - histological section of a 5-week old neonatal heart, sectioned in the same orientation, is shown; **LV** - Left ventricle; **RV** - Right ventricle; **LA** - Left atrium; **RA** - Right atrium; **AVS** - Atrioventricular septum; **IVS** - Interventricular septum; **IAS** - Interatrial septum; **LBB** - Left bundle branch; **RBB** - Right bundle branch; **Ao** - aorta [33].

for functional cardiovascular assessment; these are clear disadvantages when compared to larger experimental animals. However, the generation of transgenic and knockout mice, and the completed sequence of the mouse genome, has created opportunities for the systematic study of specific gene functions in the fields of cardiovascular pathophysiology and genetics, often justifying the substantial investment of resources in establishing mouse cardiovascular models [30].

2.1.1 Overview of the Mouse heart anatomy

Before discussing some of the specific anatomical features it is important to consider the dimensions and properties of the full-grown heart. The mouse heart weighs only about 0.2 g, and has a heartbeat of around 500-600 times per minute. Regarding the overall shape, another external feature, we must first consider that this shape is determined by the anatomical context of the adult heart within the thoracic cavity. In the Human, for example, the heart rests on the diaphragm. This is reflected in its more pyramidal shape and a flat dorsal (or inferior) surface. In comparison, the mouse heart, which in the four-legged mouse does not rest on the diaphragm and has more room to move freely within the pericardial cavity, has a more ellipsoidal shape. Another external feature is that in the mouse heart the atrial chambers and their appendages are relatively small [33]. The basic anatomical features of the postnatal heart in the mouse and human are similar (Figures 2.1 and 2.2) [33].

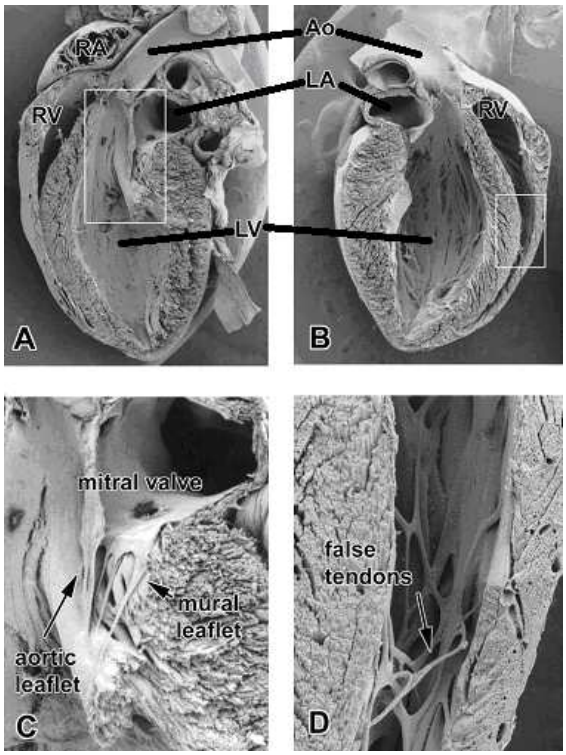

Figure 2.2 Scanning electron micrographs (SEM) of the postnatal mouse heart: A and B - SEM images of the posterior (A) and anterior (B) half of an adult mouse heart; C - an enlargement of the boxed area in A, showing the relatively small leaflets of the murine mitral valve; D - an enlargement of the boxed area in B and demonstrates some of the false tendons in the apical portion of the right ventricle; **LV** - Left ventricle; **RV** - Right ventricle; **LA** - Left atrium; **RA** - Right atrium; **Ao** - aorta [33].

In both human and mice the heart has four chambers; two atria, separated by an interatrial septum (IAS), and two ventricles, separated by an interventricular septum (IVS). In addition, located between the IAS and IVS there is a small "septal segment" which, as a result of the offset of the atrioventricular (AV) valves, is known as the atrioventricular septum (AVS), as it is situated between the subaortic outlet segment of the LV from the right atrium. In the mouse this structure is relatively thick and mostly muscular, partly as a result of delayed delamination of the septal leaflet of the tricuspid valve, and partly as a result of myocardialization of the mesenchymal tissues. In the junction situated between the atria and ventricles, the AV junction (AVJ), we find two AV valves. The arrangement of the AV valves in mouse and human is comparable. In the left AVJ we find a mitral valve, which has two distinct leaflets (a bicuspid valve), whereas in the right AVJ a tricuspid valve is located, which has three distinct leaflets. In the mouse these valves are far less prominent (Figure 2.2 A and C) in comparison with the human heart valves (Figure 2.1 A).

The inner lining of the ventricles is characterized by the presence of numerous myocardial

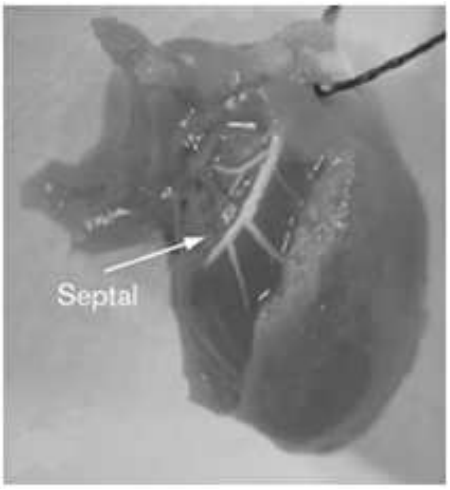

Figure 2.3 Photomicrographs of Silastic cast of septal coronary artery exposed along the right interventricular septum in an intact mouse heart [17].

protrusions better known as trabeculae (trabeculae carneae). In addition to the trabeculation, within the apical cavity of the ventricles in the mouse and human heart, it can be also discriminated thin structures that resemble the tendinous chords attached to the papillary muscle. However, despite of this resemblance, the thin structures are not really tendons, but are actually extensions of the subendocardial ventricular network of the cardiac conduction system, and are therefore nowadays generally referred to as "false tendons" (Figure 2.2 D) [33]. A slight morphological difference in the overall ventricular anatomy between mouse and human is found in the relative size and shape of the muscular ventricular septum and the position of the aortic outlet in relation to the IVS (Figures 2.1 and 2.2). In the human heart the muscular IVS is a large structure, its thickness approaching or exceeding that of the left ventricular free wall (Figure 2.1 A and B). In the mouse, the IVS is not quite as large and compact (Figure 2.2 A and B), and at the base it gradually tapers toward the AV septum [33].

2.1.2 Mouse Coronary anatomy

Mouse coronary anatomy is distinct from that of other well-studied animal models and from that of the Human. Silastic coronary casts obtained from mice (C57BL/6) demonstrated a single major septal coronary artery (Figure 2.3) [17].

The mouse septal coronary artery courses along the right interventricular septum and provides perfusion to this region of the myocardium (Figure 2.3), which is, in humans, largely supplied by septal perforator arteries arising from the left anterior descending and/or posterior descending coronary arteries. The right coronary artery proper in mice is non-dominant, perfusing the right ventricle. The mouse left coronary artery is also different, as it does not divide proximally into a left anterior descending and circumflex artery, rather it courses obliquely

across the left ventricular free wall and branches in a variable fashion. Thus, mice do not possess an anatomic left anterior descending coronary artery tracking down the interventricular septum. Therefore, myocardium infarctions produced by ligation of the left coronary artery in mice are predicted to produce regionally distinct infarctions, which involve the left ventricular free wall and apex while sparing the septum, in comparison with ligation of the left anterior descending coronary artery in other species [17].

All these features related with the anatomical knowledge of the mouse heart can help us to understand the shape and appearance of the heart. These acknowledgements also allow us to perceive that myocardial infarction from ligation of left coronary will mostly affect the LV. This will be the region under evaluation to estimate possible myocardial infarction. With these we can describe anatomical models useful for the identification of the regions of interest necessary for compute the infarct size evaluation.

2.2 Myocardial infarction

To observe and study the response of the myocardial infarction in mice, under different conditions, it is necessary to induce this heart condition in experimental animals. This experimental model for MI induction in mice by permanent ligation of the coronary artery has been extensively studied and validated by many researchers in the area [8, 19, 22]. At the INEB, the Stem Cell Biology Team established a mouse MI model and performed the standard validation protocol for its particular conditions (Nascimento DS et al., to be published elsewhere).

2.2.1 Induction of myocardial infarction

In brief, anaesthetized animals were intubated endotracheally in a supine position, and subjected to automatic ventilation. The animals were moved onto their right side, and a left thoracotomy in the third intercostal space provided access to the beating heart. After removing the pericardium, 7-0 suture was placed in the anterior myocardium to occlude the left anterior descending artery (Nascimento, DS et al; manuscript). Occlusion was confirmed by observation of left ventricular pallor immediately post ligation. The chest was closed, the lungs re-inflated and the animal moved to a prone position until spontaneous breathing occurred. All procedures in animal experiments were approved by Direcção Geral de Veterinária, conducted in strict obedience to the rules that internally apply in the Animal Facility of the Associate-Laboratory IBMC-INEB, and in accordance to the protocols of international ethics and animal welfare.

This surgical procedure allows the interruption of blood flow of the LV free wall, resulting in extensive cell death and subsequent ventricular reshuffle. The extensive deposition of collagen in the ischemia zone comes as part of the tissue response and underlying the calculation of the ventricular zone affected. Twenty one days after surgery, animal were sacrificed and the heart removed and processed for paraffin embedding and histological evaluation [8, 19, 22].

The images from figure 2.4 are longitudinal sections stained with Hematoxylin/Eosin, and

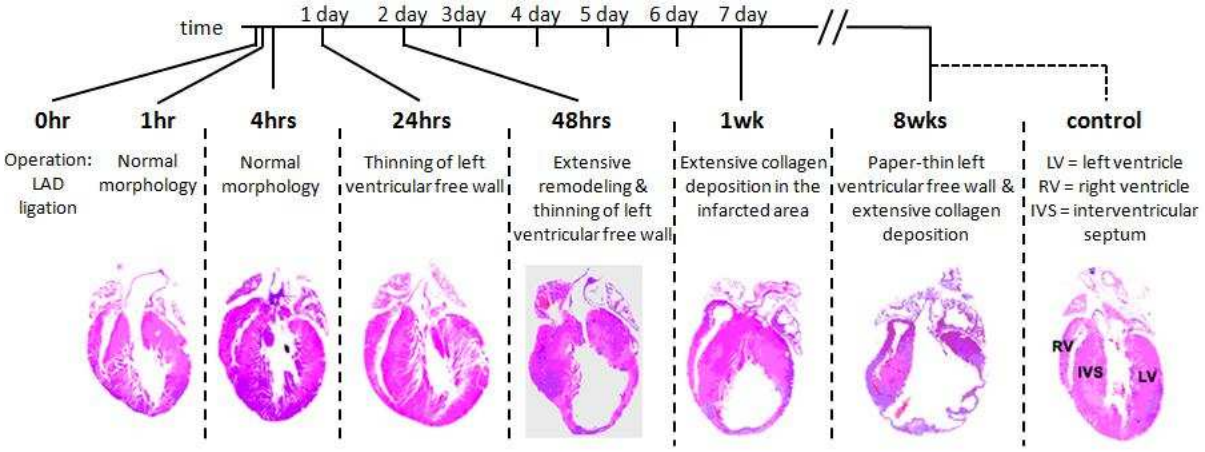

Figure 2.4 Longitudinal sections views of infarcted hearts at different time-points post-MI illustrating the increase of the myocardium compromised area.

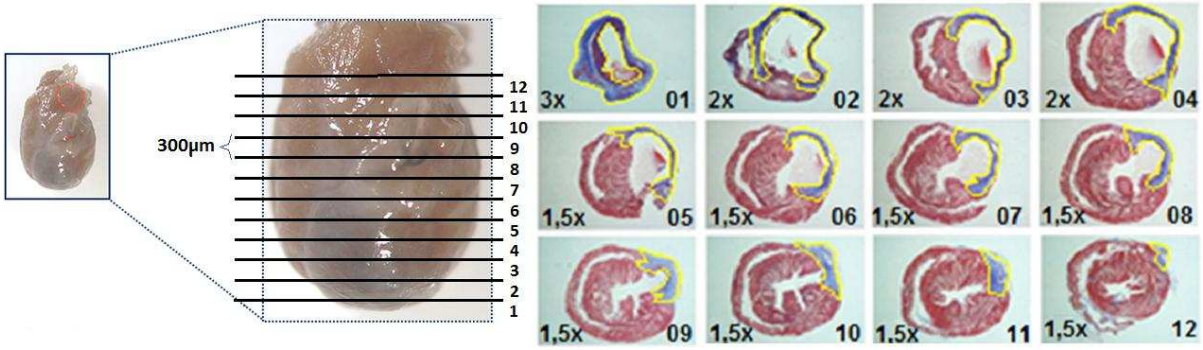

Figure 2.5 Scheme of the sections obtained from heart (left) and the corresponding 12 cross sections of the heart (right). The affected tissue is bounded in yellow, showing the narrowing of the ventricular wall and deposition of collagen (blue).

illustrate the progression of the thinning and deterioration of the LV where the infarction took place.

Based on the images of the heart it is possible to estimate the infarct size.

2.2.2 Estimation of Infarct Size

The infarct size is defined as the percentage of the LV compromised after coronary occlusion and is calculated as the mean value of infarction level over 12 cross sections of the LV. These sections are stained with Masson's Trichrome, a histological staining which enables the discrimination of the collagen deposition with Aniline Blue (Figure 2.5).

The infarct size is mainly calculated using one of the following two different evaluation methods:

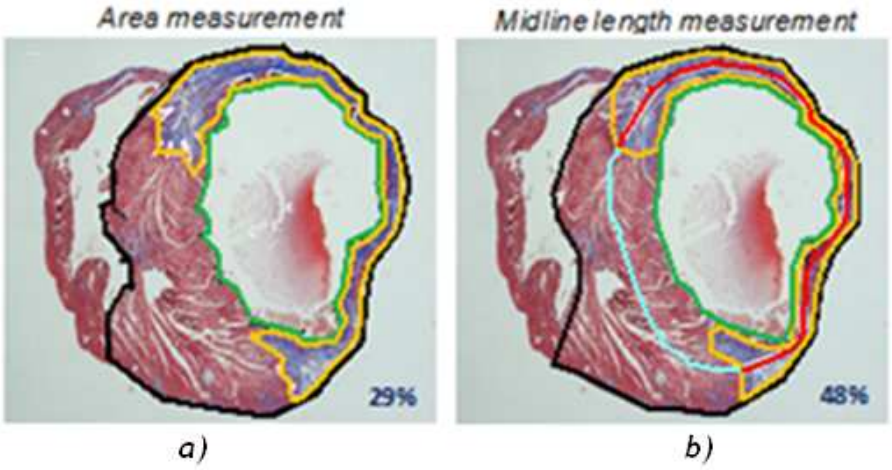

Figure 2.6 Cross section of the heart. The LV is bounded by the black line. Green line is identifying the lumen of the ventricle and the yellow one shows the tissue with infarct, reflecting the narrowing of the ventricular wall and deposition of collagen (blue). a - Infarct size obtained by area measurement. b - Infarct size obtained by midline length measurement which crosses the infarcted tissue (red line) and the normal tissue (blue line) [22].

Area measurement - Infarct scar area and the total area of left ventricular myocardium are traced manually in digital images. Infarct size is calculated by dividing the sum of infarct areas from all sections by the sum of left ventricular areas from all sections (Figure 2.6 a) (including those without infarct scar) [29].

Midline length measurement - The LV myocardial midline (Figure 2.6 b - junction of the blue and red lines) is drawn at the center line equidistant from the epicardial and endocardial regions (Figure 2.6 b - black and green lines respectively). Midline infarct length is taken as the length of the LV myocardial midline where more than 50% of the whole thickness of the myocardial wall is compromised (Figure 2.6 b - red line). Infarct size is obtained by dividing the length of the LV myocardial midline by the midline infarct length. Infarct size derived from midline length measurement is the average of all individual sections evaluation [29].

Infarct size values measured by area and length based approaches at 28 days post-myocardial infarction is highly correlated with cardiac systolic dysfunction [29]. The infarct size values obtained with area measurement are significantly compressed compared with those obtained by the midline length method. The length-based approach measures the extent to which the infarct scar radially covers the wall of the LV, without being influenced by thinning of the wall that affects the area which is the parameter measured by area-based approaches and correspond to compressed values [29].

The fundamental task required for automation of infarct estimation is tissue region delineation. In order to replace manual tissue region delineation we will apply image segmentation techniques. We will further improve the usability and automation of our approach through the

use of anatomical modeling.

The next section describes different image segmentation techniques, with and without human intervention, which can be used to perform automatic segmentation of the heart images in such a way as to identify the normal and infarcted tissues.

3 . Automatic infarct size analysis

To automatically obtain the infarct size it is necessary to separate the areas of the different tissues in each cross section of the heart. The task of tissue separation in biomedical images is tradicionaly performed using image segmentation techniques. In this work we follow the same approach.

Image segmentation is a task of fundamental importance in digital image analysis [18, 2]. It is the process of partitioning a digital image into disjoint regions with similar properties such as gray level, color, texture, brightness or contrast, each of which typically corresponds to an object of interest. It provides additional information about the contents of an image by identifying edges and regions, while simplifying the image from thousands of pixels to less than a few hundred segments [28, 35].

In the particular task of obtaining the infarct size, where it is necessary to identify sub-regions in each section to achieve the final result, image segmentation is essential.

With regards to user intervention image segmentation techniques can be classified as supervised and unsupervised. Supervised segmentation requires operator interaction throughout the segmentation process whereas unsupervised methods don't need any human intervention to obtain the final result after initial setup [28].

Since a large amount of literature refers to image segmentation the discussion presented in this chapter is restricted to the most frequently used algorithms [2]. Due to both the difficulty of the imaging segmentation task and to the specifics of each particular segmentation task, image pre-processing is required. In the next subsections we first address the image pre-processing steps applicable to our task and then present the segmentation methods explored in this work.

3.1 Image pre-processing

In order to improve image quality prior to segmentation we applied color and illumination regularization to correct for image quality variability. We also apply Gaussian smoothing for noise reduction and to remove texture detail which is not relevant for the tissue segmentation task [13]. Finally, in order to provide meaningful image information to segment each specific tissue we performed relevant channel combinations from the original image information.

3.1.1 Color and illumination regularization

Some images of the heart cross sections present a considerable variance in color and illumination. This affects the segmentation process since the variance in pixel intensity reduces the applied methodologies robustness.

We perform image regularization to reduce image variability by normalizing image contrast and color balance, allowing for subsequently more accurate image analysis [35]. Assuming that the brighter regions of the image, around the corners, represent the background, we estimate

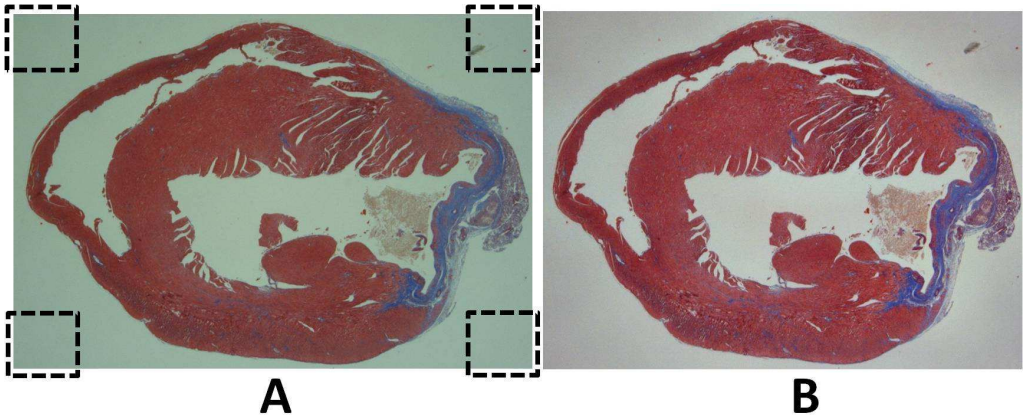

Figure 3.1 Color and illumination regularization of the heart images. The brighter regions marked in A are used to estimate the illumination. The result of color and illumination regularization is visible in B.

the illumination of the background (Figure 3.1 A). This includes both estimating overall variations in the illumination and deviations from uniform background illumination. Additionally we correct the color balance so that the brighter regions are now white and any unbalancing between channels is removed. As a final contrast enhancement step we apply adaptive histogram equalization to all images [26, 24] (Figure 3.1 B).

3.1.2 Image filtering

There is a wide variety of methods that can be applied to reduce noise in digital images. We considered three main methods for the task at hand: Gaussian smoothing [14], non-local means filtering [35, 14] and denoising by sparse 3D transform-domain collaborative filtering [7]. While the use of advanced methodologies like non-local means can lead to considerable qualitative improvements of images quality, these improvement did not correspond to greater accuracy in the delineation of the image's regions of interest. As a result we chose Gaussian filtering for noise reduction due to its simplicity and greater speed. Given an input image $\mathbf{I}_0$, the filtered image $\mathbf{I}$ is obtained by computing the convolution of the image with the Gaussian filter $\mathbf{G}$, denoted as:

$$I = G \otimes I_0, \tag{3.1}$$

where $\otimes$ denotes the spatial convolution between $\mathbf{I}_0$ and $\mathbf{G}$. The Gaussian filter is defined in terms of its standard deviation σ_0 as:

$$G_{\sigma 0} = \frac{1}{\sigma_0 \sqrt{2\pi}} \exp\left[-\left(\frac{x^2}{2\sigma_0^2} + \frac{y^2}{2\sigma_0^2} \right) \right] \tag{3.2}$$

We apply Gaussian filtering to all images prior to segmentation.

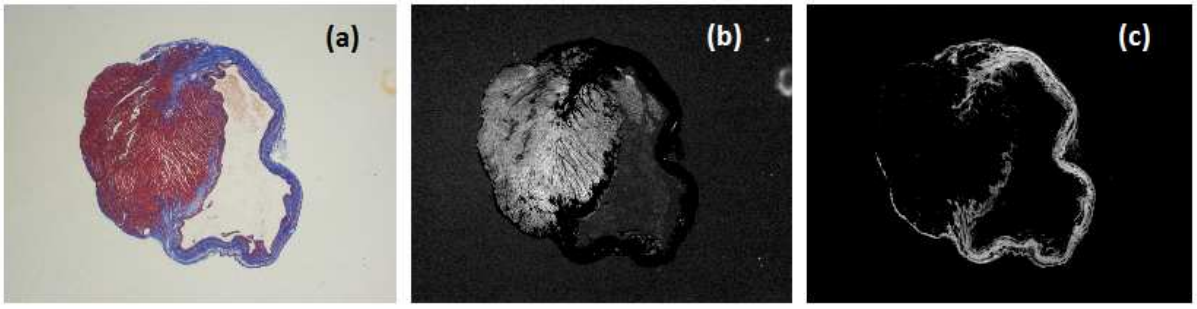

Figure 3.2 Channel combination used to better enhance the different types of tissue. (a) Cross section of the heart (original image). (b) Subtraction of the Blue channel from the Red channel enhancing the normal tissue. (c) Subtraction of the Red channel from the blue channel, enhancing the infarcted tissue.

3.1.3 Color channel combination

While the input images for the automatic infarct size system have full RGB color information most segmentation methods are more easily applicable to intensity images. However, a straightforward grey level conversion of the images would remove all color information and destroy important information. To keep meaningful information we convert the input images from RGB color to single channel greyscale images where the intensity is related to relevant information for the task of normal and infarcted heart tissue separation. As would be expected from visual inspection, we found that high values of image intensities in the Red channel were correlated with the normal-tissue, while Blue channel had high image intensity values in infarcted tissue regions. Based on these relationships the subtraction of the Blue channel from the Red channel is used in cases where we aim at obtaining the regions of the normal heart tissue (Figure 3.2 b). Conversely, we subtracted the Red channel from the Blue channel when aiming at enhancing information related to the infarcted-tissue (Figure 3.2 c).

For each specific segmentation method we either use a specific color channel combination or RGB color information. The specific combination is indicated in each method in the next subsections.

3.2 Supervised segmentation methods

Supervised segmentation methods require user input for each specific image, usually an initial region or points to start the segmentation. In other words, it requires human intervention during its operation for each example given.

Among supervised segmentation methods we tested different techniques: active contours [37, 36, 31], Gradient Vector Flow [37, 36] and region growing [35, 14]. In active contours it is necessary to define the initial contour, the same is true for the Gradient Vector Flow method. These are parameterized curves that evolve within the image to find object boundaries. The region

growing method also needs initializations of the initial positions which will form the final regions of interest. Region growing approaches exploit the fact that pixels with similar pixel information should be grouped together.

3.2.1 Parametric Active Contours

Active contours are image processing techniques used to find a contour that best approximates the perimeter of an object given an initial contour based on energy functions. Active contours (or snakes) are defined within an image domain and can move under the influence of internal forces from the contour's shape and external forces computed from the image data. Parametric active contours are widely used in segmentation [31].

Active contours synthesize parametric curves within an image domain and allow them to move toward desired features, usually edges. Typically, the curves are drawn toward the edges by potential forces, which are defined to be the negative gradient of a potential function. Additional forces, such as pressure forces, together with the potential forces comprise the external forces. There are also internal forces designed to hold the curve together (elasticity forces) and to keep it from bending too much (bending forces) [37, 31].

Active contours are represented perimetrically as:

$$c(s) = (x(s), y(s)), \tag{3.3}$$

where $x(s)$ and $y(s)$ are the coordinates of points s along the contour. The energy functional used is a sum of several terms, each corresponding to specific force acting on the contour and the goal is to minimize this functional with respect to the contour parameters:

$$E = \int \alpha Econt(s) + \beta Ecurv(s) + \gamma Eimage(s) ds, \tag{3.4}$$

where the parameters α, β and γ control the relative influence of the corresponding energy terms, *Econt* is the continuity term and forces the contour to be continuous, *Ecurv* is the smoothness term and forces the contour to be smooth and *Eimage* is the edge attraction term [31].

The *Econt* term attempts to keep the points at equal distances spreading them equally along the contour and is based on the first derivative:

$$Econt(s) = (\overline{d} - \|c(s) - c(s-1)\|)^2, \tag{3.5}$$

where $\overline{d}$ is the average distance between the points of the contour. This function is minimal for points at equal distances. This value increases when the displacement of a contour point leads to a position at a distance which differs from the average distance between points, increasing the total energy and not favoring such point displacement.

The *Ecurv* parameter enforces smoothness on the contour shape by penalizing high contour curvatures and is based on the second derivative (curvature):

$$Ecurv(s) = \|c(s-1) - 2c(s) + c(s+1)\|, \tag{3.6}$$

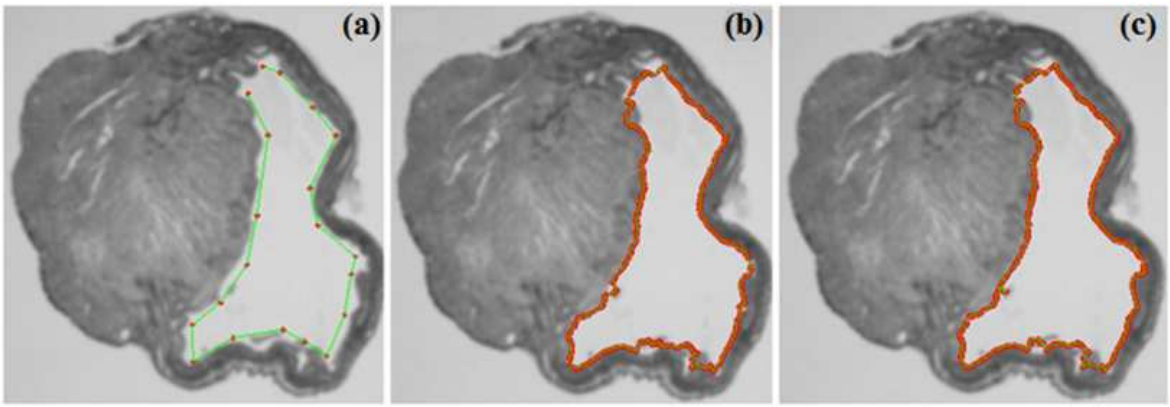

Figure 3.3 Segmentation of the lumen in a cross section of the heart using active contours: (a) A mouse heart image with the initial boundary delineated, (b) the same image with improved boundary delineation after 50 iterations and (c) final segmentation after 150 iterations.

Its value increases for irregular contours penalizing them by increasing the total energy.

The purpose of *Eimage* term is to attract the contour toward the target contour and this is achieved by the following function:

$$Eimage(s) = -\|\Delta I(x(s), y(s))\|, \tag{3.7}$$

where ΔI is the gradient of the image computed at each contour point. *Eimage* has a high negative value when the contour points approach edge locations, favoring the evolution of the contour towards those locations.

One demonstration of active contours applied to a cross section of the heart is visible in Figure 3.3 for which the delineation of the ventricle is achieved after 150 iterations. The *Eimage* term is obtained by the gradient of the green color image channel, where tissue boundaries are more evident. The user needs to specify the initial points to begin the segmentation process for each tissue or region (Figure 3.3 a).

3.2.2 Gradient Vector Flow

There are two key difficulties with parametric active contour algorithms. First, the initial contour must, in general, be close to the true boundary or else it will likely not converge to the desired result. Second, active contours have difficulties progressing into boundary concavities. Gradient Vector Flow is an external energy map for active contours models that addresses both problems [36].

Gradient vector flow fields, are dense vector fields derived from images by minimizing a certain energy functional in a variational framework. The minimization is achieved by solving a pair of decoupled linear partial differential equations that diffuses the gradient vectors of a gray-level or binary edge map computed from the image (Figure 3.4) [37].

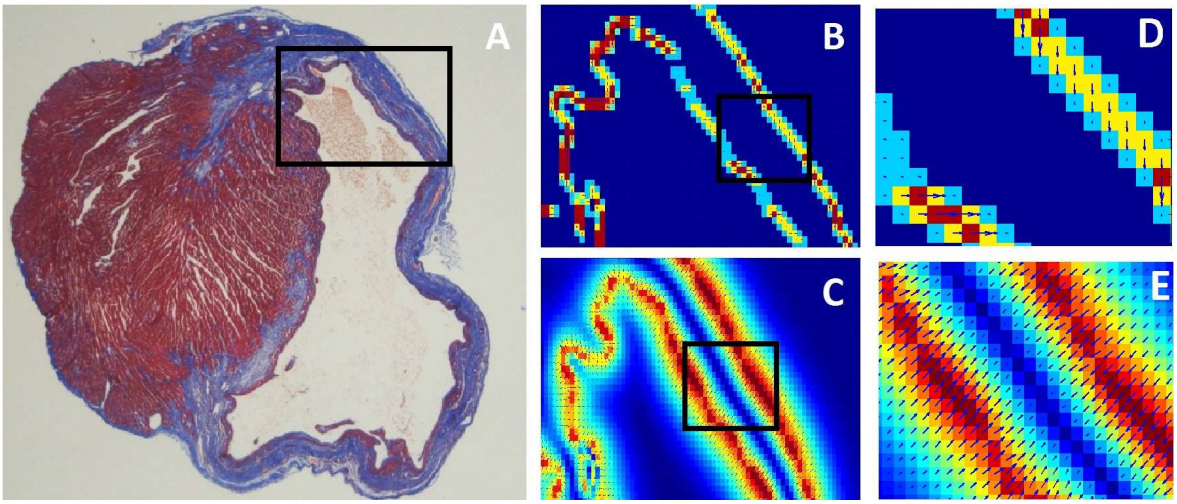

Figure 3.4 Cross section of the heart (A) with a region selected to visualize the differences between traditional gradient image (B) and gradient generated by GVF (C). D and E are enlargements of the regions selected in B and C, respectively.

Particular advantages of the GVF contours over traditional contours are its robustness with respect to initialization and its ability to move into boundary concavities. Unlike pressure forces, the active contours based on GVF does not need prior knowledge about whether to shrink or expand toward the boundary. These also have a larger capture range, which means that, barring interference from other objects, it can be initialized far away from the desired object boundary. Distance potential forces shown in (Figure 3.4 C) have vectors with large magnitudes far away from the object, explaining why the capture range is large for this external force model [37].

An example of the GVF active contour applied to a cross section of the heart is shown in Figure 3.5 where we can see that it converges to the final object boundary in less iterations than in traditional active contours. As in the active contours technique it is necessary to specify the initial points of the contour to begin the segmentation process.

3.2.3 Region Growing

Region growing exploits spatial context by grouping pixels or sub-regions into larger regions. Homogeneity is the main criterion for merging regions based on a selected similarity criteria which depends on the problem under consideration and also on the type of image data available [14].

Region growing starts by dividing the input image into regions. These initial regions can be small neighborhoods or individual pixels known as seeds which are manually defined. For each region a set of image property values are computed that define the membership properties for that region. Each region's property values reflect the membership to that same region. These

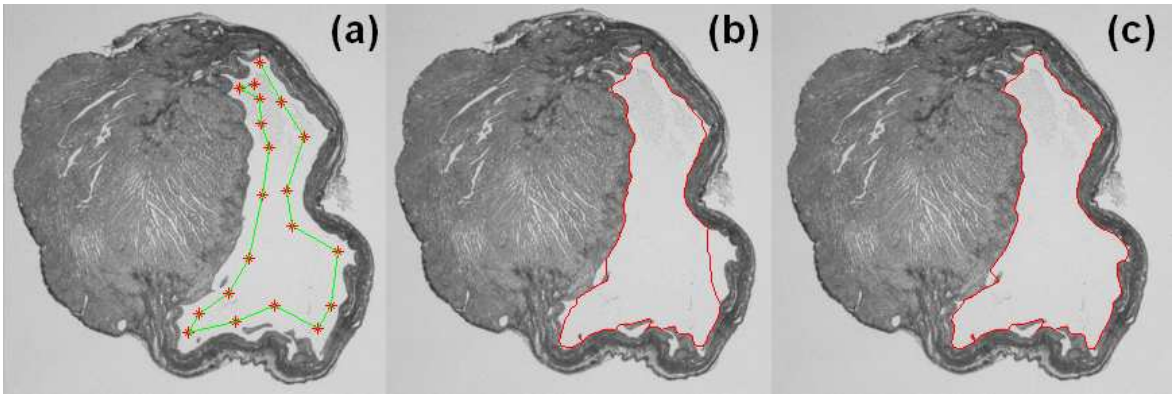

Figure 3.5 Segmentation of the lumen in a cross section of the heart using GVF active contours: (a) A mouse heart image with the initial boundary delineated, (b) the same image with improved boundary after 20 iterations and (c) final segmentation after 60 iterations.

property parameters may vary and some usual choices are: average gray level, texture, color, etc. The second step of the method is the merging of regions which do not show separating boundaries between them. To do this all boundaries between adjacent regions are examined. The boundary strength between regions is estimated by the difference of property values between those adjacent regions. A given boundary is strong if the parameters differ significantly on either side of that boundary, and it is weak if they do not. Strong boundaries are allowed to remain unaltered; weak boundaries are removed and the adjacent regions merged. This process is iterated by alternately recomputing the region membership parameters for the enlarged regions and once again dissolving weak boundaries, until it reaches a point where no weak boundaries remain [35].

Region-growing methods often produce good segmentation results that correspond well to the visually apparent edges of objects in the image [35, 14]. Observing this procedure in our task of segmenting a cross section of the heart (Figure 3.6) we see that regions in the interior of an object are growing until their boundaries reach the edge of the object. For the task of segmenting the normal and the infarcted heart tissue it is necessary to define the initial points for the process of region growing in each of the tissue-conditions. To apply region growing we select the average region's pixel intensity as the homogeneity criteria. In this example, the objective is the segmentation of the normal tissue and for that purpose we use the color image combination referred in section 3.1.3. We subtract the Blue channel from the Red channel in order to select the intensity information related to the normal tissue. The same process can be applied to the infarcted tissue by selecting different initial points and using a different color channel combination.

An extra issue occurs when, due to image variability, the region does not grow until its desired extension. In this case the user can give additional initial points for the algorithm or the homogeneity evaluation criteria can be altered.

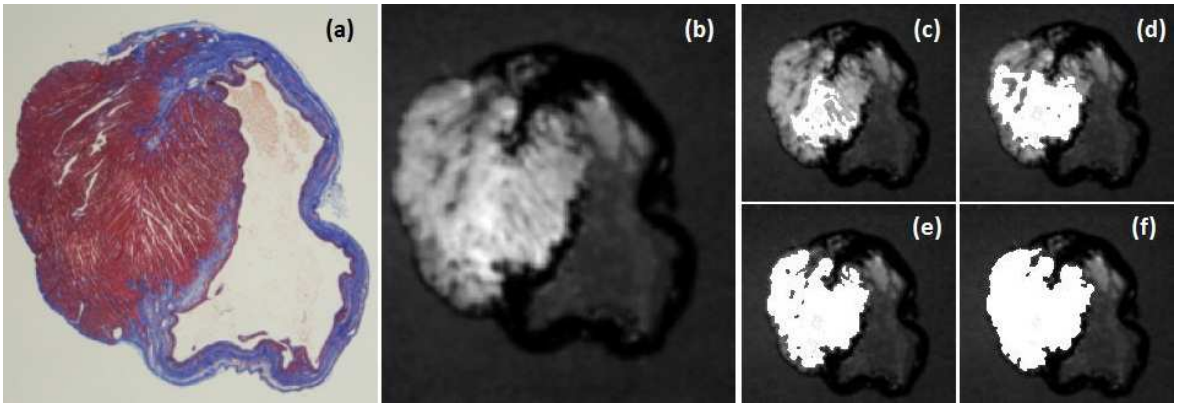

Figure 3.6 Region-growing segmentation of the healthy tissue of a mouse heart image section: (a) original image, (b) channel combination between the Red and Blue channel used as the information for normal tissue membership. (c), (d) and (e) shows three stages of the region growing evolution and (f) shows the final healthy tissue segmented region.

While the use of supervised methods gives the user confidence on the results for each image, since the segmentation is guided by the user, the need for interaction still requires considerable time and effort. In the next section we will explore unsupervised methods to the problem of heart tissue image segmentation, which require only the setting of initial parameters for the segmentation of all images.

3.3 Unsupervised segmentation methods

Unsupervised segmentations methods do not require user interaction for the segmentation of each image, but require validation of initial parameters. Among unsupervised segmentation techniques those more adequate for the task of heart tissue segmentation are: automatic thresholding [18, 34], watershed segmentation [28], k-means [16] and mean-shift segmentations [2, 23]. Automatic thresholding technique uses a histogram to represent the pixel's intensity. Based on the histogram it defines a partition grouping pixels into two classes. Watershed is a region based segmentation that analyze the image as a topographic surface and detects regions based on an immersion simulation. K-means and mean-shift are cluster based segmentation methods. K-means groups pixels with similar properties not taking into account their positions in the image. Mean-shift also groups pixels but considering both pixel spatial and color spaces.

In the next subsections we discuss these approaches for the problem of heart tissue segmentation.

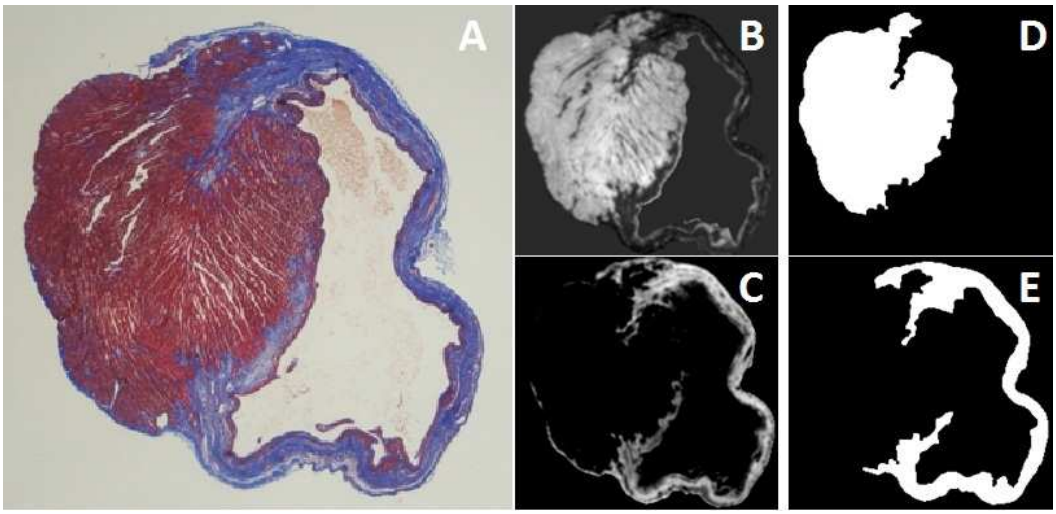

Figure 3.7 Otsu heart tissue segmentation result: A - original image (cross section of mouse heart), B and C - color image combinations used for the segmentation of the normal and infarcted tissue respectively, D and F - segmentation result of the normal and infarcted tissues respectively.

3.3.1 Automatic Thresholding Segmentation

In automatic thresholding a single value called threshold is used to create a binary partition of the image intensities. All intensities greater than the threshold are grouped together into one class and those below the threshold are grouped together into another class [18]. The use of a single threshold Th thus results in a binary segmented image:

$$I_{Th}(i,j) = \begin{cases} 1 \; if \; I(i,j) > Th \\ 0 \; if \; I(i,j) \leq Th \end{cases} \tag{3.8}$$

where $I_{Th}(i,j)$ is the binary segmented image at a threshold Th and (i,j) are the coordinates of each pixel of the image. The specific threshold value is chosen based on the image's pixel properties and some assumed model. While the simplicity of thresholding approaches is an advantage, this type of approaches can only be applied when several assumption are possible. First, the pixel's region membership must be encoded into its intensity value. Secondly, the image must have uniform illumination. These assumption are neither trivial nor frequently possible. This makes automatic thresholding highly dependent on efficient image pre-processing.

Manual adjustment of thresholds is common in order to obtain a result considered correct by visual inspection, however with this approach different segmentation results are likely to be obtained by different users for the same image [26]. A number of algorithms have been developed for automatically obtain a threshold value [18, 23, 27]. A usual approach is the Otsu method [21]. In this case the method assumes that the image under analysis has a bimodal distribution of the pixel's greylevel values, one corresponding to the foreground and another to the background. The value of the threshold is, in this case, calculated by maximizing the

separability of the resultant classes so that their intra-class variance is minimal.

A segmentation by threshold of the normal and infarcted tissue is observed in figure 3.7. We apply Otsu automatic thresholding to color image combinations which enhance infarcted and normal tissue information as described in section 3.1.3. We used the result of the subtraction of the Blue channel from the Red channel (Figure 3.7 B). Then the segmentation is achieved by applying an threshold value obtained by Otsu's method, where pixels with intensity values above the threshold are selected to form the binary image (Figure 3.7 D). For the segmentation of the infarcted tissue we subtract the Red channel from the Blue channel (Figure 3.7 C) and use that result for the thresholding segmentation (Figure 3.7 D). In appendix J, several other examples of segmentation by threshold are presented.

The main drawback of this technique is that the results are too tightly coupled with the thresholds used. Any change in the threshold values can originate a different segmented region. Another drawback which is a direct consequence of the previous one is that the technique is very sensitive to noise and to irregular illumination since this method does not take into account the spatial characteristics of an image [18, 23, 27].

3.3.2 Watershed Segmentation

Watershed segmentation or watershed transform is a region based method since it takes into account spatial information in the segmentation process [28, 15].

The most intuitive description of the watershed transform is based on a flooding simulation. Consider the input grayscale image as a topographic surface. The goal is to produce the watershed lines on this surface. To do so, holes are punched at each regional minimum in the image. The topography is slowly flooded by allowing water to rise from each regional minimum at a uniform rate across the image. When the rising water coming from two distinct minima is about to merge, a dam is built to prevent the merging. The flooding will eventually reach a stage when only the tops of the dams are visible above the water surface, and these correspond to the watershed lines. The final segmented regions arising from the various regional minima are called catchment basins [35, 26, 16].

For image segmentation, watershed segmentation is usually, but not always, applied to a gradient image. Since real digitized images present many regional minima in their gradients, this typically results in an excessive number of catchment basins. This problem is known as watershed oversegmentation [26, 16].

The watershed transform can also be used with initial markers. This is a technique usually used to reduce oversegmentation, if one can place markers within the objects to be segmented. In this case the topographic surface is only flooded from the selected maker locations, limiting the number of final regions in the segmentation [35, 26]. However, to apply marker based watershed segmentation to an image we need either user given locations for the markers or an initial segmentation of high confidence regions to be considered as markers.

In figure 3.8 is visible a segmentation of a cross section of the heart by watershed which

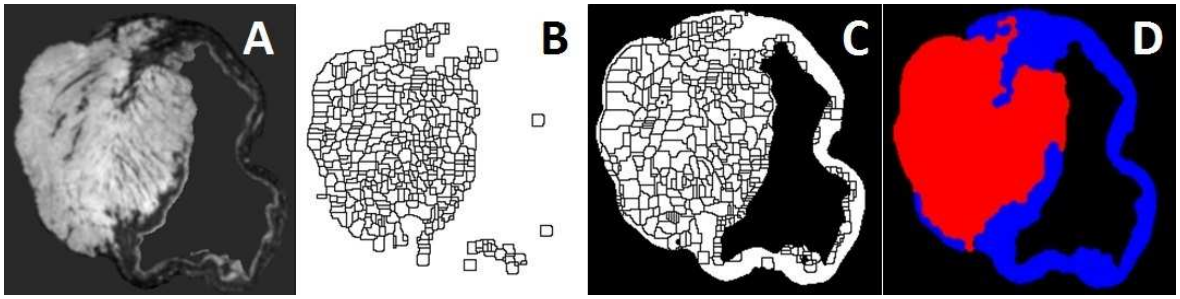

Figure 3.8 Segmentation of a cross section of the heart using watershed transform: A) input image obtained by color channel combination; B) watershed segmentation result; C) watershed segmentation result limited by the mask of the heart tissue which allows to focus the analysis only on the heart tissue; D) identification of each segmented region as normal (red) or infarcted tissue (blue).

resulted in oversegmentation. For this technique we applied the traditional watershed segmentation without markers. We used the subtraction result of the Blue channel from the Red channel (see Section 3.1.3) as the input image (Figure 3.8 A) for the segmentation process. Performing watershed segmentation originates an oversegmentation of the tissue since it has many regional minima (Figure 3.8 B). To deal with the oversegmented result we limit our analysis to the heart tissue and use color clues to separate all regions into infarcted and healthy tissue regions. In appendix K, several other examples of watershed segmentation are presented.

To focus on the heart tissue we use Otsu automated segmentation, based on the direct greyscale conversion of the input image (Figure 3.8 C). This eliminates watershed regions that are not within the tissue regions. Finally, by comparing the RGB color values in each region we decide if each segmented region corresponds to normal or infarcted tissue (Figure 3.8 D). This is done through the comparison of the R and B average image color values for each region, if R grater than B the region corresponds to healthy tissue and it corresponds to infarcted tissue otherwise.

3.3.3 K-means Segmentation

K-means segmentation is a clustering approach to segmentation [15, 18]. Image segmentation using clustering is based on the grouping of pixels with similar properties. Similar properties may be any property the data pixel possesses, like intensity, gradient or color (for a color dataset) among others.

K-means assigns N data points to k disjoint subsets, S_j, j = 1,2,...,k, each containing N_j data points, by minimizing the sum-of-squares criterion given by

$$J = \sum_{j=1}^{k} \sum_{n \in S_j} \sqrt{|x_n - \mu_j|^2}, \tag{3.9}$$

where x_n is the value of n^{th} data point and μ_j is the mean value of the data points within the

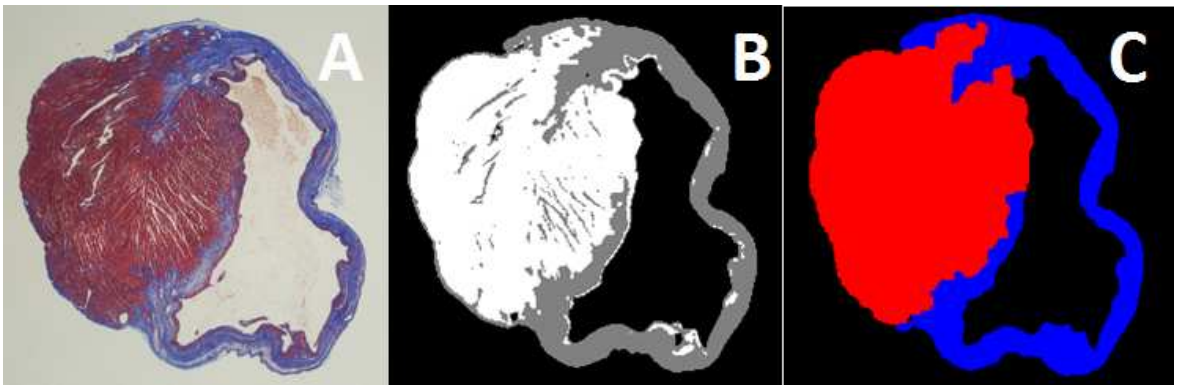

Figure 3.9 Segmentation of a cross section of the heart using k-means clustering algorithm: A - original image, B - k-means segmentation result and C - identification of each tissue type (red - normal tissue and blue - infarcted tissue).

cluster Sj.

K-means applied to image segmentation assigns each pixel from an image to specific clusters according to their color or intensity properties and a measure of similarity [15]. By maximizing similarity of each subset locally, the algorithm will globally yield an optimal dissimilarity of all subsets. The dissimilarity for a pixel is its distance from the mean of each of the clusters in the feature space. The mean for each cluster is computed iteratively. The pixel is added to the cluster whose mean is the nearest to the pixel (maximum similarity between the pixel property and the cluster's mean) [18].

In the case of heart tissue segmentation we first select the region of heart tissue through Otsu thresholding. Considering only those pixels from the heart tissue region we choose $k = 2$ and use the RGB color information to obtain the two tissue pixel clusters corresponding to healthy and infarcted tissue (see Figure 3.9 B). These are then identified based on each cluster's average color. If the average color of that region in the R channel is greater than the average color of the same region in the B channel, the region corresponds to healthy tissue otherwise it corresponds to infarcted tissue. In appendix L, several other examples of k-means clustering segmentation are presented.

While k-means segmentations has the considerable advantage of allowing for the setting of the number of different tissues of interest, it has the disadvantage that by taking no spacial information into account it can produce multiple irregular regions. To tackle this problem we use morphological operations to join small regions and smooth the contours, and select only the largest region of each tissue type (Figure 3.9 C).

3.3.4 Mean-shift Segmentation

Mean-shift image segmentation is also a clustering approach, but in this case the clustering is performed jointly in the pixel spatial and color spaces [32, 25, 6]. This technique searches for

the local maximal density using a estimation kernel. After maxima density locations are found data points are grouped based on which maximal density point they converged to [16].

Mean-shift does not require prior knowledge of the number of clusters, and does not constrain the shape of the clusters. It only requires the definition of the radius of the kernel used for the density estimation. Given n data points of x on d-dimensional space, the multivariate kernel density estimate obtained with kernel $K(x)$ and windows radius h is [16, 32, 25, 6]:

$$f(x) = \frac{1}{nh^d} \sum_{i=1}^{n} K\left(\frac{x - x_i}{h}\right), \tag{3.10}$$

For radially symmetric kernel, it suffices to define the profile of the kernel $K(x)$ satisfying:

$$K(x) = c_{k,d} K(\|x\|^2), \tag{3.11}$$

where $c_{k,d}$ is a normalization constant which assures $K(x)$ integrates to 1. The modes of the density function are located at the zeros of the gradient density estimator [32, 6]:

$$\nabla f(x) = \frac{2c_k}{nh^d} \sum_{i=1}^{n} (x - x_i) K\left(\left\|\frac{x - x_i}{h}\right\|\right), \tag{3.12}$$

The mean-shift clustering works in three steps:

1. From initial data points, run mean shift to find the estimated maxima of the density function.

2. Prune the obtained density points by retaining only the local maxima.

3. Set of all initial data points that converge to the same density maxima (mode) to correspond to the same cluster.

The quality of a kernel density estimator is measured by the mean of the square error between the density and its estimate, integrated over the domain of definition [25, 6].

A digital image can be represented as a two-dimensional array of p-dimensional vectors (pixels), where $p = 1$ in the gray level case and $p = 3$ for color images. The space of the pixel coordinates is the *spatial* domain, while the pixel gray level or color information is the *range* domain [25, 16].

In order for mean-shift segmentation to take into account both spatial and range information, location and range feature vectors are concatenated in a joint spatial-range domain. The different nature of each domain requires some compensation by proper normalization. Thus, the multi-variate kernel is defined as the product of two radially symmetric kernels and the Euclidean metric allows a single bandwidth for each domain, that is:

$$K_{h_s,h_r}(x) = \frac{c}{h_s^2 h_r^2} K(\|\frac{x^s}{h_s}\|^2) K(\|\frac{x^r}{h_r}\|^2), \tag{3.13}$$

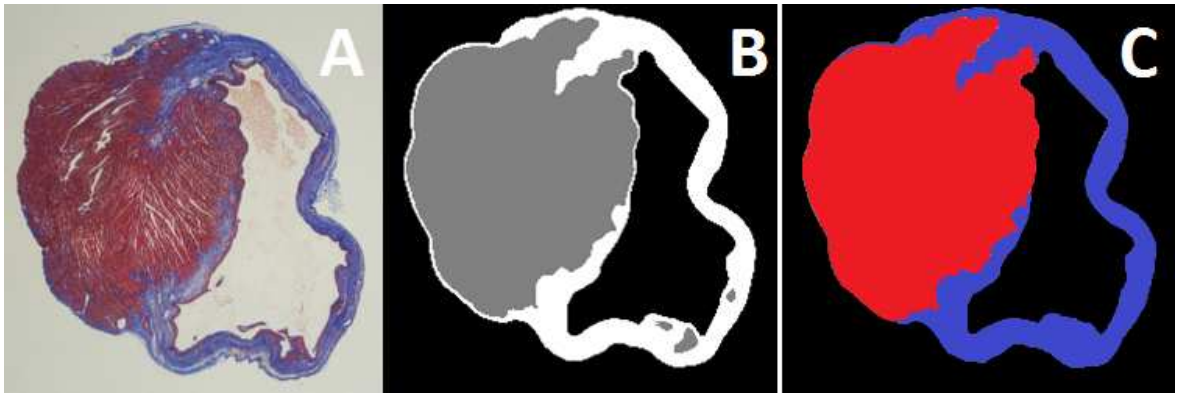

Figure 3.10 Segmentation of a cross section of the heart using mean shift clustering technique. A - original image of a mouse heart cross section. B - respective mean-shift clustering. C - identification of each tissue type (red region identifies normal tissue and blue region identifies infarcted tissue)

were x^s is the spatial part, x^r is the range part of a feature vector, $K(x)$ the common profile used in both domains, h_s and h_r the employed kernel bandwidths, and c the corresponding normalization constant. Each data point becomes associated to a point of convergence which represents the local mode of the density in the d-dimensional space. The process, having the parameters h_s and h_r, takes into account spatial and range information jointly. For the segmentation task, the convergence points sufficiently close in the joint domain are fused to obtain the homogenous regions in the image [25, 6].

We can observe the application of this technique to our task of segmenting heart tissue regions in figure 3.10. As in the k-means technique we decided to obtain at most three clusters. If we obtain more than three clusters we iteratively increase the radius of the kernel used and repeat the process. In this case we based our segmentation on the Red and Blue channels since they lead to better results than the use of all channels or anyone of the color image combination referred on section 3.1.3. As in the case of K-means based segmentation we identify which final regions belong to infarcted or normal tissue through the analysis of the red and blue channel. If the average intensity of the region under analysis in the red channel is greater than the sane region in the blue channel the region is considered healthy region otherwise is an infarcted region. The final result showed regions less dispersed when compared with the k-means result. It is a consequence of the spatial information that is taken into account. For example, by examining the segmented regions obtained with k-means and mean-shift techniques, in figures 3.9 and 3.10, we identify small regions inside the region related to normal tissue in case of using the k-means technique. In case of mean-shift the segmentation result explores spatial information and the final regions are more homogeneous. In appendix M, several other examples of segmentation by mean-shift technique are presented.

While all presented unsupervised segmentation methods do not require user interaction, some pos-processing is required to obtain the final identification of the normal and infarcted

tissues in most cases, such as:

1. identify each tissue type by comparing color intensities;
2. reduce oversegmentation;
3. adjuste the segmentation result using morphological operations;
4. redefine parameters of the segmentation techniques (if necessary) and repeat the segmentation.

Furthermore, since the user has no interaction with the segmentation process, results can be unusable and reduce user confidence in the automatic analysis approach.

Another issue is that for evaluation of infarct size researchers only consider the left ventricle region. The images of the cross sections of the heart show both right and left ventricle. The right ventricle is a part of healthy tissue that is not distinguishable from the left ventricle and can only be detected based on anatomical information. In our experimental setup the right ventricle is ignored by manually delineating the left ventricle. However, this is itself a time consuming task that should be automated.

Considering these problems we propose in the next section an unsupervised tissue segmentation approach through anatomical model adaptation.

3.4 Unsupervised tissue segmentation through model adaptation

While supervised and unsupervised methods for heart tissue segmentation provide high performance solutions for infarct size estimation, they ignore the structure of the heart. This structure may be assumed to be stable to a certain extent and we propose to explore this assumption towards an increase in the robustness of the automated analysis. Furthermore, by recognizing the heart structure we can recognize the left ventricle region and avoid the user manual task of ventricle region delineation.

In order to perform heart tissue segmentation by using an anatomical model we must define a model and a way to adapt such a model to existing image data. As we observe in images from the heart sections, the heart tissue has an oval shape with two holes inside its overall region (lumens). Based on this standard structure the design of the anatomical model chosen for this task was based on an overall ellipsoid heart shape with two smaller ellipsoids inside the heart. The model governs the size and position of each ellipsoid as well as the spatial relationships between them (Figure 3.11). The spatial relationships are simple: all lumen ellipsoids must be inside the overall heart ellipsoid, and left and right lumen ellipsoids must be on separate side of the minor axis of the overall ellipsoid.

Considering as hidden variable the real location and scale of the heart tissue regions Z and the input image data as X we can assume a model for our anatomical model parameterized by

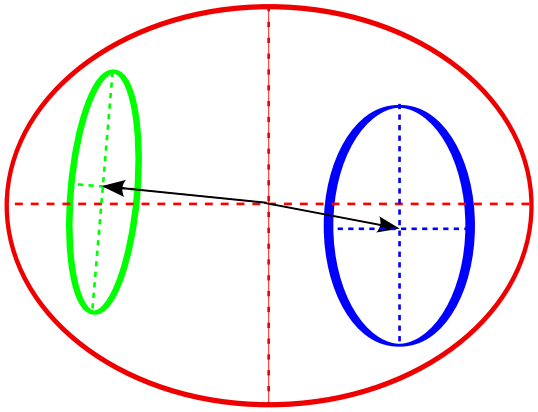

Figure 3.11 Anatomical model assumed for the heart tissue: red ellipse represents the full tissue; blue ellipse represents the left ventricle lumen; green ellipse represents the right ventricle lumen.

θ for which the likelihood functional is:

$$L(\theta;X,Z) = P(X,Z|\theta). \tag{3.14}$$

Given that we have three different regions to adapt the model parameters θ can be divided into those responsible for the modeling of each part:

$$\theta = \{\theta_{ht}, \theta_{rl}, \theta_{ll}\}, \tag{3.15}$$

where θ_{ht} are the parameters for the heart tissue ellipsoid and θ_{rl} and θ_{ll} are the parameters for the right and left lumen ellipsoids respectively.

As the parameters govern the position and shape properties of ellipsoids we have that:

$$\theta_{ht} = \{c_{ht}, e_{ht}, \sigma_{ht}, o_{ht}\}, \tag{3.16}$$

where c_{ht}, e_{ht}, σ_{ht} and o_{ht} are the centroid position, eccentricity, scale and orientation of the ellipsoid of the total heart tissue respectively. Similar parametrization is performed for the lumen ellipsoids' parameters ($\theta_{rl}\theta_{ll}$).

In a similar way the heart regions hidden variable can be specified for each different parts of the model:

$$P(X,Z|\theta) \quad = \quad P(X,Z_{ht},Z_{ll},Z_{rl}|\theta) \tag{3.17}$$

where Z_{ht}, Z_{ll} and Z_{rl} correspond to the real heart tissue, left lumen and right lumen regions, respectively.

By using Bayes rule and exploring inherent conditional independence between the different regions and parameters we can factorized equation (3.17) as:

$$P(X,Z_{ht},Z_{ll},Z_{rl}|\theta) \quad = \quad P(X,Z_{rl}|\theta)P(X,Z_{ll}|\theta)P(X,Z_{ht}|\theta) \tag{3.18}$$

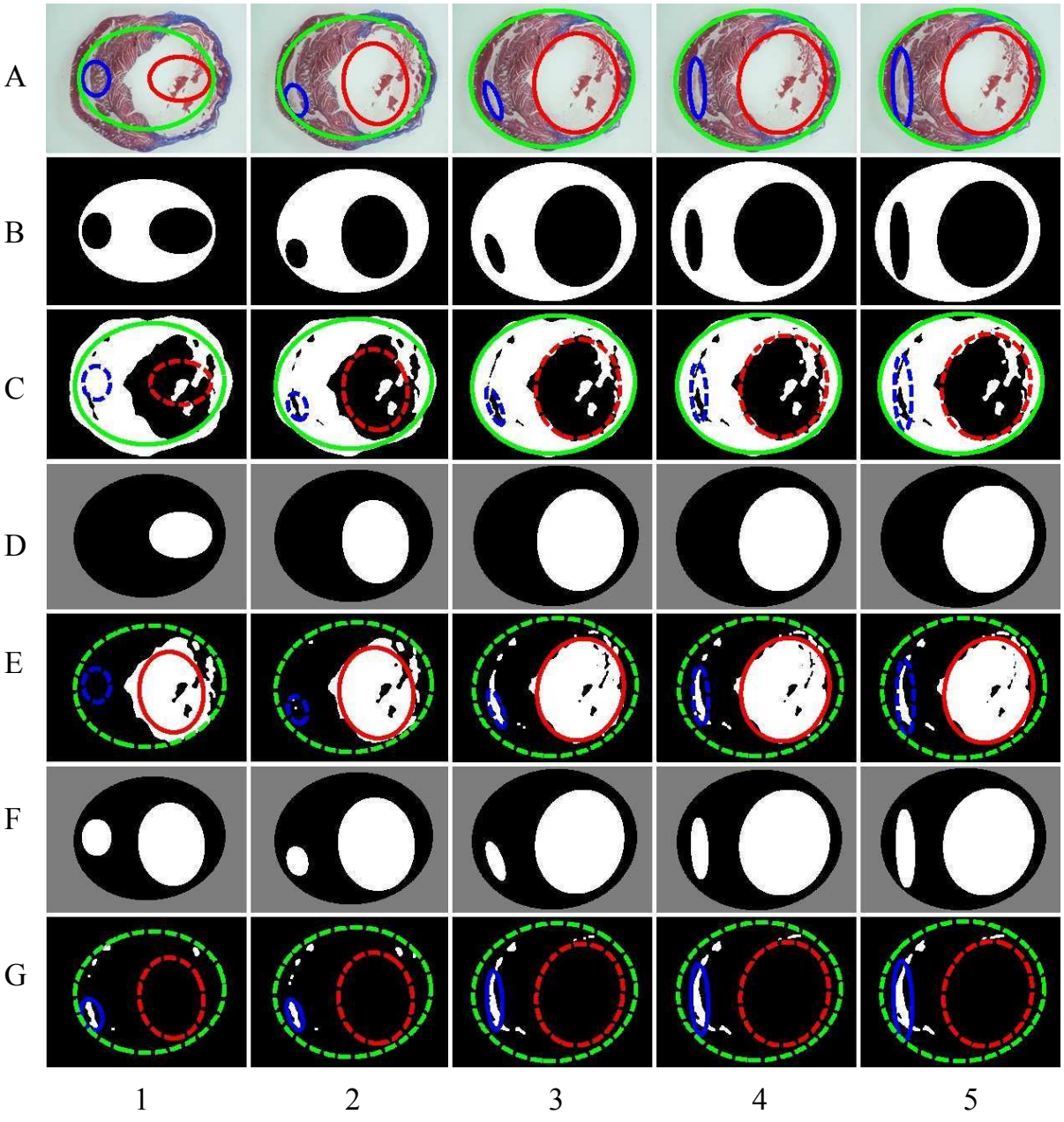

Figure 3.12 Five iterations of the adaptation of the anatomical model: A) current stage of the anatomical model's adaptation to the heart; B) mask obtained from the model parameters used to obtain compute $P(X, Z_{ht}|\theta)$; C) the model's shape after the adaptation of θ_{ht}; D) mask obtained from the new model parameters used to obtain compute $P(X, Z_{ll}|\theta)$; E) the model's shape after the adaptation of θ_{ll}; F) mask obtained from the new model parameters used to obtain compute $P(X, Z_{rl}|\theta)$; G) the model's shape after the adaptation of θ_{rl}. All the masks have the region of interest represented as white and the background represented as black. The gray color represents a region not used in the specific adaptation step.

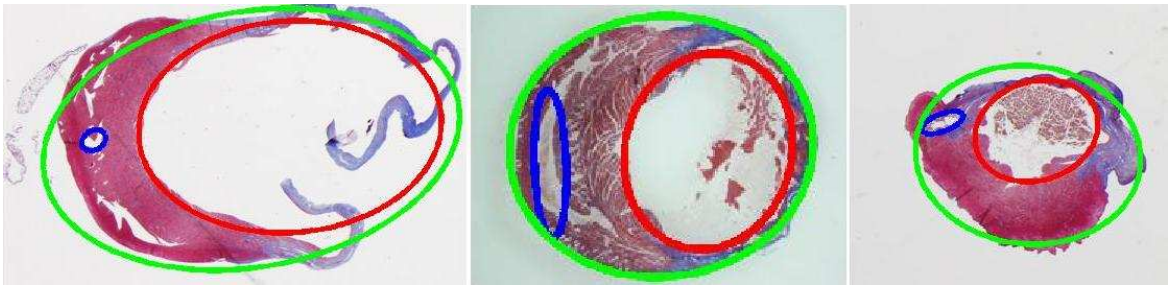

Figure 3.13 Model adaptation results in irregular heart cross sections: heart with torn left ventricle wall (left); heart with blood in the left ventricle (middle and right).

where we assume that each tissue regions' probability distribution is independent of all other given the parameters of the model. This provides an adequate framework where we can sequentially estimate the heart, left ventricle and right ventricle tissue regions and the corresponding parameters through the Expectation Maximization (EM) algorithm [9, 4].

The model adaptation process using EM is initiated with the placement of the anatomical model in the middle of the image with a scale adequate to the image dimensions. Given the initial model parameters the adaptation of the anatomical model is performed iteratively, starting with the overall heart tissue ellipsoid them the left and right ventricles' lumens.

In Figure 3.12 we can observe the sequential steps of the anatomical model's adaptation. At each step, from the current parameters (figure 3.12 A) C) E)), a mask of the current model position is built (figure 3.12 B) D) F)). From the image information inside the regions of the current mask in white and also the background regions in black we analyze image green channel and obtain an estimate of the true region under adaptation (figure 3.12 C) E) F)). This estimated region, together with the current parameter estimated values, then allows the maximization of the related parameters (solid lines in figure 3.12 C) E) G)). It is at this point that the restriction on each ellipsoid size and position are enforced by limiting the estimated parameters to only possible values (position and size limitations). The process is continued until no alteration of parameter is performed or a limit number of iterations has been reached. An additional test must be performed to verify that a right ventricle lumen is present as this is not always the case in this type of images.

The robustness of this method allows for usable results even when the heart cross section show a highly deformed anatomical structure, when there is blood in the ventricle and even when the heart tissue is torn, situations that would make all previously presented methods fail, see figure 3.13.

To measure the infarct size we use the final adapted anatomical model spatial configuration. First we estimate the region of the left ventricle, where the infarct size evaluation is performed. This is performed by obtaining the distance from the center of the left ventricle lumen to the center of the right ventricle lumen estimated by the anatomical model). The circular limit defined by that distance and the center of the left ventricle is where we assume the left ventricle

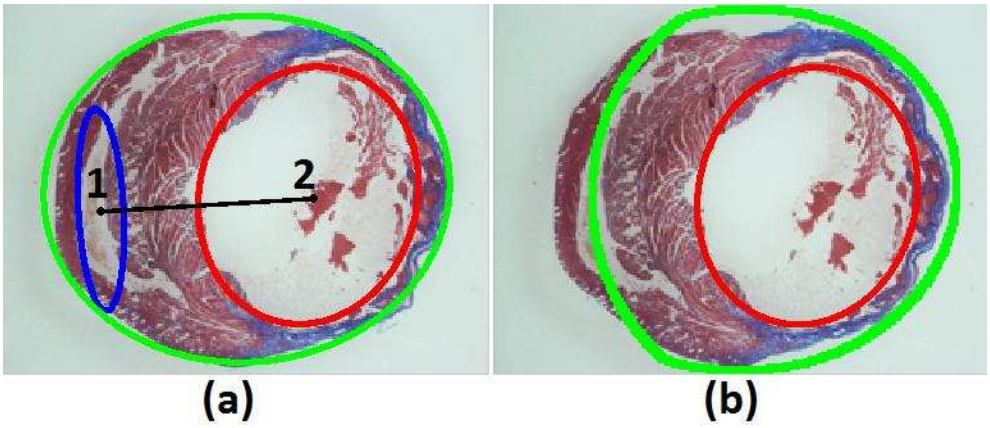

Figure 3.14 Left ventricle tissue region estimation: (a) distance from the center of the right ventricle lumen (1) to the center of the left ventricle lumen (2); (b) anatomical regions of the left ventricle (region perimeter in green and lumen in red).

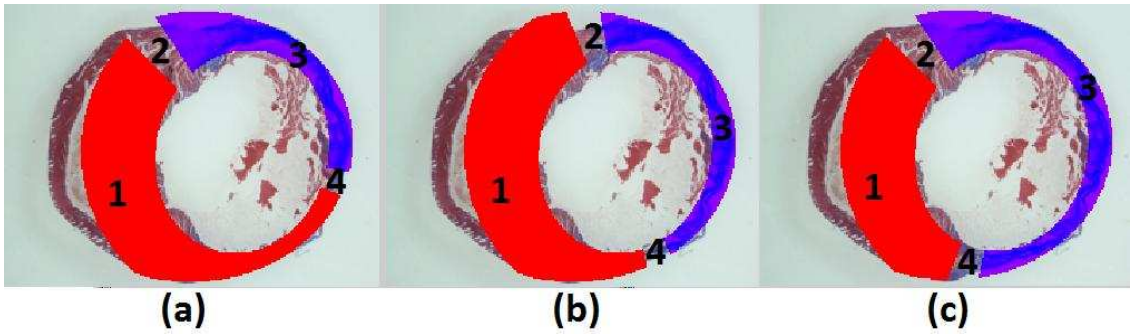

Figure 3.15 Infarct and healthy tissue region estimation process: (2) and (4) are limiting radial separators in the model. The red region identifies normal tissue and blue region identifies infarcted tissue; (a) first iteration; (b) fifth iteration; (c) final position of each section, identifying the infarcted and healthy tissue regions.

tissue ends. Figure 3.14 shows the radial distance between lumen centers and the final left ventricle tissue region estimated.

Finally, to measure the infarct size it is necessary to define the regions of normal and infarct tissue within the left ventricle. This is performed by dividing the left ventricle into two regions using two radial separations. We then iteratively improve the initial position for each section by analyzing the average intensity of the green image channel within each region (Figure 3.15). We move the separators so that the difference between the average green image channel level intensity value within each of the two regions is increased. The change of the separators position is performed iteratively in 5 degree steps. The process stops when no further improvements are possible.

Figure 3.16 shows the final result of this process and the two determined regions of the left

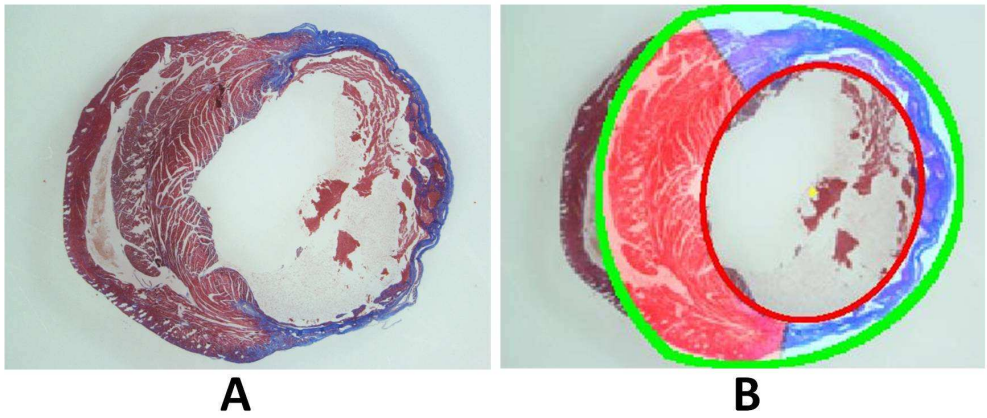

Figure 3.16 Final healthy and infarcted heart regions estimated within the left ventricle.

ventricle. In appendix N, several other examples of anatomical model adaptation are presented. From the information of the regions of infarcted and healthy heart tissue we are able to estimate the infarct size.

3.5 Experimental results

To evaluate the performance of the proposed methods we performed the infarct size evaluation on sections of two complete hearts. All the images were provided by INEB - Instituto Nacional de Engenharia Biomédica by the NEWTherapies Group.

Myocardial infarction is evaluated in the left ventricle region of each heart cross-section [8, 29]. The infarcted tissue to be considered can been seen in figure 3.17 (A) as a shaded region. However, it is not easy to determine the left ventricle region as it is variable in morphology and even most biologists vary in their assessment of where the right ventricle (RV) ends and the left ventricle (LV) begins. As such, we obtain automatic infarct size estimation results on the LV by delineating the RV through manual using image editing tools and not considering this during the evaluation. In the case of the tissue segmentation through model adaptation that task is performed automatically.

3.5.1 Infarct size evaluation

Heart infarct size is the percentage of the left ventricle affected by myocardium infarction. To measure and estimate the infarct extension it is necessary to identify the normal and infarcted tissue.

To better define the calculation of the infarct size we must define the heart anatomy regions involved. In Figure 3.17 (A) we can observe the heart bounded by the exterior black continuous

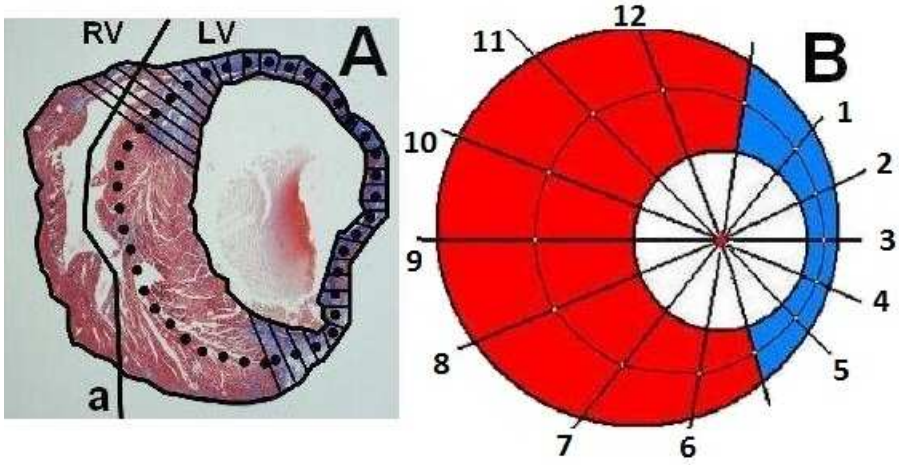

Figure 3.17 Image of a heart cross section. A - The heart is bounded by the outside black continuous line which includes the LV and RV separated by line **a**. The interior black continuous line is identifying the lumen of the left ventricle and the region marked by lines shows the tissue with infarct. The dotted line is the midline between the inside and outside black continuous lines. B - Scheme of a cross section of the heart.

line. It is formed by right (RV) and left ventricles (LV). The RV consists of normal heart tissue and the right ventricle lumen. The LV includes the infarcted tissue, which is represented by the shaded region, the lumen, clear region which is bounded by the interior black continuous line and also normal tissue. The infarct size is calculated by two different methods:

- **Area measurement** - The infarct size is calculated by dividing the LV infarct area by the total area of the LV tissue [8, 29]. This is trivial based on the obtained regions from the automatic segmentation results.

- **Midline length measurement** - The infarct size is calculated by dividing the LV infarct region midline by the length of LV midline [29]. Figure 3.17 (B) shows a scheme that represents a cross-section of a heart. To perform the midline measurement we first automatically find the midline by tracing lines from the center of the lumen to the exterior of the heart tissue. The midline is given by midpoint between tissue borders. The points of the middle line where there is more infarcted tissue than normal tissue (in the radial direction) are considered as infarcted points. Infarct size is obtained bydividing the length of the LV infarct midline by the total length of the LV midline.

The infarct size measurement for the complete heart is defined as the mean value of infarct size for all the heart cross sections.

Table 3.1 Results of infarct size measurement in mice assays. The results are the average value of infarct size obtained for all transverse sections of each heart.

Heart #1			
Measurement	Midline length (%)	Area (%)	Time (min)
Manual	43%	22%	31
Region growing	**40**%	**22**%	2,26
Thresholding	39%	20%	1,51
Watershed	40%	20%	6,15
K-means	40%	23%	1,95
Mean-shift	36%	17%	6,96
Model based	44%	27%	20,68

Heart #2			
Measurement	Midline length (%)	Area (%)	Time (min)
Manual	52%	36%	25
Region growing	47%	35%	2,24
Thresholding	47%	30%	1,52
Watershed	49%	35%	5,99
K-means	**50**%	**36**%	2,25
Mean-shift	49%	36%	6,95
Model based	44%	31%	18,34

3.5.2 Validation and discussion

The infarct size was calculated manually and automatically in images from two hearts. The calculation was performed on the cross-section tissue without considering the right heart ventricle. To automatically segment the tissue without taking into account the right ventricle we first manually identify this region and it is not considered during the evaluation. For automatic tissue segmentation through model adaptation this task is not necessary since it correctly identifies the right and the left ventricle. Table 3.1 shows the results for the infarct size evaluation using our approaches and manual annotation. The results are the average value of the infarct size over all cross-sections of each independent heart. The time spent in the evaluation using the different approaches is also presented.

The difference between the proposed approaches and manual annotation are never greater than 8%. Within the unsupervised segmentation approaches, the k-means technique produced better results and the differences were never above 3% when compared with manual results. The differences from the supervised technique used were at most 5% but considering the heart #1 this technique produced better results in both midline length and area measurements. Tissue segmentation through anatomical model adaptation by EM produced results with differences never more than 8%. This may be both due to an oversimplified model and also due to errors

in determining the left ventricle region (for which all other methods have manual selection). However, this approach is completely automatic and that represents a considerable advantage in term of analysis work by the researcher. Regarding the times each technique takes to evaluate the infarct size, all the tested approaches are faster than manual annotation.

The results for each section of the Heart #1 using the different segmentation techniques are presented from table 3.2 to table 3.3. The results for each section of the Heart #2 are presented from table 3.4 to table 3.5.

Table 3.2 Results of infarct size measurement in Heart #1 using different approaches. The method for estimate the infarct size is the midline measurement.

Heart #1 - Midline measurement							
Section	Manual	Region Growing	Thresholding	Watershed	K-means	Mean-shift	Model-Based
2	87,42%	84,44%	80,40%	82,85%	68,73%	81,57%	100%
3	68,40%	67,01%	65,52%	65,24%	65,24%	63,07%	62,85%
4	60,70%	53,32%	59,45%	57,07%	63,20%	39,05%	52,53%
5	52,16%	49,63%	53,32%	48,13%	54,41%	46,04%	59,40%
6	50,94%	48,91%	45,16%	45,05%	46,78%	43,93%	41,11%
7	48,04%	46,93%	43,54%	42,89%	44,54%	41,07%	48,17%
8	39,07%	35,35%	34,70%	35,27%	38,33%	33,85%	37,25%
9	33,30%	28,90%	28,66%	25,35%	30,95%	25,08%	28,84%
10	20,26%	14,67%	10,29%	12,26%	12,26%	8,97%	18,96%
11	17,03%	14,19%	13,41%	28,46%	14,30%	11,99%	30,84%
12	0%	0%	0%	0%	0%	0%	0%
Average	43,39%	40,30%	39,50%	40,23%	39,88%	35,87%	43,63%

Table 3.3 Results of infarct size measurement in Heart #1 using different approaches. The method for estimate the infarct size is the area measurement.

Heart #1 - Area measurement							
Section	Manual	Region Growing	Thresholding	Watershed	K-means	Mean-shift	Model-Based
2	51,83%	58,44%	54,24%	58,14%	48,24%	54,79%	100%
3	34,83%	30,24%	33,86%	32,61%	35,95%	28,87%	35,59%
4	29,47%	23,31%	24,77%	24,59%	29,78%	13,85%	26,14%
5	22,44%	17,89%	18,96%	18,99%	25,32%	16,53%	28,39%
6	23,12%	22,71%	17,48%	17,52%	20,68%	17,20%	19,25%
7	17,58%	22,38%	16,62%	15,96%	23,35%	14,39%	27,57%
8	17,59%	16,82%	14,84%	15,94%	18,34%	14,28%	20,22%
9	19,56%	21,70%	15,14%	14,41%	18,46%	13,76%	14,59%
10	14,41%	15,71%	12,06%	11,38%	15,27%	6,83%	10,30%
11	11,01%	11,71%	8,26%	8,86%	10,20%	7,50%	19,10%
12	3,44%	4,95%	3,63%	3,48%	3,09%	0%	0%
Average	22,30%	22,35%	19,99%	20,17%	22,61%	17,09%	27,38%

Table 3.4 Results of infarct size measurement in Heart #2 using different approaches. The method for estimate the infarct size is the midline measurement.

Heart #2 - Midline measurement							
Section	Manual	Region Growing	Thresholding	Watershed	K-means	Mean-shift	Model-Based
1	94,36%	89,54%	79,11%	87,94%	79,35%	91,29%	100%
2	86,10%	78,60%	75,78%	83,30%	79,94%	83,26%	49,92%
3	82,82%	73,47%	71,24%	74,72%	70,61%	79,06%	66,94%
4	78,38%	58,53%	68,00%	64,80%	72,14%	70,85%	37,98%
5	54,60%	46,72%	43,91%	45,40%	44,62%	43,66%	36,76%
6	43,45%	39,32%	38,43%	35,58%	48,64%	37,47%	33,40%
7	37,97%	36,42%	31,62%	36,61%	45,44%	32,23%	37,19%
8	34,27%	34,22%	30,93%	34,62%	43,22%	33,04%	40,25%
9	28,95%	28,07%	27,39%	28,90%	27,42%	25,02%	33,30%
10	15,98%	19,30%	18,62%	18,51%	17,44%	17,59%	24,02%
11	17,51%	10,79%	26,70%	30,71%	26,10%	25,90%	29,20%
Average	52,22%	46,82%	46,52%	49,19%	50,45%	49,03%	44,45%

Table 3.5 Results of infarct size measurement in Heart #2 using different approaches. The method for estimate the infarct size is the area measurement.

Heart #2 - Area measurement							
Section	Manual	Region Growing	Thresholding	Watershed	K-means	Mean-shift	Model-Based
1	81,52%	81,14%	51,75%	78,82%	61,08%	87,01%	100%
2	49,52%	49,97%	51,79%	61,89%	58,12%	70,09%	32,82%
3	56,63%	43,94%	43,73%	50,71%	43,07%	53,29%	36,09%
4	53,98%	47,34%	33,63%	35,23%	41,21%	45,59%	17,33%
5	21,68%	20,18%	18,75%	20,13%	21,21%	18,82%	16,47%
6	16,76%	16,86%	14,78%	13,91%	33,02%	16,24%	14,54%
7	19,89%	19,31%	15,98%	16,71%	30,36%	15,43%	19,11%
8	24,76%	27,26%	21,76%	23,00%	32,24%	19,99%	28,63%
9	28,06%	29,96%	27,17%	26,89%	25,97%	24,10%	27,02%
10	24,20%	27,08%	20,33%	26,29%	24,28%	15,46%	22,76%
11	22,19%	24,67%	26,88%	26,67%	26,15%	25,60%	25,80%
Average	36,29%	35,25%	29,69%	34,57%	36,07%	35,60%	30,96%

4. MIQuant

Based on the validated approach we developed a software for infarct size evaluation named MIQuant. The software was developed for use in the laboratory to aid in the analysis of biological experimental results. Due to the preference by biologists of some interaction in the analysis process we chose a supervised approach, based on region growing segmentation. The speed and easy interaction of this method associated with the agreement between the results obtained by this method and the manual results were the basis for this choice. The graphical user interface of the developed software application is showed in figure 4.1.

The developed software, based on requirements specified by biologists, allows the user to:

- Perform analysis of one or more heart cross sections;
- Edit images allowing operations such as tissue deliniation;
- Segment different heart tissue regions with the ability to change the obtained segmentations;
- Compute the infarct size value;
- Manually edit the left ventricle midline from the infarct estimation by midline length measurement;
- Save results as excel worksheet and images with segmented regions.

The MIQuant was developed to allow the quantification of infarct size, expressed as percentage, by two previously validated methods: area and midline length measurements. The user must follow several steps prior to myocardium infarction size calculation. To guide the user, a footnote bar is display with basic instruction on the next steps and available options (figure 4.1 A).

In Figure 4.1 B is visible the menu bar of the software. The "File" menu includes commands to load the image or multiple images. The user may either analyze a single image or multiple images. If multiple images are loaded MIQuant computes the average myocardium infarction size of all sections and the intermediate results obtained for each section. After loading the image, the software automatically adjusts image quality (as explained in section 3.1.1), this pre-processing step can be removed on the “Image quality" section. The “Edit" menu displays commands for original image edition. The commands available are:

- Remove tissue: ignores undesired tissue regions by hand delineation of those tissues on the original image separating the tissue to be ignored. The user must click to define a line path and double-click/ENTER at last to complete the line drawing (figure 4.2).

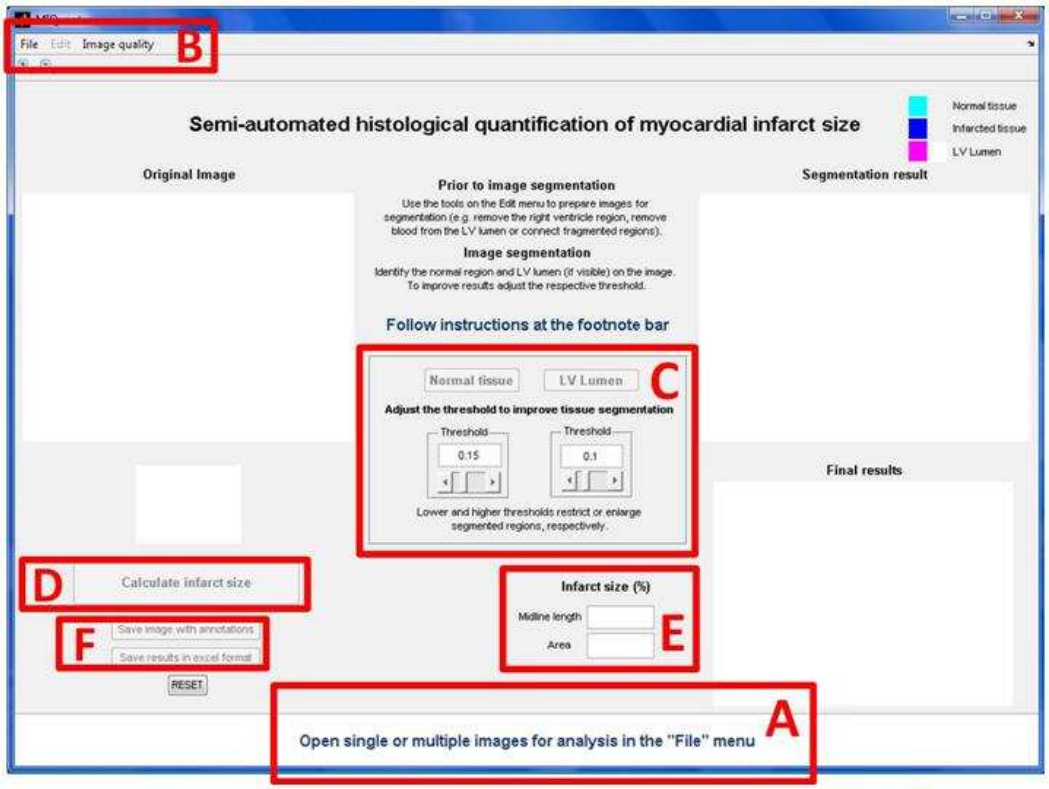

Figure 4.1 MIQuant user interface with labeled interface details: A is the footnote bar where hints are displayed on how to work with MIQuant; B is the menu bar where are located the "File", "Edit" and "Image Quality" menus. This allows to load images, edit the input image and chose to improve image quality or not; C are the interface controls that correspond to the parameters of the segmentation process. Here it is possible to control the segmentation by adjust the threshold values used in the process; D is the button that initialize the calculation of infarct size; E is where the results are displayed and F are the buttons that allow to save the results in excel format or in image format.

- Connect tissue regions: creates a connection between tissue regions that were previously disjoint. The user need to click on the image sequentially on the two regions to be connected. A path with mean intensity from the begin and end points selected is created connecting the regions (figure 4.3).

- Clean left ventricle lumen: erases selected regions that can interfere with tissue segmentation, it can be used to remove blood from the left ventricle lumen. The user must define the region to be removed by clicking to define the path and double-click/ENTER at last to complete the drawing (figure 4.4). The defined region is replaced with background intensity values.

- Undo: erases all the performed image editions.

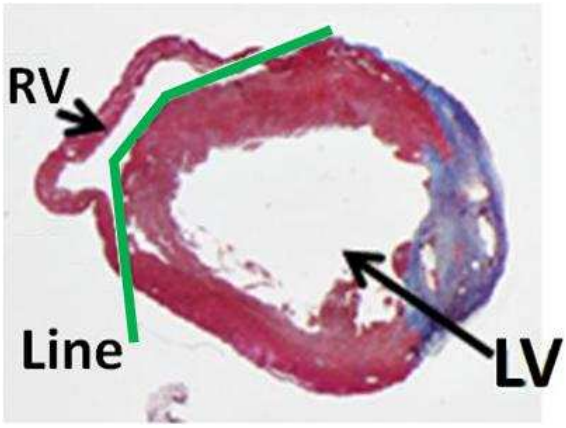

Figure 4.2 Demonstration of the command “Remove tissue" available in “Edit" menu of the MIQuant software by creating a separation line.

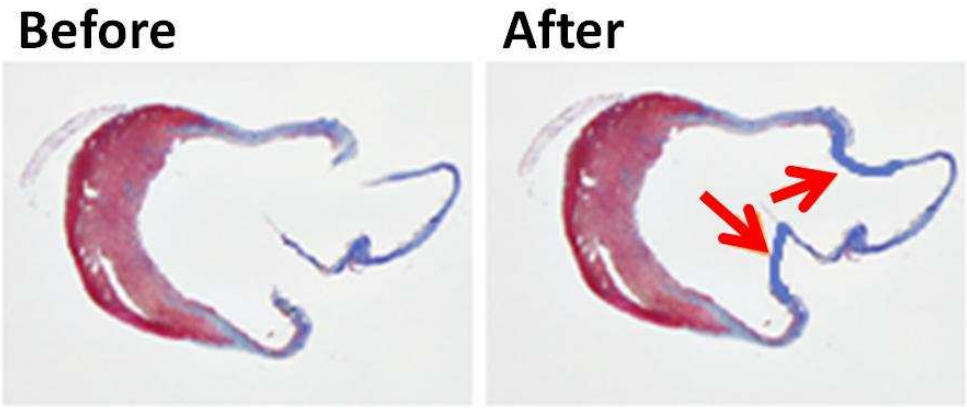

Figure 4.3 Demonstration of the command “Connect tissue regions" available in “Edit" menu of the MIQuant software by introduce a line with the mean intensity of the begin and end points defined.

In Figure 4.1 the interface controls indicated by "C" correspond to the region growing parameters. The user must select one of the “Normal tissue" or the “LV Lumen" buttons to identify the region to be selected. For each type of tissue it is possible to adjust the threshold if required and repeat segmentation. The segmentation can be repeated until the user is satisfied with the segmentation results.

After performing the tissue segmentation it is possible to obtain the infarct size results by clicking on the respective buttons (figure 4.1 D). The myocardial infarction size, calculated by both midline length and area measurements are shown in the MIQuant interface (figure 4.1 E). Results are also printed on the image under analysis.

Figure (figure 4.5) shows an example of how the software works. When the final results are displayed there is also the option to edit the midline result. The user may adjust the midline

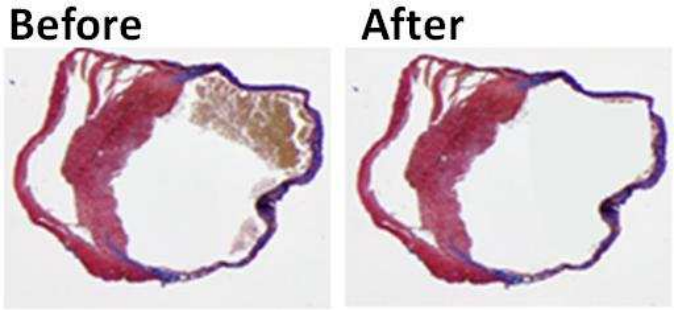

Figure 4.4 Demonstration of the command“Clean left ventricle lumen" available in “Edit" menu of the MIQuant software by selecting a region and change the intensity information in that region by the intensity of the background.

when wrongly predicted using the “Edit midline" tool and repeat the myocardial infarction size calculation. The midline can be edited by clicking first in the midline dot to be corrected and then on the desired final position for the respective dot (figure 4.6).

After obtaining the final results and visually inspecting that they are in accordance with the users criteria, it is possible to save the visual result and save the data result to an excel file (figure 4.1 F). The visual result also contains in part of the image the values of the infarct levels obtained for that image.

The developed tool is currently being used in several laboratories for the infarct size estimation. For evaluate the performance of the software a study was conducted [20]. It reports that MIQuant is a reliable alternative to the manual estimation of infarct size and the time spent to obtain the infarct size is a fraction of the time spent in the manual evaluation. The paper concludes that MIQuant is a valid and easy-to-use software application and the software contributes for the standardization of infarct size quantification across studies and, therefore, to the systematization of the evaluation of cardiac regenerative potential of newly developed therapies.

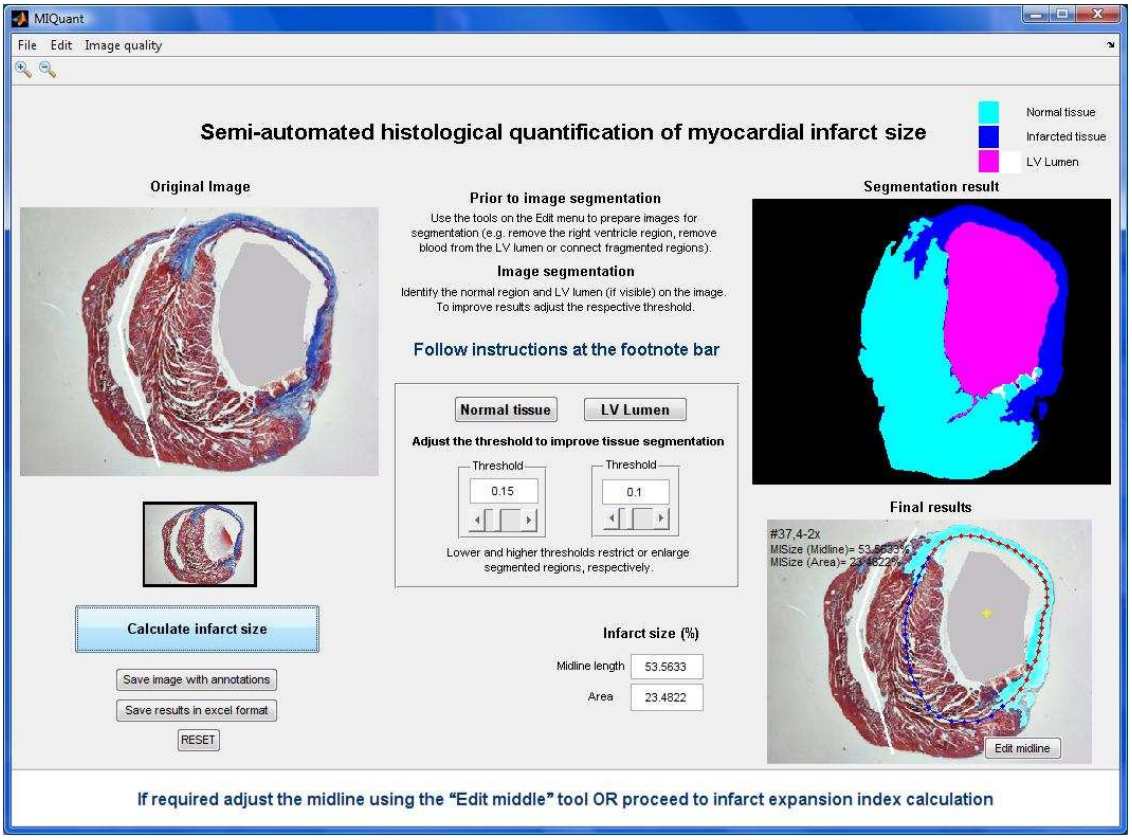

Figure 4.5 Infarct size evaluation using the tool. The segmentation are displayed for the user decide if it is necessary to repeat the segmentation process or if it is well segmented. The final results are also displayed and the option to edit the midline result becomes available.

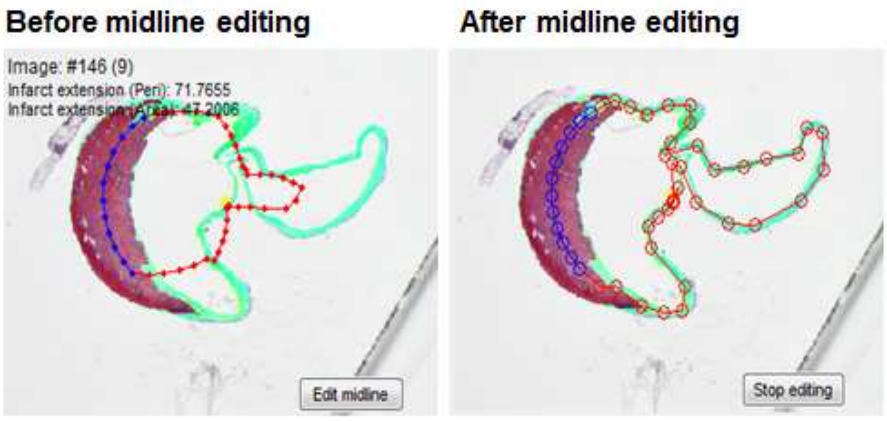

Figure 4.6 Adjust of the midline result. The user must select one dot and then select the new position to change his position.

5 . Conclusions

In this work we propose an automated heart infarct size estimation tool, for animal assays. During this work several image segmentation approaches where tested, comparing each with manual annotation. The segmentation of the heart tissue was performed by supervised and unsupervised techniques and also through anatomical model adaptation by expectation maximization. Given the segmentation results, the infarct size was automatically estimated. The results of infarct size obtained using different segmentation techniques were in close agreement with the manual annotation with differences never higher than 8%. By using the developed methodology it was possible to obtain an analysis of the infarct size within a fraction of the manual method measure time.

Within the automatic segmentation approaches, the watershed technique produced better results, with the differences never above 3%. The differences from the supervised approach used were at most 5%. Tissue segmentation through anatomical model adaptation produced results with differences never more than 8%. The use of anatomical modeling did not provide the best performing results but it does provide a fully automatic approach for the analysis of heart tissue, requiring no human intervention during analysis. Furthermore, it enables the possibility to handle images where there are tissue discontinuities and badly defined lumens and enables the detection of the right and left ventricle regions.

Although the performance was lower in the supervised approach, not considering the segmentation by anatomical model adaptation, the biologists prefer the possibility to control the segmentation results in relation to fully unsupervised approaches where they do not control the segmentation process.

Based on this preference we developed a tool for infarct size evaluation named MIQuant. This tool is operated by biomedical investigators and is based on region growing segmentation technique. The developed tool is currently under evaluation at the INEB-Institute of Biomedical Engineering, by the Stem Cell Biology Team led by Dr. Pinto-do-Ó whose research focus is the biology of cardiac regeneration.

A . Manuscript submitted to IbPRIA conference

Manuscript entitled "Automatic and semi-automatic analysis of the extension of myocardial infarction in an experimental murine model" submitted and accepted for oral presentation in the Proceedings of IbPRIA, LNCS 6669 held in Las Palmas de Gran Canaria (Spain), pages 151-158, 2011.

Automatic and semi-automatic analysis of the extension of myocardial infarction in an experimental murine model

Tiago Esteves[1,2], Mariana Valente[2], Diana S. Nascimento[2], Perpétua Pinto-do-Ó[2], and Pedro Quelhas[1,2]

1 - Departamento de Engenharia Electrotécnica e de Computadores, Faculdade de Engenharia, Universidade do Porto, Rua Dr. Roberto Frias, 4200-465 Porto, Portugal
2 - INEB - Instituto de Engenharia Biomédica, Rua do Campo Alegre, 823, 4150-180 Porto, Portugal
meb09026@fe.up.pt

Abstract. Rodent models of myocardial infarction (MI) have been extensively used in biomedical research towards the implementation of novel regenerative therapies. Permanent ligation of the left anterior descending (LAD) coronary artery is a commonly used method for inducing MI both in rat and mouse. Post-mortem evaluation of the heart, particularly the MI extension assessment performed on histological sections, is a critical parameter for this experimental setting. MI extension, which is defined as the percentage of the left ventricle affected by the coronary occlusion, has to be estimated by identifying the infarcted- and the normal-tissue in each section. However, because it is a manual procedure it is time-consuming, arduous and prone to bias. Herein, we introduce semi-automatic and automatic approaches to perform segmentation which is then used to obtain the infarct extension measurement. Experimental validation is performed comparing the proposed approaches with manual annotation and a total error not exceeding 8% is reported in all cases.

Keywords: Infarct extension evaluation, image segmentation, region growing, otsu, k-means, meanshift, watershed

1 Introduction

Acute myocardial infarction is a major public health problem, resulting mainly from the occlusion of coronary arteries, due to the build-up of arteriosclerotic plaques, and the establishment of tissue ischemia eventually leading to end-stage heart failure. Permanent ligation of the left anterior descending (LAD) coronary artery in animal models, including the rat and the mouse, is a commonly used method for reproducing several of the human-associated pathological events. This surgical procedure also allows the implementation of pre-clinical models of disease which are a pre-requisite for testing cell/drug-therapies before proceeding into clinical trials [1]. The tissue extension of the induced myocardial

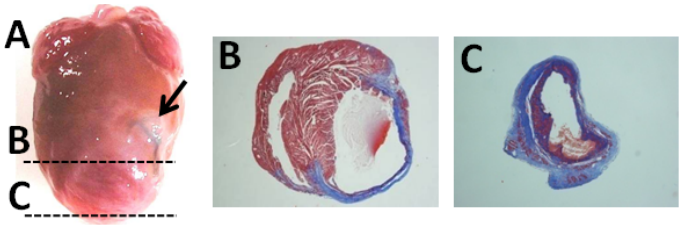

Fig. 1. Experimental myocardial-infarction mouse model. A - Macroscopic view of 21 days post-infarction heart; black arrow indicates the anatomical location of the LAD coronary artery ligation. B and C - Histological cross-sections of apical and mid region of LV stained with Masson Trichrome. Apex and free LV wall are fully compromised by ischemia, wich is illustrated by the collagen deposition (blue region) replacing the viable myocardium tissue (red region).

infarction, which is defined as the percentage of the left ventricle affected by coronary occlusion, is a critical parameter to evaluate the effect of any applied therapy at the experimental setting. This is calculated as the average value of infarct extension over all cross-sections of the dissected heart stained with Masson's Trichrome, a histological stain that enables the identification of collagen deposition, a hallmark of established infarction [1, 2]. To determine the infarct extension it is necessary to indentify the infarcted-tissue (blue area) and the normal-tissue (red area) in each section (Figure 1). Currently these tasks are performed manually by the biologists, which is a time-consuming and arduous endeavor. The latter is a driving force to the development of approaches to aid the analysis of the experimental MI extension. Our approaches entail the segmentation of the cross sections of the heart, which can be performed by means of automated image processing techniques.

The multiple techniques that may be applied to the segmentation of animal tissue can be discriminated in two major classes: automatic and semi-automatic techniques. In the former case the user needs to define initial parameters for each image in order to start the segmentation. Thus, automatic segmentation requires only the validation of the initial parameters and then the algorithms segment all the images in study without further user intervention.

Region growing is a semi-automatic technique that can be used to segment the cross sections of the heart. Alattar et al. describe the use of this technique in segmentation of the left ventricle in cardiac MRI (magnetic resonance imaging) scans [3]. This technique exploits spatial context by grouping pixels or subregions into larger regions. Homogeneity is the main criterion for merging the regions. However, the selection of similarity criteria used depends on the problem under consideration and also on the type of image data available [4, 5].

Regarding automatic segmentation there are techniques such as thresholding, region based segmentation and cluster based segmentation that can also be used in tissue segmentation [4, 6]. Sharma et al. introduce the segmentation of CT (computurized tomography) abdomen images using a threshold segmenta-

tion technique to separate different regions in the images [6]. In a thresholding technique a single value (threshold) is used to create a binary partition of the image intensities. All intensities greater than the threshold are grouped together into one class and those below the threshold are grouped into a separate class [4, 7]. Watershed is also a method applied in medical images segmentation. It is a region based segmentation which involves the concept of topography and hydrography. Hamarneh et al. present MR (magnetic resonance) cardiac images segmented with watershed transform [8]. Watershed can be described as a flooding simulation. Watersheds, or crest lines, are built when the water rise from different minima. All pixels associated with the same catchment basin are assigned to the same label [8, 9]. For image segmentation, the watershed is usually, but not always, applied to a gradient image. Since real digitized images present many regional minima in their gradients, this typically results in an excessive number of catchment basins (oversegmentation) [5, 9]. Ahmed et al. describe the segmentation of MR brain images using k-means clustering algorithm [10]. K-means segments the entire image into several clusters according to some measure of dissimilarity [8, 10]. Mean-shift technique has also been used in segmentation of MR brain images [11]. The mean-shift algorithm is a clustering technique which does not require prior knowledge of the number of clusters, and does not constrain the shape of the clusters, requiring only the definition of the radius of the kernel used [9].

We use these techniques to (1) segment all histology processed cross-sections of the excised mouse-hearts, (2) calculate the infarct extension and finalize by (3) comparing the results with manual annotation.

This paper is organized as follows: Section 2 introduces the methodology and describes automatic and semi-automatic techniques used in segmentation of the heart, Section 3 defines how to measure the infarct extension Section 4 presents the results obtained and finally the conclusion is presented in Section 5.

2 Methodology

To obtain the infarct extension it is necessary to segment the different tissues in each cross section of the heart. This can be performed with semi-automatic and full automatic techniques. Within the existing semi-automatic methods for image segmentation we had chosen to use region growing due its speed and ease of interaction. Otsu thresholding technique, watershed segmentation, k-means and mean-shift clustering are the fully automatic techniques that we selected to segment the cross sections of the heart.

In order to improve the segmentation process we applied noise reduction, using a Gaussian filter [5]. This noise reduction is applied in all the images before any segmentation process.

2.1 Semi-automatic tissue segmentation

Region growing exploits spatial context by grouping pixels or sub-regions into larger regions according to some criterion. The average gray level information is

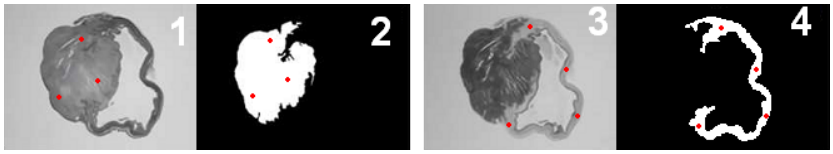

Fig. 2. Segmentation of normal tissue using the Red channel (1) and infarcted tissue using the Blue channel (3) in a cross section of the heart by region growing technique. The results of the segmentation process are binary images (2 and 4). The red points indicate the initial positions of the region growing process.

the criterion chosen for merging the neighboring regions in our work. Regions are merged if they satisfy the chosen criterion and no merging occurs when the criterion is not met [5, 4]. The user needs to specify the initial points to begin the segmentation process. For the task of segmenting the normal and the infarcted heart tissue it is necessary to define the initial points for the process of region growing in each of the tissue-conditions. To segment the normal-tissue we used the gray level information present in the Red channel. For the segmentation of the infarcted-tissue we used the gray level information from the Blue channel. The result is a set of binary images, one for each tissue condition (Figure 2). Results are improved using morphological operations, for example to fill small holes inside the segmentation results.

Given the segmentation areas we can then calculate the infarct extension.

2.2 Automatic tissue segmentation

To automatically segment the different tissue-conditions in each of the heart cross-sections we use otsu thresholding, watershed segmentation, k-means and mean-shift clustering. All these image segmentation techniques allow the partition of the image in regions which we can associate to the distinct tissue-conditions by analyzing their color.

Otsu thresholding technique selects an adequate threshold of gray level for extracting objects from their background. This threshold is used to convert an intensity image to a binary one. All intensities greater than the threshold are grouped together into one class and those below the threshold are grouped into a separate class [12].

Using this technique, with different channels of the RGB image, we can obtain segmentations of the normal and infarcted-tissue. High values of image intensities in the Red channel relate to normal-tissue. The Blue channel has high image intensity values in infarcted areas. Based on these relationships between the Red and Blue color channels and the tissue properties we decided to subtract the Blue channel to the Red channel for the segmentation of the normal-tissue. We subtract the Red channel to the Blue channel for the segmentation of the infarcted-tissue (Figure 3 (a)).

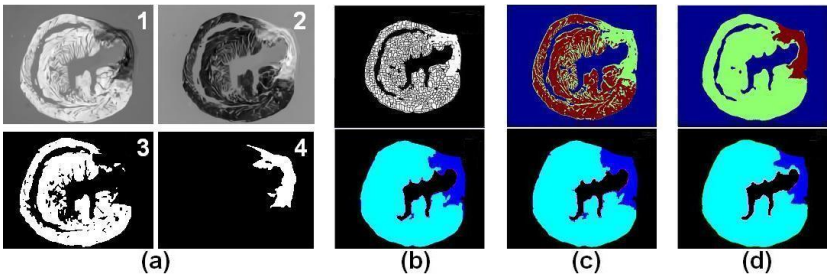

Fig. 3. Segmentations of a heart cross section and identification of the normal and infarted tissue: (a) Combination of the channels (1 and 2) and respective otsu thresholding results (3 and 4), (b) Watershed segmentation result, (c) K-means and (d) Mean-shift clustering results (top) and respectively identification of the regions (down).

Watershed technique is based on immersion simulation. The input image is considered as a topographic surface which is flooded by water starting from regional minima. Watershed lines are formed on the meeting points of water coming from distinct minima. All pixels associated with the same catchment basin are assigned to the same label [13, 14].

For the application of this technique we use the same image channel combination as for otsu thresholding. Performing watershed segmentation originates an oversegmentation of the tissue since it has many regional minima. However, by comparing the color intensities in each region we are able to decide if each region is from normal-tissue or from infarcted-tissue. Using also the otsu thresholding technique that allows to easily obtain the full tissue segmentation we focus our analysis only on the tissue region. The resulting tissue areas are coherent with normal/infarct tissue-areas (Figure 3 (b)).

K-means clustering technique assigns cluster labels to data points from the entire image [8]. For this technique we use the information of the three channels, selecting three clusters which will correspond to the background, normal- and infarcted-tissue. After obtaining the segmentation result we identify each segmented cluster from its average color intensity. To improve the segmentation we fill the holes using morphological operations (Figure 3 (c)).

Mean-shift clustering technique does not require prior knowledge of the number of clusters and only needs the definition of the radius of the kernel used. As in the previous technique we decided to obtain at most three clusters. If we get more than three clusters we iteratively increase the radius of the kernel used (Figure 3 (d)).

For this technique we decided to use only the information present in the Red and Blue channel because it showed better results than the use of all channels.

Following the segmentation results of full automatic and semi-automatic techniques we can measure the infarct extension.

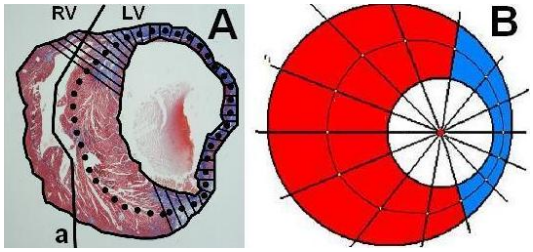

Fig. 4. Image of a heart cross section. A - The heart is bounded by the outside black continuous line which includes the left ventricle (LV) and right ventricle (RV) separated by line **a**. The interior black continuous line is identifying the lumen of the left ventricle and the region marked by lines shows the tissue with infarct. The dotted line is the midline between the inside and outside black continuous lines. B - Scheme of a cross section of the heart.

3 Infarct extension evaluation

To better understand the calculation of the infarct extension we must analyze the different regions in the heart. In Figure 4 (A) we can observe the heart bounded by the exterior black continuous line. It is formed by right and left ventricles. The first consists only in normal-tissue. The left ventricle includes the infarcted-tissue, which is represented by the shaded region, lumen, which is bounded by the interior black continuous line and also normal-tissue. The infarct extension is usually calculated by two different methods:

Area measurement - Infarct extension is calculated by dividing the infarct area by the area of the heart tissue [1, 2] (Figure 4 (A)). This is trivial based on the segmentation results obtained.

Midline length measurement - Infarct extension is calculated by dividing the midline infarct length by the length of midline [2] (Figure 4 (A)). Figure 4 (B) shows a scheme that represents a cross-section of the heart. To perform the midline measurement we first automatically find the midline by tracing lines from the centre of the lumen to the outside of the tissue. The midline is given by the middle distance between tissue borders. The points of the middle line where there is infarcted-tissue in bigger percentage than the normal-tissue (in the radial direction) are considered infarcted points. Secondly we divide the length of infarct midline by the length of the midline. To obtain the lumen of the heart we get a segmentation of all the heart tissue by otsu thresholding technique, which is trivial and we identify the biggest hole inside that segmentation.

The infarct extension is defined as the mean value of infarct extension in all the cross-sections of the heart.

Infarct extension is evaluated in the heart cross-sections considering or not the right ventricle [1, 2] (Figure 4 (A)). However, it is not easy to find a robust way to remove the RV as it is variable in morphology and most biologists vary in their assessment of where the RV ends and the LV begins. As such, we perform

Table 1. Results of infarct extension measurement in mice's hearts. The results are the average value of infarct extension obtained in transverse sections of each mouse heart. In the manual analysis the results only consider the left ventricle.

Infarct extension						
Midline length measurement						
Heart	Manual	Region growing	Otsu	Watershed	K-means	Mean-shift
#1 with RV	-	39%	38%	39%	37%	34%
#1 without RV	43%	38%	40%	41%	38%	36%
#2 with RV	-	47%	47%	48%	46%	47%
#2 without RV	52%	48%	48%	49%	47%	49%
Area measurement						
Heart	Manual	Region growing	Otsu	Watershed	K-means	Mean-shift
#1 with RV	-	29%	18%	17%	17%	14%
#1 without RV	22%	25%	21%	21%	20%	17%
#2 with RV	-	34%	29%	31%	28%	33%
#2 without RV	36%	38%	32%	36%	32%	36%

both the analysis on the full heart, including the RV, and also obtain results on the LV only by removing the RV through image editing tools (manually).

4 Results

The infarct extension was calculated manually and automatically in two independent hearts. The calculation was performed both on the whole cross-section tissue and also without considering the right heart ventricle for comparison. To automatically segment the tissue without taking into account the right ventricle we manually remove this region before the segmentation process. Table 1 shows the results for the infarct extension evaluation using our approaches and the manual annotation. The results are the average value of the infarct extension over all cross-sections of each independent heart.

Differences between the proposed approaches and manual annotation are never greater than 8% in the case of the evaluation considering the right ventricle. Removing the right ventricle the differences are never greater than 7%. The differences among the proposed approaches considering the right ventricle tissue are at most 15% and without this are never greater than 8%.

5 Conclusion

The proposed approach enabled the full and semi-automatic calculation of infarct extension. The results obtained using our approaches were in close agreement with the manual annotation with differences never higher than 8%. The segmentation allowed an analysis of the infarct extension in a fraction of the manual method measure time.

Within the automatic segmentation approaches, the watershed technique produced better results, with the differences never above 5% (reduced to 3% by removing the right ventricle). The differences from the semi-automatic approach used were at most 7% considering the right ventricle (5% without this one). Although the differences were slightly higher in the semi-automatic approach, the biologists prefer the possibility to control the segmentation results in relation to fully automatic approaches.

Future research will focus on integrating automatic image segmentation methods with anatomical models. This will enable the automatic segmentation and measurement of only the left ventricle of the heart, leading to better results.

Acknowledgments

These studies were supported by a FCT Grant Project PTDC/SAU-OSM/68473/2006. PQ and PPÓ are, respectively, *Ciência2008* and *Ciência2007* awardees; DSN is recipient of SFRH/BPD/42254/2007 by FCT (Portuguese government Fellowships).

References

1. N. Degabriele, U. Griesenbach, and K. Sato, "Critical appraisal of the mouse model of myocardial infarction," *Experimental Physiology*, vol. 89, no. 4, pp. 497–505, 2004.
2. J. Takagawa, Y. Zhang, and M. Wong, "Myocardial infarct size measurement in the mouse chronic infarction model: comparison of area- and length-based approaches," *Journal of Applied Physiology*, vol. 102, pp. 2104–2111, March 2007.
3. M. Alattar, N. Osman, and A. Fahmy, "Myocardial segmentation using constrained multi-seeded region growing," *Image Analysis and Recognition (ICIAR 2010)*, vol. 6112, pp. 89–98, 2010.
4. Q. Wu, F. Merchant, and K. Castleman, *Microscope Image Processing*, chapter 7, Elsevier, 1996.
5. Raf. Gonzalez, R. Woods, and S. Eddins, *Digital Image Processing Using MATLAB*, chapter 9, Pearson Education, 2004.
6. N. Sharma and L. Aggarwal, "Automated medical image segmentation techniques," *Journal of Medical Physics*, vol. 35, no. 1, pp. 3–14, 2010.
7. D. Pham and C. Xu, "A survey of current methods in medical image segmentation," *Annual Review of Biomedical Engineering*, vol. 2, pp. 315–338, 1998.
8. G. Hamarneh and X. Li, "Watershed segmentation using prior shape and appearance knowledge," *Image and Vision Comp.*, vol. 27, no. 1–2, pp. 59–68, 2009.
9. S. Khadir and R. Ahamed, "Moving toward region-based image segmentation techniques: A study," *Journal of Theoretical and Applied Information Technology*, vol. 5, no. 1, pp. 1–7, 2009.
10. M. Ahmed and D. Mohamad, "Segmentation of brain mr images for tumor extraction by combining kmeans clustering and perona-malik anisotropic diffusion model," *International Journal of Image Processing*, vol. 2, no. 1, pp. 1–8, 2010.
11. A. Mayer and H. Greenspan, "An adaptive mean-shift framework for MRI brain segmentation," *IEEE Trans. on Medical Imaging*, vol. 28, no. 8, pp. 1–12, 2009.
12. N. Otsu, "A threshold selection method from gray level histograms," *IEEE Transactions Systems, Man and Cybernetics*, vol. 9, no. 1, pp. 62–66, 1979.
13. M. Marcuzzo, P. Quelhas, A. Campilho, A. Maria Mendonça, and Aurélio Campilho, "Automated arabidopsis plant root cell segmentation based on svm classification and region merging," *Computers in Biology and Medicine*, vol. 39, no. 9, pp. 1–9, 2009.
14. A. Bleau and J. Leon, "Watershed-based segmentation and region merging," *Computer Vision and Image Understanding*, vol. 77, no. 3, pp. 317–370, 2000.

B . Oral presentation in IbPRIA conference

Oral presentation performed in the IbPRIA Conference related with the manuscript "Automatic and semi-automatic analysis of the extension of myocardial infarction in an experimental murine model" submitted in the IbPRIA 2011 conference held in Las Palmas de Gran Canaria (Spain).

Automatic and semi-automatic analysis of the extension of myocardial infarction in an experimental murine model

Tiago José Arieira Esteves
Mariana Valente
Diana Nascimento
Perpétua Pinto-do-Ó
Pedro Quelhas

INEB – Instituto de Engenharia Biomédica
Universidade do Porto
Porto, Portugal

IbPRIA 2011
Las Palmas de Gran Canaria
Spain, June 8-10, 2011

U.PORTO UNIVERSIDADE DO PORTO

I3S CONSÓRCIO DE INVESTIGAÇÃO EM SAÚDE

IBMC INEB Laboratório Associado . Associate Laboratory

INEB - INSTITUTO DE ENGENHARIA BIOMÉDICA

20 1989 - 2009 U.PORTO

Outline

- Motivation
- Methodology
  - Supervised tissue segmentation
  - Unsupervised tissue segmentation
- Infarct extension evaluation
- Results
- Conclusion

Motivation

- Cardiovascular diseases remain the major cause of premature morbidity and mortality worldwide. It accounted for over 4.3 million deaths in Europe in 2009.

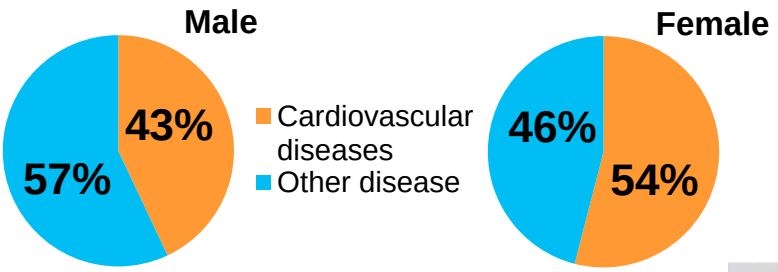

- An important cardiovascular disease is myocardial infarction.
- To study this important health problem, experimental rodent models of myocardial infarction are extensively used. Permanent ligation of the left anterior descending coronary artery is a commonly used method for inducing myocardial infarction both in rat and mouse.
- These experiments aims the implementation of novel regenerative therapies to apply to this problem.

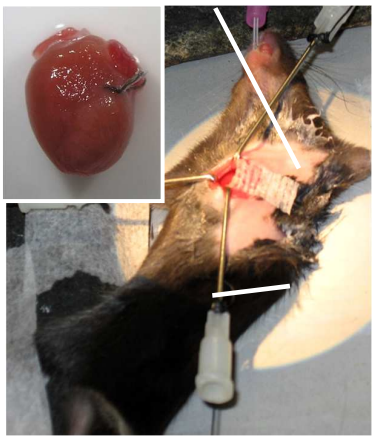

Methodology

- Particularly, the infarct extension is an important parameter analyzed.
- The infarct extension is defined as the percentage of the left ventricle affected by coronary artery occlusion, typically calculated on 12 transverse histological sections stained with Masson´s Trichrome.
- The determination of the infarct extension is time-consuming, arduous and prone to bias because requires manual definition of infarcted tissue and the non affected tissue in each section.

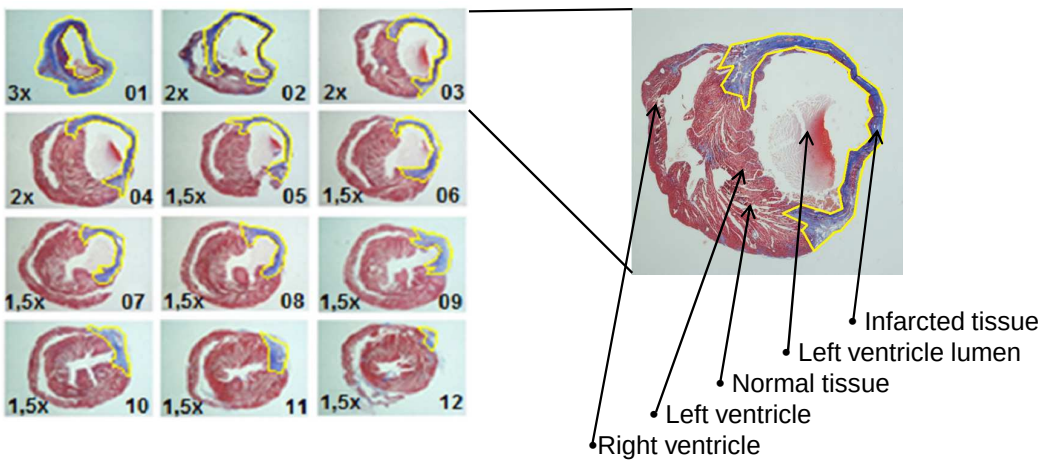

Methodology

- **Schematics of the approach**

Histological cross section of the heart → **Segmentation of the heart cross section** → **Infarct extension evaluation**

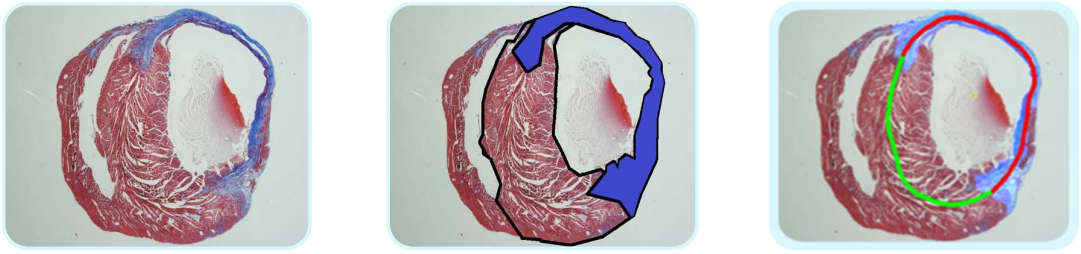

- The analysis is done on the tissue of the heart cross sections and this requires its segmentation.
- Therefore we tested several techniques for image segmentation and the segmentation results are then used for evaluating the infarct extension.

Methodology

- **Segmentation methods**

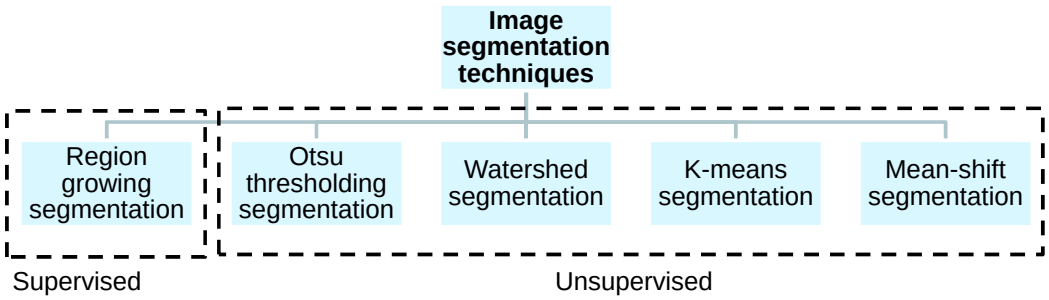

- **Pre-processing**
  - Gaussian filtering for noise reduction.
  - Noise reduction is applied to all images prior to segmentation.
  - Color and illumination regularization is also applied.

Supervised tissue segmentation

- **Region growing**
  - Region growing examines neighboring pixels of initial “seed points” and determines whether the pixel neighbors should be added to the region according to some criterion.
  - We chose the average gray level information as the criterion for merging the neighboring regions.

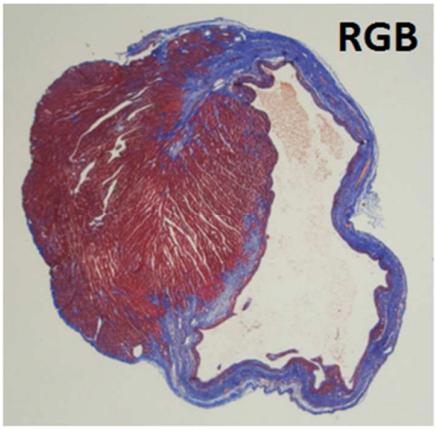

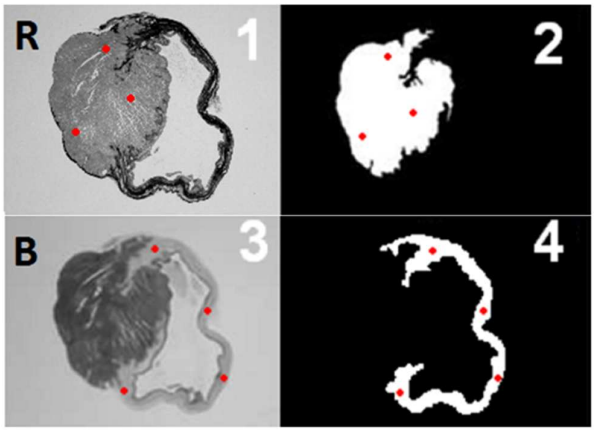

Unsupervised tissue segmentation

- **Otsu thresholding**
  - This technique selects an adequate threshold of gray level for extracting objects from their background.
  - This threshold is used to convert an intensity image to a binary one.
  - For the segmentation of the normal and infarcted tissue we use image channel combinations to convert color images into intensity images with relevant information:
    - **(A) Normal tissue = Red channel – Blue channel**
    - **(B) Infarcted tissue = Blue channel – Red channel**

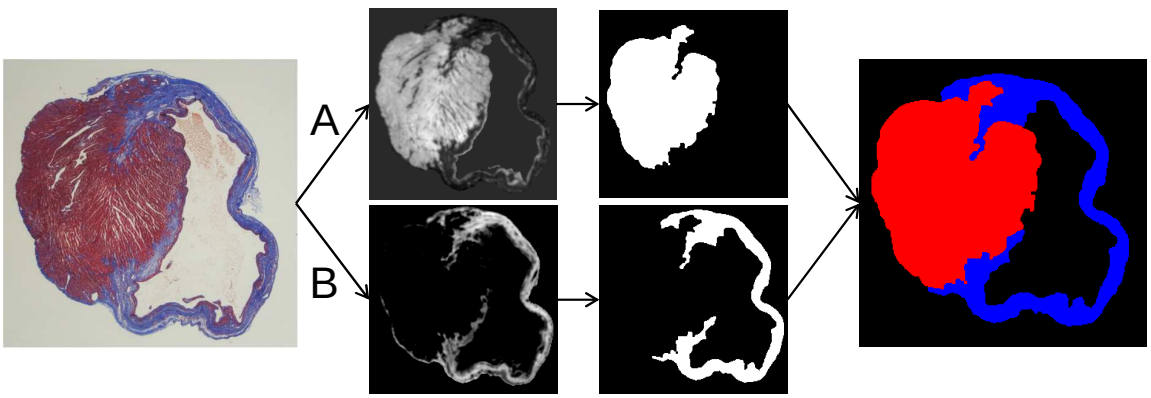

Unsupervised tissue segmentation

- **Watershed technique**
  - Watershed technique is based on immersion simulation.
  - The input image is considered as a topographic surface which is flooded by water starting from regional minima.
  - The final segmented regions arising from the various regional minima are called catchment basins. All pixels associated with the same catchment basin are assigned to the same label.
  - For the application of this technique we used the image channel combination A as for Otsu thresholding. We subtract the Blue channel to the Red channel.
  - Watershed is evaluated only in tissue areas, which were selected using Otsu thresholding.
  - Given the watershed segmentation we decide if each segmented region corresponds to normal or infarcted tissue based on color intensities.

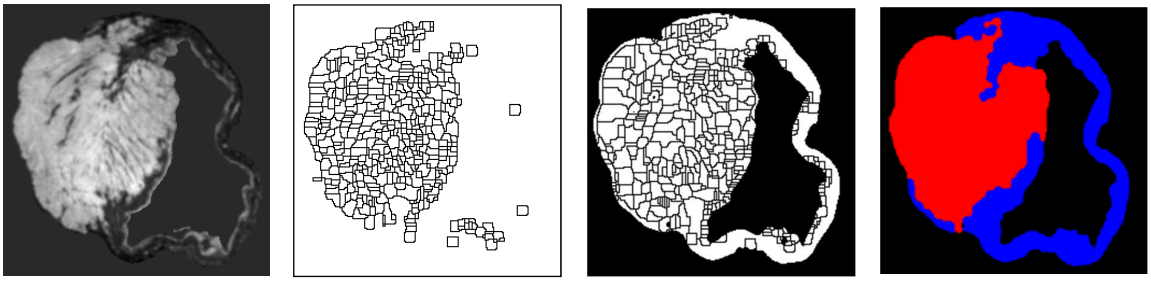

Unsupervised tissue segmentation

- **K-means clustering technique**
  - This technique assigns cluster labels to pixels with similar color properties.
  - We used the information of the three channels and we selected three clusters which correspond to the background, normal and infarcted tissue.
  - After obtaining the segmentation result we identify each segmented cluster based on the color properties of the corresponding cluster center.
  - To improve the final segmentation morphological operations are used.

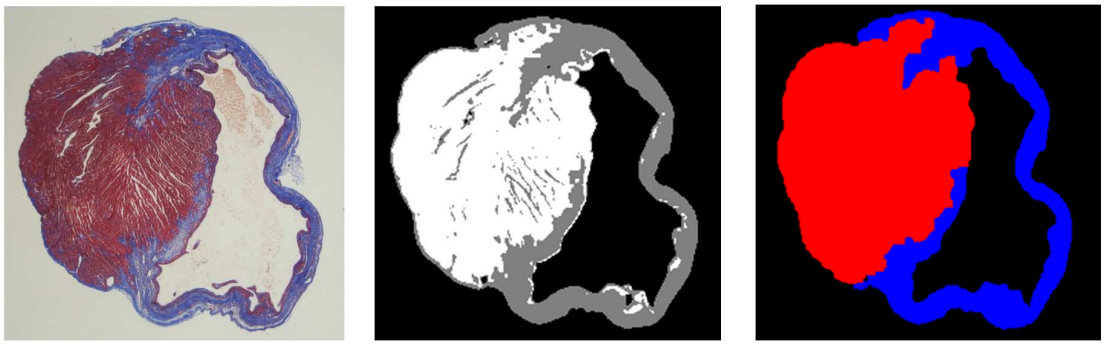

Unsupervised tissue segmentation

- **Mean-shift clustering technique**
  - Mean-shift is a clustering technique which does not require prior knowledge of the number of clusters.
  - This technique needs the definition of the radius of the kernel used.
  - We select a kernel with an initial radius in order to obtain three clusters. If more than three clusters are obtained we adjust the radius of the kernel and repeat the segmentation process.
  - In this case we base our segmentation only on the Red and Blue channels since they led to better results.

r = 0.05 → r = 0.06 → r = 0.07

6 clusters | 5 clusters | 3 clusters

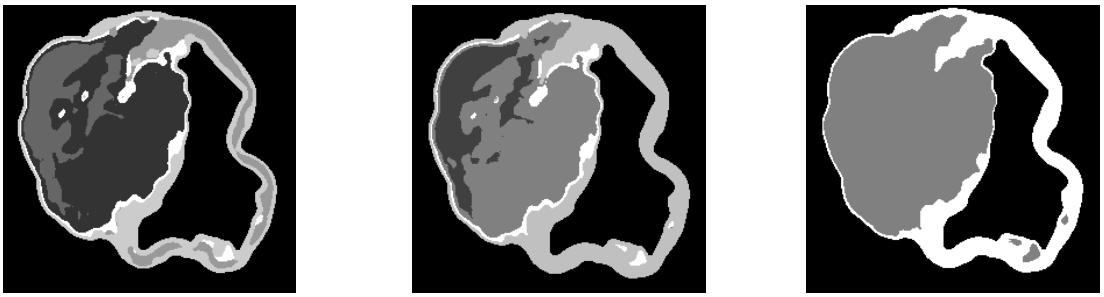

Infarct extension evaluation

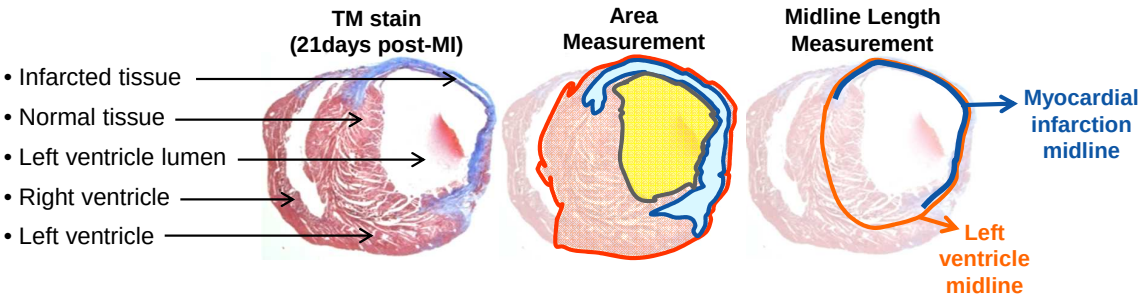

- **Area measurement:**
  - Infarct extension is calculated by dividing the infarct area by the area of the heart tissue.

- **Midline length measurement:**
  - Infarct extension is calculated by dividing the midline infarct length by the length of midline.

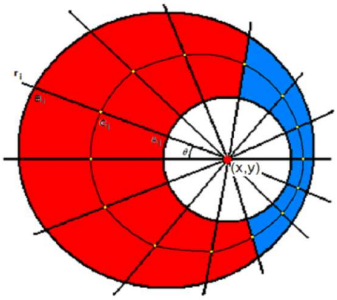

Results

- The infarct extension was calculated manually and automatically in two independent hearts.
- The calculation was performed both on the whole cross-section tissue and also without considering the right heart ventricle for comparison.
- To automatically segment the tissue without taking into account the right ventricle we manually remove this region prior to segmentation.

Infarct extension						
Midline length measurement						
Heart	Manual	Region growing	Otsu	Watershed	K-means	Mean-shift
#1 with RV	-	39%	38%	39%	37%	34%
#1 without RV	43%	38%	40%	41%	38%	36%
#2 with RV	-	47%	47%	48%	46%	47%
#2 without RV	52%	48%	48%	49%	47%	49%
Area measurement						
Heart	Manual	Region growing	Otsu	Watershed	K-means	Mean-shift
#1 with RV	-	29%	18%	17%	17%	14%
#1 without RV	22%	25%	21%	21%	20%	17%
#2 with RV	-	34%	29%	31%	28%	33%
#2 without RV	36%	38%	32%	36%	32%	36%

Differences between the proposed approaches and manual annotation are never greater than 9% in the case of the evaluation considering the right ventricle. Removing the right ventricle the differences are never greater than 7%.

Conclusion

- The proposed segmentation techniques enabled the supervised and unsupervised calculation of infarct extension.
- The results of the methods to automatically measure the infarct extension evaluation were coherent with manual annotations.

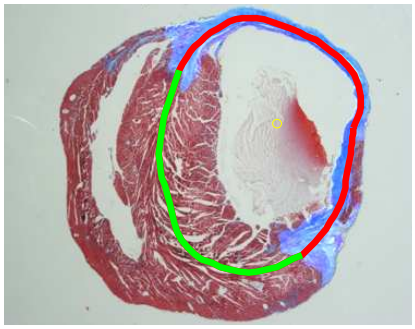

- The results obtained using our approaches were in close agreement with the manual annotation with differences never higher than 9%. The segmentation allowed an analysis of the infarct extension in a fraction of the manual method measure time.
- Although the differences were slightly higher in the semi-automatic approach, the biologists prefer the possibility to control the segmentation results in relation to fully unsupervised approaches.

Acknowledgments

- **INEB – Biomedical Imaging and Vision Computing Group**
  - Pedro Quelhas;
  - Aurélio Campilho;
- **INEB – NEWTherapies Group**
  - Mariana Valente;
  - Diana Nascimento;
  - Perpétua Pinto-do-Ó
- **These studies were supported by a FCT Grant Project PTDC/SAU-OSM/68473/2006. PQ and PPÓ are, respectively, *Ciência2008* and *Ciência2007* awardees; DSN is recipient of SFRH/BPD/42254/2007 by FCT (Portuguese government Fellowships).**

FCT Fundação para a Ciência e a Tecnologia
MINISTÉRIO DA CIÊNCIA, TECNOLOGIA E ENSINO SUPERIOR

INSTITUTO DE ENGENHARIA BIOMÉDICA

Universidade do Porto
FEUP Faculdade de Engenharia

INEB - INSTITUTO DE ENGENHARIA BIOMÉDICA
20
1989 - 2009
U.PORTO

C . Manuscript submitted to RecPad conference

Manuscript entitled "Semi-automatic extraction of the level of infarction in mouse hearts" submitted and accepted for poster presentation in the RecPad conference held in Vila Real, Portugal, pages 1-2, 2010.

Semi-automatic extraction of the level of infarction in mouse hearts

Tiago Esteves, Perpétua Pinto do Ó and Pedro Quelhas
INEB - Instituto de Engenharia Biomédica
meb09026@fe.up.pt

Abstract

Despite considerable advances in diagnosis and management over the last three decades, acute myocardial infarction continues to be a major public health problem. Almost all myocardial infarctions result from occlusion of pre-existing arteriosclerotic plagues of coronary arteries. This can be mimicked by assay by ligation of the left coronary artery in a variety of animal models, including rats and mice. This allows the collection of information that leads to a better understanding of this problem.

An important aspect that is required for evaluation is the calculation of infarct extension. However, it is done manually. The present work is aimed to create a tool for semi-automatic calculation of infarct extension in such experiments.

1. Introduction

Acute myocardial infarction is a major public health problem and almost all result from occlusion of pre-existing arteriosclerotic plagues of coronary arteries. This aspect has been mimicked by ligation of the left coronary artery in a variety of animal models, including rats and mice. This allows the execution of clinical trials where one can obtain important information in order to better understand this problem [4].

The infarct extension is the most important information obtained from the clinical trials. It is defined as the percentage of the left ventricle affected by coronary occlusion. We calculate this rate as the mean value of infarction extension in 12 cross sections that represents the left ventricle stained with Massons Trichrome, an histological staining that enables the discrimination of collagen deposition that occurs in the infarcted tissue with Aniline Blue [1, 2, 3, 4]. To determine the infarct extension it is necessary to indentify and measure the blue area (infarcted tissue) and the red area (normal tissue) in each section. Currently these tasks are made manually by the biologists which is a time-consuming and exhausting task. These factors motivate the development of a tool for semi-automatic calculation of infarct extension which involves the segmentation of the cross sections of the heart.

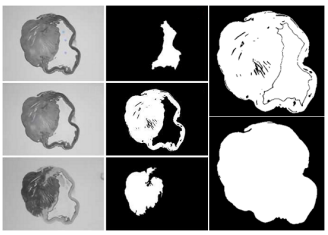

Figure 1. Segmentation of different regions in a cross section of the heart (left) and morphological operation to fill the holes inside for obtain the final result (right).

2. Methodology

To obtain the infarct extension it is necessary to segment the different tissues in each cross section of the heart. Within the existing methods for image segmentation we chose to use the region growing method due to the speed and easy interaction. After the identification of infarcted and normal tissue we can measure the infarct extension.

2.1. Tissue segmentation by region growing

Region growing exploits spatial context by grouping pixels or sub-regions into larger regions according to some criterion. The average gray level is the criterion chosen for merging the neighbouring regions. Regions merge if they satisfy the chosen criterion and stop growing when the criterion is not met [5, 6]. The user needs to specify which are the initial points to begin the process of grouping pixels, for all regions. To improve the segmentation we fill the holes using morphological operations. The result is a set of binary images, one for each tissue type (Figure 1).

Given the segmentation areas we can then calculate the infarct extension.

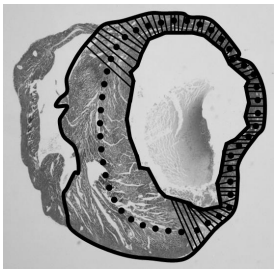

Figure 2. Cross section of the heart. The left ventricle is bounded by the outside black continuous line. The interior black continuous line is identifying the lumen of the left ventricle and the region marked by lines shows the tissue with infarct. The dotted line is the midline between the inside and outside black continuous lines.

2.2. Infarct extension evaluation

In Figure 2 we can observe the left ventricle bounded by the exterior black continuous line and outside of this line there is the right ventricle which is not relevant for the clinical trials. The left ventricle is the region where we evaluate the infarct extension and it is formed by infarcted tissue, marked by the shaded region, lumen, bounded by the interior black continuous line and normal tissue. The infart extension is usually calculated by two different methods:

Area measurement - Infarct extension is calculated by dividing the infarct area by area of the left ventricle tissue [1, 2, 3, 4](Figure 2).

Midline length measurement - Infarct extension derived from midline length measurement is calculated by dividing the sum of midline infarct lengths by the length of midline circumference [2](Figure 2).

The infarct extension was calculated manually and by computer using the referred methods and the results were compared (Table 1).

3. Results

We developed a tool based on requirements specified by biologists that allows the user to: segment and view the various regions of the heart with possibility to change the segmentations produced to find the one considered correct, display the segmentations in the original image to best visually the results, get the infarct extension by area and midline length methods and obtain the results.

In the results of experiments performed in two hearts shown in Table 1 we can observe the differences between the manual method to obtain the infarct extension and the program. The results are the average value of the infarct extension in each slice of the heart and the differences are never greater than 5%. For each slice the differences in infarct extension are never greater than 15%. The time it takes to get the infarct extension for each slice is approximately 1 minute. This is at least 10 times faster than the manual method.

Table 1. Results of infarct extension measurement in mouse hearts (heart #37 and heart #40) expressed as a percentage. The results are the mean value of infarct extension obtained in transverse sections of each mouse heart.

Infarct extension				
	Midline length measurement		Area measurement	
Heart	Manual	Program	Manual	Program
#37	48%	43%	29%	28%
#40	52%	47%	36%	34%

4. Conclusion

The proposed method enabled the semi-automatic calculation of infarct extension faster than the manual method. We tested our approach in two hearts and the results were in close agreement with the manual method.

The developed tool is currently under evaluation at the Institute of Biomedical Engineering in the Division of Biomaterials where the infarctions are performed on animals and may still be subject to some modifications.

Future research will focus on applying automatic image segmentation methods together with anatomical models in order to automate the program.

References

[1] E. D. d. M. Esther Lutgens, Mat J.A.P. Daemen. Chronic myocardial infarction in the mouse: cardiac structural and functional changes. *Cardiovascular Research*, 41:586–593, June 1998.

[2] M. L. W. Junya Takagawa, Yan Zhang. Myocardial infarct size measurement in the mouse chronic infarction model: comparison of area- and length-based approaches. *Journal of Applied Physiology*, 102:2104 2111, March 2007.

[3] M. F. MA Pfeffer, JM Pfeffer. Myocardial infarct size and ventricular function in rats. *Circulation Research*, 44:503–512, 1979.

[4] K. S. Naomi M. Degabriele, Uta Griesenbach. Critical appraisal of the mouse model of myocardial infarction. *Experimental Physiology*, 89(4):497–505, May 2004.

[5] K. R. C. Qiang Wu, Fatima Merchant. *Microscope Image Processing*. Elsevier, 1996.

[6] S. L. E. Rafael C. Gonzalez, Richard E. Woods. *Digital Image Processing Using MATLAB*. Pearson Education, 2004.

D . Poster presentation in RecPad conference

Poster entitled "Semi-automatic extraction of the level of infarction in mouse hearts" presented in the RecPad conference held in Vila Real, Portugal, 2010.

Semi-automatic extraction of the level of infarction in mouse hearts

Tiago Esteves (meb09026@fe.up.pt) Perpétua Pinto do Ó Pedro Quelhas

INEB – Instituto de Engenharia Biomédica Signal and Image Division

Universidade do Porto FEUP Faculdade de Engenharia

Abstract

Despite considerable advances in diagnosis and management over the last three decades, acute myocardial infarction continues to be a major public health problem. Almost all myocardial infarctions result from occlusion of pre-existing arteriosclerotic plagues of coronary arteries. This can be mimicked by assay by ligation of the left coronary artery in a variety of animal models, including rats and mice. This allows the collection of information that leads to a better understanding of this problem.

An important aspect that is required for evaluation is the calculation of infarct extension. However, it is done manually. The present work is aimed to create a tool for semi-automatic calculation of infarct extension in such experiments.

References

[1] - Naomi M. Degabriele, Uta Griesenbach, Kaori Sato, **Critical appraisal of the mouse model of myocardial infarction**, Experimental Physiology, vol. 89, no. 4, pp 497-505, May 2004.

[2] - Esther Lutgens, Mat J.A.P. Daemen, Ebo D. de Muinck, **Chronic myocardial infarction in the mouse: cardiac structural and functional changes**, Cardiovascular Research, vol. 41 pp 586-593 June 1998.

[3] - MA Pfeffer, JM Pfeffer, MC Fishbein, **Myocardial infarct size and ventricular function in rats,** Circulation Research, vol. 44, pp 503-512, 1979.

[4] - Junya Takagawa, Yan Zhang, Maelene L. Wong, **Myocardial infarct size measurement in the mouse chronic infarction model: comparison of area- and length-based approaches,** *J Appl Physiol*, vol. 102, pp 2104–2111, March 2007.

[5] - Rafael C. Gonzalez, Richard E. Woods, Steven L. Eddins, **Digital Image Processing Using MATLAB**, pp 48-49, 2004.

[6] - Qiang Wu, Fatima Merchant, Kenneth R. Castleman, **Microscope Image Processing**, Elsevier, pp 173-174, 1996.

RecPad 2011
29 October 2010, Vila Real

Introduction

- Infarct assays in lab animals allow the execution of clinical trials leading to a better understanding of myocardial infarct.
- Infarcts are mimicked by ligation of the left coronary artery in a variety of animal models, including rats and mice.
- The infarct extension is the most important information obtained from the clinical trials. It is defined as the percentage of the left ventricle affected by coronary occlusion.

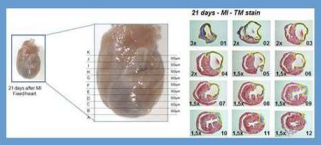

- Infarction extension is evaluated over 12 heart cross sections.
- Tissue is stained with an histological staining that enables the discrimination of collagen deposition that occurs in infarcted tissue.
- To determine the infarct extension it is necessary to indentify and measure the blue area (infarcted tissue) and the red area (normal tissue) in each section.

Tissue segmentation

- Tissue image segmentation is based on a gray level representation of the original colour image.
- Segmentation is obtained through *region growing*. Using the average gray level as the criterion chosen for merging the neighbouring regions.
- The user needs to specify which are the initial points to begin the process of grouping pixels. To improve the segmentation we fill the holes using morphological operations.
- Independent initial segmentation points are required for the full tissue, the lumen (empty are within the ventricle) and normal tissue.

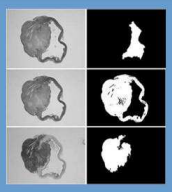

Infarct extension evaluation

- Infarct extension is calculated based on the previously segmented normal tissue and infarcted tissue.
- Two different methods of infarct extension calculation are used:

Area measurement – Infarct extension is calculated by dividing the infarct area by area of the left ventricle tissue.

Midline length measurement - Infarct extension derived from midline length measurement is calculated by dividing the midline infarcted length by the total midline length.

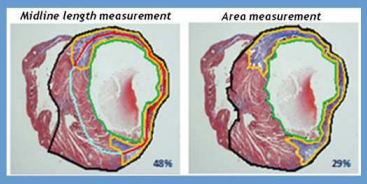

- **Area measurement** based on segmented regions is trivial.
- In **midline measurement** we automatically find the midline, by tracing lines from the centre of the lumen to the outside of the tissue. The midline is given by tracing the middle distance between tissue borders. The length of the middle line where infarcted tissue is more than half the length of the corresponding radial line is considered infarcted length.

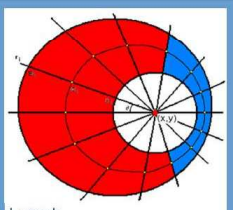

Legend:
- Red: Normal tissue;
- Blue: Infarcted tissue;
- White: Lumen;
- (X,Y): Center of the lumen;
- θ: Angle between each line *i*;
- Ai: Inside point of the tissue;
- Bi: Outside point of the tissue;
- Ci: Midpoint between the inside and outside points.

Prototype and results

- We developed a program based on requirements specified by biologists and taking into account their needs.
- The program allows to obtain the infarct extension by area and midline length methods.
- The results of the prototype were in close agreement with the manual measurements.

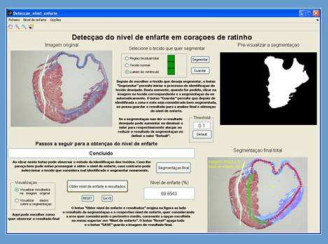

Image	Infarct extension (%)			
	Midline length measurement		Area measurement	
	Manual	Program	Manual	Program
#37-1	100	100	100	100
#37-2	87	79	52	55
#37-3	68	65	35	38
#37-4	61	55	29	25
#37-5	52	47	22	17
#37-6	51	47	23	19
#37-7	48	43	18	17
#37-8	39	34	18	15
#37-9	33	24	20	17
#37-10	20	10	14	12
#37-11	17	12	11	12
#37-12	0	0	3	4
Mean	**48**	**43**	**29**	**28**

Image	Infarct extension (%)			
	Midline length measurement		Area measurement	
	Manual	Program	Manual	Program
#40-1	94	87	82	72
#40-2	86	71	50	43
#40-3	83	71	57	43
#40-4	78	69	54	49
#40-5	55	44	22	18
#40-6	43	38	17	19
#40-7	38	31	20	18
#40-8	34	30	25	25
#40-9	29	25	28	28
#40-10	16	19	24	25
#40-11	18	27	22	30
Mean	**52**	**47**	**36**	**34**

- Measurement obtained on images from two hearts enable the comparison between our semi-automated approach and manual measurement.
- The results are the average value of the infarct extension in each slice of the heart and the differences are never greater than 5%.
- For each slice the differences in infarct extension are never greater than 15%.
- The time it takes to get the infarct extension for each slice is approximately 1 minute. This is at least 10 times faster than the manual method.

Future research

- Increase robustness by introducing automatic segmentation methods and anatomical heart models.
- Fully automate the methodology, comparing it to both manual and the current implementation.

E . Manuscript submitted in Pattern Recognition Journal

Abstract of the manuscript entitled "Automated myocardial infarction analysis in an experimental model using image segmentation and model adaptation" submitted and under evaluation in Pattern Recognition Journal, pages 1-26, 2011.

Automated myocardial infarction analysis in an experimental model using image segmentation and model adaptation

Tiago Esteves[a,b], Mariana Valente[b], Diana S. Nascimento[b], Perpétua Pinto-do-Ó[b], Pedro Quelhas[a,b]

[a] *Departamento de Engenharia Electrotécnica e de Computadores, Faculdade de Engenharia, Universidade do Porto, Rua Dr. Roberto Frias, 4200-465 Porto, Portugal*
[b] *INEB - Instituto de Engenharia Biomédica, Rua do Campo Alegre, 823, 4150-180 Porto, Portugal*

Abstract

Experimental rodent models of myocardial infarction have been extensively used in biomedical research to study molecular, cellular and histological alterations following myocardial infarction.

These models have been recently applied to assess the therapeutic potential for functional restoration of damaged myocardium. Such studies are based on myocardial infarction induction by permanent ligation of the left anterior descending coronary artery, some therapeutic treatment and subsequent analysis infarct size to estimate heart damage. Infarct size is defined as the percentage of the left ventricle affected by coronary artery occlusion.

The infarct size is estimated by manually delineating the infarcted and normal tissue areas in the left ventricle of the dissected heart. However, this is a time-consuming, arduous and prone to bias process. Herein, we explore the use of automatic image segmentation approaches to perform infarct size estimation. To further improve automation we developed an anatomic model, adapted through expectation maximization, which allows for fully automatic analysis of the data.

Experimental validation is performed comparing the proposed automatic approaches with manual annotation.

Keywords: Infarct size evaluation, tissue segmentation, anatomical model adaptation

F . Poster presentation in I3S conference

Poster entitled "Analysis of the extension of myocardial infarction in an experimental murine model" presented in the Second I3S Scientific Retreat IBMC | INEB | IPATIMUP together in Science , Axis Vermar, Póvoa do Varzim, Portugal, 2011.

Analysis of the extension of myocardial infarction in an experimental murine model

Tiago Esteves (meb09026@fe.up.pt), Mariana Valente, Diana S. Nascimento,
Perpétua Pinto-do-Ó and Pedro Quelhas
INEB – Instituto de Engenharia Biomédica Signal and Image Division

Universidade do Porto
FEUP Faculdade de Engenharia

Abstract

Despite considerable advances in diagnosis and management over the last three decades, acute myocardial infarction continues to be a major public health problem. Rodent models of myocardial infarction (MI) have been used in biomedical research towards the implementation of novel regenerative therapies. Permanent ligation of the left anterior descending coronary artery is a commonly used method for inducing MI both in rat and mouse. The assessment of MI extension on histological sections of dissected hearts is a critical parameter for this experimental setting. Currently, this is obtained manually, making it a time-consuming and arduous task and prone to bias. These factors motivate the development of a tool for automatic estimation of the infarct extension.

References

[1] - Naomi M. Degabriele, Uta Griesenbach, Kaori Sato, **Critical appraisal of the mouse model of myocardial infarction**, Experimental Physiology, vol. 89, no. 4, pp 497-505, May 2004.

[2] - Esther Lutgens, Mat J.A.P. Daemen, Ebo D. de Muinck, **Chronic myocardial infarction in the mouse: cardiac structural and functional changes**, Cardiovascular Research, vol. 41 pp 586-593 June 1998.

[3] - Gonzalez, Woods, Eddins, **Digital Image Processing Using MATLAB**, Pearson Education, 2004.

FCT Fundação para a Ciência e a Tecnologia
MINISTÉRIO DA CIÊNCIA, TECNOLOGIA E ENSINO SUPERIOR

Aknowledgements

The work presented in this manuscript was performed in collaboration with Mariana Valente, Diana S. Nascimento and Perpétua Pinto-do-Ó from the INEB's NEWTherapies group within the scope of the project PTDC-SAU-OSM-68473/2006, co-funded by the Fundação para a Ciência e a Tecnologia (FCT), FEDER and Programa POFC/QREN

I3S
5-6 May 2011
Póvoa de Varzim

Introduction

- Infarct assays in lab animals allow the execution of clinical trials leading to a better understanding of myocardial infarct.
- Infarcts are mimicked by ligation of the left coronary artery in a variety of animal models, including rats and mice.
- The infarct extension is the most important information obtained from the clinical trials. It is defined as the percentage of the left ventricle affected by coronary occlusion.

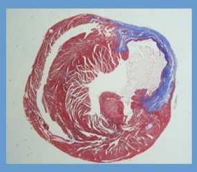

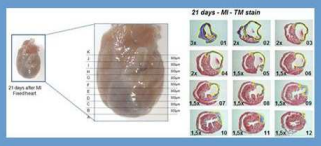

- Infarction extension is evaluated over 12 heart cross sections.
- Tissue is stained with an histological staining that enables the discrimination of collagen deposition that occurs in infarcted tissue.
- To determine the infarct extension it is necessary to identify and measure the blue area (infarcted tissue) and the red area (normal tissue) in the left ventricle in each section. The right ventricle is not considered in the evaluation.

Tissue segmentation

- The segmentation of the tissue allows the identification of infarcted tissue and normal tissue that enables the evaluation of myocardial infarction.
- Tissue segmentation is performed by semi-supervised and unsupervised image segmentation techniques and also through model adaptation.
- The semi-supervised technique require definition of initial points for start the segmentation. Unsupervised techniques do not require user interaction and the segmentation process is automatic.
- However, both semi-supervised and unsupervised segmentation techniques require the removal of the right ventricle before the segmentation process, since it is not considered in the evaluation. Tissue segmentation based on model adaptation contemplates this step. With this technique we identify all the tissues and remove the right ventricle automatically.

Image segmentation techniques

Semi-supervised	Unsupervised				Model based
Region growing segmentation	Automatic thresholding segmentation	Watershed segmentation	K-means segmentation	Mean-shift segmentation	Tissue segmentation through model adaptation

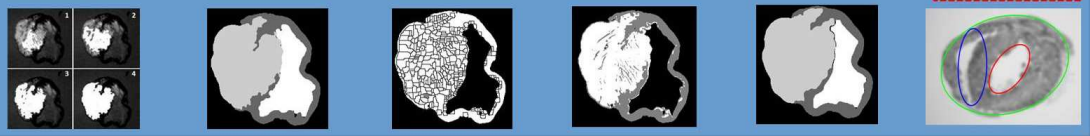

Infarct extension evaluation

- Infarct extension is calculated based on the previously segmented normal tissue and infarcted tissue.
- Two different methods of infarct extension calculation are used:

Area measurement – Infarct extension is calculated by dividing the infarct area by area of the left ventricle tissue.

Midline length measurement - Infarct extension derived from midline length measurement is calculated by dividing the midline infarcted length by the total midline length.

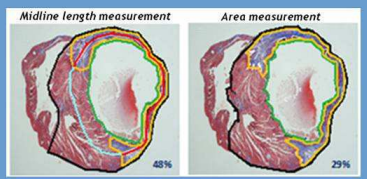

- **Area measurement** based on segmented regions is trivial.
- In **midline measurement** we automatically find the midline, by tracing lines from the centre of the lumen to the outside of the tissue. The midline is given by tracing the middle distance between tissue borders. The length of the middle line where infarcted tissue is more than half the length of the corresponding radial line is considered infarcted length.

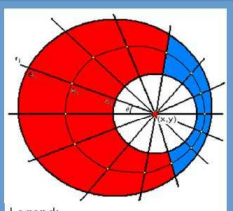

Legend:
- Red: Normal tissue;
- Blue: Infarcted tissue;
- White: Lumen;
- (X,Y): Center of the lumen;
- θ: Angle between each line *i*;
- Ai: Inside point of the tissue;
- Bi: Outside point of the tissue;
- Ci: Midpoint between the inside and outside points.

Prototype and results

- We developed a program based on requirements specified by biologists and taking into account their needs. The program is based on region growing segmentation technique.
- The program allows to obtain the infarct extension by area and midline length methods.
- The results of the prototype were in close agreement with the manual measurements.
- Measurement obtained on images from two hearts enable the comparison between our semi-automated approach and manual measurement.
- The results are the average value of the infarct extension in each slice of the heart and the differences are never greater than 8%.

Infarct extension							
Midline length measurement							
Heart	Manual	Region growing	Otsu	Watershed	K-means	Mean-shift	EM
#1 without RV	43%	38%	40%	41%	38%	36%	43%
#2 without RV	52%	48%	48%	49%	47%	49%	44%
Area measurement							
Heart	Manual	Region growing	Otsu	Watershed	K-means	Mean-shift	EM
#1 without RV	22%	25%	21%	21%	20%	17%	27%
#2 without RV	36%	38%	32%	36%	32%	36%	31%

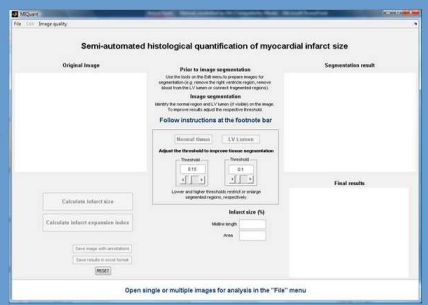

- The time it takes to get the infarct extension for each heart is approximately 9 minutes (average time). This is at least 5 times faster than the manual method.

G . Poster presentation in I3S conference

Poster entitled "MIQuant - towards standardization of cardiac regenerative therapies experimental assessment" presented in the Second I3S Scientific Retreat IBMC | INEB | IPATIMUP together in Science , Axis Vermar, Póvoa do Varzim, Portugal, 2011 and also in the 6^{th} International Meeting of the Portuguese Society for stem Cells and Cell Therapies (SPCE-TC), Biocant, Cantanhede, Portugal, 2011.

MIQuant – towards standardization of cardiac regenerative therapies experimental assessment

INEB - Instituto de Engenharia Biomédica

U.PORTO UNIVERSIDADE DO PORTO

Nascimento, DS[1]; Valente, M[1,2,3,4*]; Esteves, T[1,5*]; Freire, A[1,5]; Quelhas, P[1,5] and Pinto-do-Ó, P[1]

* equal contribution

(1) INEB – Instituto Nacional de Engenharia Biomédica, Porto, Portugal, (2) Instituto Politécnico de Saúde do Norte, IPSN, Portugal, (3) IBMC - Instituto de Biologia Molecular e Celular, Porto, Portugal, (4) Instituto de Ciências Biomédicas Abel Salazar (ICBAS) da Universidade do Porto, Portugal, (5) Faculdade de Engenharia da Universidade do Porto, Porto

marianavalente@ineb.up.pt

INTRODUCTION

Acute myocardial infarction is a major public health problem, resulting mainly from the occlusion of coronary arteries, due to the build-up of arteriosclerotic plaques, and the establishment of tissue ischemia eventually leading to end-stage heart failure. Experimental rodent models of myocardial infarction (MI) are extensively used to study molecular, cellular and histological alterations following MI. Moreover, these models have been recently applied to access the regenerative potential of newly developed therapies. The infarct size, defined as the percentage of the left ventricle affected by coronary artery occlusion, is calculated as the average value of infarct extension over all cross-sections of the infarcted heart. After MI, the collagen-based scar can be visualized in blue following Masson's Trichrome (TM) that enables the identification of collagen deposition, as soon as 7 days post-injury. The determination of the infarct extension is time-consuming, arduous and prone to bias because it requires manual definition of the infarcted-tissue and the non-affected region in each section. Aiming at the standardization and simplification of this task, a user-friendly semi-automatic tool was developed. The acronym MIQuant that stands for MI quantification was attributed to the program.

MATERIALS & METHODS

Experimental myocardial infarction (MI) model - 8-12 weeks old C57BL/6 mice were anesthetized, mechanically ventilated, and subjected to MI via permanent ligation of the left anterior descending (LAD) coronary artery. Sham-operated mice underwent the same surgical procedure without ligation of the coronary artery. All animals were kept and handled in compliance with the IBMC-INEB Animal House guidelines and the European Convention.

Histological analysis - For histological analysis, 3µm thick transverse sections were cut from the apex to the base of paraffin-embedded hearts with an interval of 300µm among each section (Takagawa et al., 2007). Sections were stained with Hematoxylin-Eosin (HE) and TM for morphologic and quantitative analysis of the infarct region.

Calculation of the Myocardial Infarction - The percentage of the affected LV wall was calculated by two different and previously validated methods: the area measurement (calculated by dividing the infarct area by the total LV area) (Michael et al., 1995) and the midline length measurement (calculated by dividing the midline of the infarcted ventricle wall by the midline of total LV wall). Midline infarct length was defined as the length of the midline on regions with >50% of the myocardial wall thickness with collagen deposition (Takagawa et al., 2007). The MI size determination was performed either manually, by drawing points to outline different anatomical/pathological regions of LV using the Image J 1.42 software or by using a novel semi-automated program - *MIQuant*, designed in MATLAB® (Mathworks®, Inc.)

MIQuant Software – The semi-automated software was designed by applying the region growing method, which exploits the spatial context by grouping pixels or sub-regions into larger regions according to a determined criterion. Regions are merged if they satisfy the chosen criterion and no merging occurs when the criterion is not met (Gonzalez et al., 2004; Wu et al., 1996). The lumen region is identified as a biggest hole inside the heart segmentation. The user needs to specify the initial points to begin the segmentation process in each of the tissue-conditions and the segmentation areas obtained by the software are used to calculate the infarct extension by area measurement. To perform the midline measurement the MIQuant software automatically traces lines from the lumen centre to the outside of the tissue, and finds the middle distance between tissue boundaries.

Statistical analysis – All statistics were performed using SPSW statistic software 18 and P <0.05 was considered statistically significant. Values presented in text and figures are mean ± standard error of the mean (SEM). Statistical significance among "Experts" and "Volunteers" users for midline length and area measurements were determined by the Independent-Samples Mann-Whitney U test.

REFERENCES

1. Michael LH, Entman ML, Hartley CJ, Youker KA, Zhu J, Hall SR, Hawkins HK, Berens K and Ballantyne CM (1995) Myocardial ischemia and reperfusion: a murine model. Am J Physiol 269:H2147-2154.
2. Takagawa J, Zhang Y, Wong ML, Sievers RE, Kapasi NK, Wang Y, Yeghiazarians Y, Lee RJ, Grossman W and Springer ML (2007) Myocardial infarct size measurement in the mouse chronic infarction model: comparison of area- and length-based approaches. J Appl Physiol 102:2104-2111.
3. Gonzalez R, Woods R and Eddins S (2004) Digital Image Processing Using MAT-LAB, Pearson Education.
4. Wu Q, Merchant F and Castleman K (1996) Microscope Image Processing, Elsevier, USA.

ACKNOWLEDGMENTS

The authors would like to acknowledge members of the NEWTherapies Group (INEB) for their input, in particular to José Henrique Teixeira, Joana Guedes, Estrela Neto, António Ribeiro, Catarina Almeida and Nuno Nogueira and the IBMC-INEB animal care-takers for their invaluable assistance.

This work was funded by the PTDC/SAU-OSM-68473/2006) from the Portuguese Foundation for Science and Technology (FCT), Quadro de Referência Estratégico Nacional (QREN) and American Portuguese Biomedical Research Fund (APBRF). MV is the recipient of BI (PTDC/SAU-OSM- This work was funded by a grant (68473/2006); DN is recipient of SFRH/BPD/42254/2007; AF is recipient of SFRH/BD/64715/2009 and PPO is granted by *Ciência 2007*.

PTDC/SAU-OSM-68473/2006 FCT Fundação para a Ciência e a Tecnologia COMPETE QREN QUADRO DE REFERÊNCIA ESTRATÉGICO NACIONAL EUROPEAN REGIONAL DEVELOPMENT FUND

I[3]S Second Scientific Retreat

IBMC | INEB | IPATIMUP

May 5th – 6th 2011, Póvoa de Varzim - PORTUGAL

IBMC INEB Laboratório Associado . Associate Laboratory

www.ineb.up.pt

Histopathological Evolution of Mouse Induced Myocardial Infarction

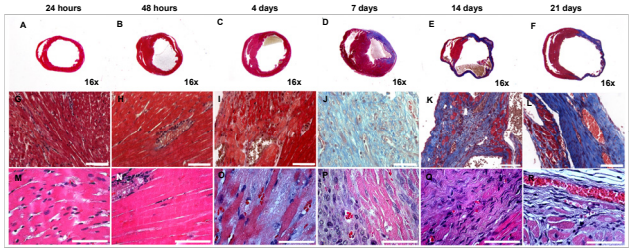

Fig 1. Histopathological evolution of mouse induced myocardial-infarction. At first and second row (magnification 16x), cross sections stained with TM demonstrated the LV remodeling after permanent ligation of LAD coronary artery with progressive thinning of LV wall, chamber dilation and collagen deposition. In higher magnification, the HE staining showed histological alterations at the cellular level in response to MI. Scale bar 50µm.

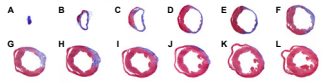

Fig 2. Transverse sections representative of the LV sampling of the paraffin-embedded hearts. Sections were obtained from the apex to the base (300µm of interval between each section) and stained with TM. Magnification 16x.

Quantification of Myocardial Infarction Size

Manual measurement

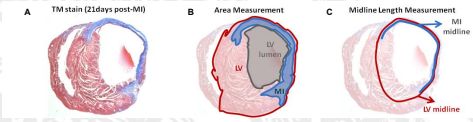

Fig 3. Manual measurement of the MI extension with Image J® 1.42 software. **A –** TM-stained cross sections from an infarcted heart 21 days post-surgery. **B –** Area approach – total LV tissue (red line), lumen region (gray line) and MI tissue (blue line) were manually defined. **C –** Midline length approach – red line marks the LV myocardium middle line and the blue line was drawn on the extent of the infarct that includes 50% of the whole thickness the myocardium.

MIQuant measurement

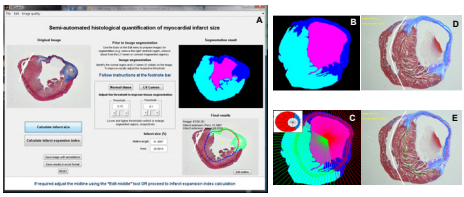

Fig 4. A – MIQuant layout. **B –** Virtual view of the cross-section segmentation obtained by the region growing method using the *MIQuant* software. Normal tissue was segmented in light blue, delimitation of the lumen hole was done in pink and the infarcted tissue was identified in dark blue . **C –** The midline was drawn at the middle of the LV wall and the infarcted tissue was considered when the collagen deposition affected more than 50% of ventricular wall **(C). D** and **E** images demonstrated the MI tissue identified on the photography by area and midline length measurements.

MIQuant validation

Manual *vs.* MIQuant

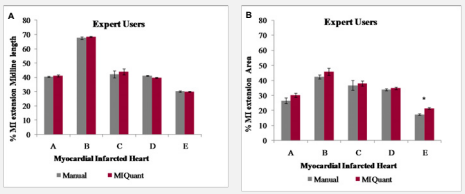

Fig 5. Comparative analysis of the MI size obtained by manual quantification and using the *MIQuant* software. The percentage of the affected LV wall was calculated by two different methods: the midline length measurement **(A)** and the area measurement **(B)**. No statistically significant differences were observed on the results retrieved by the midline length measurements. Concerning to the area measurements, and with the exception of the heart E, no statistically significant differences were observed between the manual and software results. *p<0,05 (mean±S.E.M.)

Time consumed during analysis

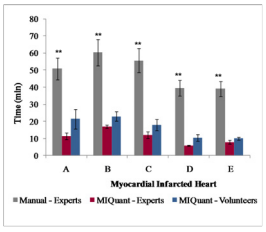

Fig 7. The time consumed during the calculation of the MI size either manually or using the MIQuant approaches. Although the *MIQuant* requires the definition of initial parameters by the user prior to segmentation, it was significantly quicker (MIQuant expert and MIQuant volunteers) than the manual method measurements. **p<0,01 (mean±S.E.M.)

Expert users *vs.* Volunteer users

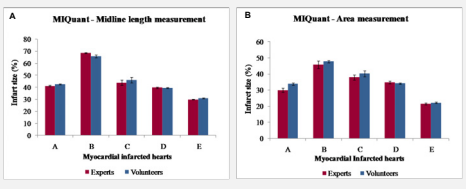

Fig 6. Comparative analysis of the MI size obtained by *experts* or *volunteers* using the *MIQuant*. No statistically significant differences were observed neither by the midline length **(A)** or by the **(B)** area measurements. *p<0,05 (mean±S.E.M.)

CONCLUSIONS

Overall, the *MIQuant*, when accessible as a *freeware*, will be a valuable tool for the simplification and standardization of MI size calculation among laboratories and will therefore contribute to normalize the evaluation of cardiac regenerative potential of newly developed therapies.

I[3]S CONSÓRCIO DE INVESTIGAÇÃO EM SAÚDE IBMC INEB IPATIMUP

20 1989 - 2009 20 years of Biomagical engineering in Porto

H. Poster presentation in the 1st Advanced Summer School

Poster entitled "MIQuant - towards standardization of cardiac regenerative therapies experimental assessment" presented in the 1st Advanced Summer School, Interrogations at the Biointerface, *Cancer/Regeneration Interface* and also in the Spring Biointerfaces Lab Meeting both held in Porto, Portugal, 2011.

MIQuant – Semi-automation of Infarct Size Assessment in Models of Cardiac Ischemic Injury

INEB - Instituto de Engenharia Biomédica

U.PORTO UNIVERSIDADE DO PORTO

Nascimento, DS*[1]; Valente, M*[1,2,3,4]; Esteves, T[1,5]; Pina, MF[1,6]; Guedes, JG[1]; Freire, A[1,5]; Quelhas, P[1,5] and Pinto-do-Ó, P[1]

*** equal contribution**

(1) INEB – Instituto Nacional de Engenharia Biomédica, Porto, Portugal; (2) Instituto Politécnico de Saúde do Norte, IPSN, Portugal; (3) IBMC - Instituto de Biologia Molecular e Celular, Porto, Portugal; (4) Instituto de Ciências Biomédicas Abel Salazar (ICBAS) da Universidade do Porto, Portugal; (5) Faculdade de Engenharia da Universidade do Porto, Porto; (6) Departamento de Epidemiologia Clínica, Medicina Preditiva e Saúde Pública, Faculdade de Medicina da Universidade do Porto, Porto, Portugal

marianavalente@ineb.up.pt

INTRODUCTION

In recent years, the evaluation of cardiac regenerative potential of newly developed therapies, as is the case of gene-delivery and transplantation of stem/progenitor-cells, has been primarily explored in rat and mouse models of surgically-induced myocardial infarction (MI) [1,2,3]. The left anterior descending (LAD) coronary artery ligation is the prominent model in these studies, and the infarct size has been considered a key parameter for assessing the success of the novel therapy. In studies involving an experimental MI setting, the calculation of the infarct size is typically evaluated by histological measurements of either: (a) the endocardial and epicardial length [5,6], (b) the midline length [5], (c) the endocardial length [4] or (d) the area [7] of infarcted *versus* non-infarcted left-ventricle (LV) regions. Despite the widespread use of the aforementioned approaches, the infarction size can vary depending on the used method [5,8] and thus no direct comparison can be withdrawn across laboratories. Moreover, several aspects of MI size quantification that can also account for infarct size variation are inconsistent across studies and not always clearly defined, *e.g.* the number of sections used for the calculation, the histological staining and criteria used to identify the infarcted region. Accordingly, the purpose of the present work is to standardize and simplify the infarct size calculation in experimental models of MI by making accessible, as freeware, an easy-to-use semi-automatic software application, which we developed and validated at the "bench".

MATERIALS & METHODS

Experimental myocardial infarction (MI) model - 8-12 weeks old C57BL/6 mice were anesthetized, mechanically ventilated, and subjected to MI via permanent ligation of the LAD coronary artery. Sham-operated mice underwent the same surgical procedure without ligation of the coronary artery. All animals were kept and handled in compliance with the IBMC-INEB Animal House guidelines and the European Convention.

Histological analysis - For histological analysis, 3µm thick transverse sections were cut from the apex to the base of paraffin-embedded hearts with an interval of 300µm among each section [5]. Sections were stained with Hematoxylin-Eosin (HE) and Masson's Trichrome (TM) for morphologic and quantitative analysis of the infarct region, respectively.

Calculation of the Myocardial Infarction - The percentage of the affected LV wall was calculated by two different and previously validated methods: the area measurement (calculated by dividing the infarct area by the total LV area) [7] and the midline length measurement (calculated by dividing the midline of the infarcted ventricle wall by the midline of total LV wall). Midline infarct length was defined as the length of the midline on regions with >50% of the myocardial wall thickness with collagen deposition [5]. The MI size determination was performed either manually, by drawing points to outline different anatomical/pathological regions of LV using the Image J 1.42 software or by using a novel semi-automated program - *MIQuant*, designed in MATLAB® (Mathworks®, Inc.)

MIQuant Software – The semi-automated software was designed by applying the region growing method, which exploits the spatial context by grouping pixels or sub-regions into larger regions according to a determined criterion. Regions are merged if they satisfy the chosen criterion and no merging occurs when the criterion is not met [9,10]. The lumen region is identified as a biggest hole inside the heart segmentation. The user is asked to provide input seed points for the LV lumen and viable myocardium prior to automated segmentation. Following segmentation, the image displayed in the screen will be the support for the infarct size computation by area measurement. To perform the midline measurement the *MIQuant* software automatically traces lines from the lumen centre to the outside of the tissue, and finds the middle distance between tissue boundaries.

Statistical analysis – To validate *MIQuant*, 4 expert researchers analyzed 5 hearts by midline and area methods, manually and with *MIQuant*. All experts repeated measures at 3 distanced moments and a one-way repeated measures analysis of variance (ANOVA) was conducted to evaluate repeatability. Seven non-trained volunteers measured the same samples using *MIQuant*. The association between manual and *MIQuant* results was investigated by the Person product-moment-correlation coefficient (*r*) and to address agreement amongst methods, the Bland-Altman agreement statistical method was used. A two-way between-groups ANOVA and post-hoc Turkey HSD test was applied to attend the impact of observers and heart samples in the results. Expert and volunteer results were compared by an independent-samples t-test and the time spent during the MI size quantification manually and with *MIQuant* software was compared by an Independent-Samples Mann-Whitney U test.

REFERENCES

1. Gonzales C and Pedrazzini T (2009) *Exp Cell Res* 315:3077-3085.
2. Ahmed RPH, et al. (2010) *PLoS ONE* 5:e8576.
3. Smits AM, et al. (2009) *Nat Protoc* 4:232-243.
4. Pfeffer MA, et al. (1979) *Circ Res* 44:503-512.
5. Takagawa J, et al. (2007) *J Appl Physiol* 102:2104-2111.
6. Patten RD, et al. (1998) *Am J Physiol* 274:H1812-1820.
7. Michael LH, et al. *Am J Physiol* 269;H2147-2154.
8. Minicucci MF, et al. (2007) *Arq Bras de Cardiol* 89:93-98.
9. Gonzalez R, et al. (2004) *Digital Image Processing Using MATLAB*, Pearson Education.
10. Wu Q, et al. (1996) *Microscope Image Processing*, Elsevier, USA.

Quantification of Myocardial Infarction Size

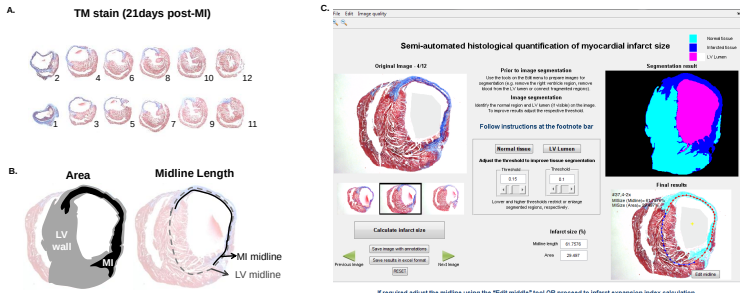

Fig 1. Manual and *MIQuant* semi-automated calculation of MI size in chronic infarcts. A. LV representative MT stained sections, numbered from the apex to the LV base, were obtained from an infarcted hearts harvested at 21 days post-surgery. **B.** Histological infarct size calculation by the *area* method requires manual tracing of the LV myocardium (light gray) and of the scarred LV tissue (black). The infarct size, expressed as a percentage, is the division of the infarct area by the LV area multiplied by 100. For the *midline length* approach (right) the midline, herein defined as the mid-region between the epicardial and endocardial surfaces, of the total LV (dashed line) and of scarred region (full line) are manually traced. The infarct size, expressed as a percentage, is the division of the infarct midline length by the LV midline length multiplied by 100. The total LV infarct extent is the average of infarct size obtained for the LV representative cross-sections A.. (C) Screen shot of *MIQuant* layout following infarct size calculation. Multiple images can be uploaded in TIFF or JPEG file-formats and the software calculates the intermediate values of infarct size for each image (bottom right). A total MI size is also generated assuming that the uploaded images were representative sections of the LV. For selection of the scarred myocardium (top right) the software requires the user to double-click in a normal tissue region and in the LV lumen, if applicable, over the uploaded image (top left).

MIQuant validation

MIQuant repeatability (intra-observer) and reproducibility (inter-observer)

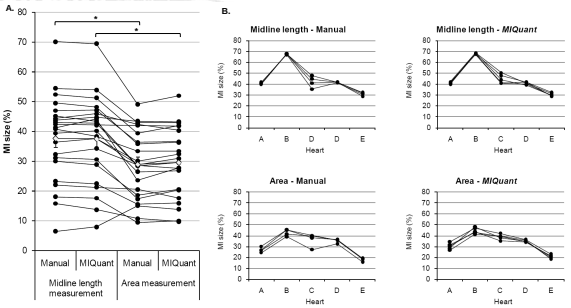

Fig 2. A. Consistency of manual and *MIQuant* infarct size results obtained using the area and midline length measurements. Hearts were harvested at 21 days post-surgery and infarct size determinations are the mean value of 12 cross-sections representative of the LV. Mann-Whitney statistical analysis demonstrated significant differences between the area and midline length methods, as already described by Takagawa [10]. **B.** Reproducibility of *MIQuant* measurements. Although ANOVA demonstrated no significant influence of the observer on the LV infarct size scores obtained, neither manually nor using *MIQuant*, the latter displays a tendency for lower discrepancy between operators.

Validation of *MIQuant* by non trained volunteer-users

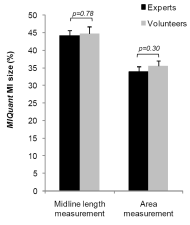

Fig 3. *MIQuant* efficacy is not affected by user proficiency. *MIQuant* infarct size values obtained by competent (experts) and non-trained (volunteer) users were compared and the mean values are displayed as graph bars. Independent-samples *t*-test showed no significant differences between infarct scores calculated by the experts *vs.* volunteers. Furthermore, a two-way ANOVA demonstrated no significant influence of the user on the obtained infarct size value.

MIQuant vs. Manual

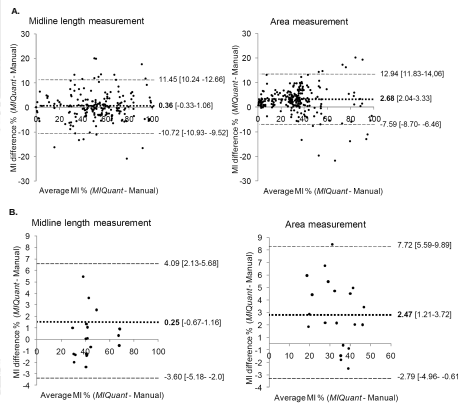

Fig 4. A. Bland-Altman analysis was conducted with manual and *MIQuant* results obtained *per* LV section. The visual inspection of Bland-Altman plot denoted that differences between *MIQuant* and manual measurements are scattered around the bias with no obvious pattern for the midline length results whereas, the area differences appear to increase for higher infarction values. The estimated bias is 0.36% with concordance limits of -10.72% and 11.45% for the midline length method, whereas for the area approach the bias is 2.68% with limits of agreement of -7.58% and 12.94%. Hence, for both methodological approaches, the predicted confidence interval is within acceptance limits and so *MIQuant* is considered equivalent to the established manual quantification method. **B.** Measurements of the infarct size *per* heart, i.e. mean value of 12 sections representative of the LV, obtained by the manual and *MIQuant* calculation were also compared. For the midline length, the predicted bias is 0.25% and the limits of agreement are -3.60% and 4.09%, resulting on 7.74% amplitude of concordance. The analysis of the area measurements retrieves a mean difference of 2.47% (95% confidence interval (CI) from 1.21% to 3.72%), suggesting that *MIQuant* tends to give a higher reading from 1.21% to 3.72%. The area method concordance interval ranges from -2.79% to 7.72%. Thus, for *MIQuant per* heart infarct size results the confidence interval of the predicted bias and concordance limits are within acceptance limits (bias ±2%, concordance limits ±7%) for both midline length- and area-measurements, which show that the performance of *MIQuant* is equivalent to the manual infarct size calculation.

Time-efficiency of *MIQuant* infarct size quantification

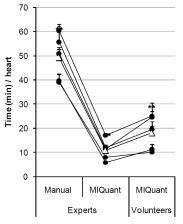

Fig 5. The time consumption of the infarct size determination *per* heart (mean value of 12 representative sections of the LV) was compared between the manual and *MIQuant* approaches. Although the *MIQuant* requires the definition of initial parameters by the user prior to segmentation, the semi-automated software resulted on a significant overall ↓4,5- and 3-fold decrease in the time spent on the analysis when performed by experts and volunteer users, respectively. The Δ indicates the mean value of each group. ***p*<0,001 (mean±S.E.M.).

CONCLUSIONS

The *MIQuant* is a valid, easy-to-use software application that assists on infarct size calculation. The widespread use of *MIQuant* will contribute to the reduction of time spent on the analysis and for the standardization of infarct size quantification across studies and, therefore, to the systematization of the evaluation of cardiac regenerative potential of newly developed therapies.

ACKNOWLEDGMENTS

The authors would like to acknowledge members of the NEWTherapies Group (INEB) for their input, to Dr. Pedro Oliveira for statistical coaching and IBMC-INEB animal care-takers for their invaluable assistance. This work would not have been possible without the collaboration of all those who volunteered as non-trained operators for the statistical validation of the *MIQuant* software. This work was funded by the PTDC/SAU-OSM-68473/2006) from the Portuguese Foundation for Science and Technology (FCT), Quadro de Referência Estratégico Nacional (QREN) and American Portuguese Biomedical Research Fund (APBRF); MV is the recipient of BI (PTDC/SAU-OSM-68473/2006); DN is recipient of SFRH/BPD/42254/2007; AF is recipient of SFRH/BD/64715/2009, PQ is granted by Ciência2008 and PPO is granted by Ciência2007.

1st Advanced Summer School

Interrogations at the Biointerface

Cancer/Regeneration Interface

INEB | IPATIMUP | IBEC

June 20th – 24th 2011, Porto - PORTUGAL

IBMC INEB Laboratório Associado . Associate Laboratory

www.ineb.up.pt

I3S CONSÓRCIO DE INVESTIGAÇÃO EM SAÚDE IBMC INEB IPATIMUP

20 1989 - 2009 20 years of Biomagical engineering in Porto

FCT Fundação para a Ciência e a Tecnologia COMPETE

Ⅰ. Oral presentation in the XII Congresso Técnico de Anatomia Patológica

Oral presentation performed in the XII Congresso Técnico de Anatomia Patológica, Centro Multimeios de Espinho, Espinho, Portugal entitled "MIQuant - towards standardization of cardiac regenerative therapies experimental assessment".

MIQuant

Towards standardization of cardiac regenerative therapies experimental assessment

Nascimento DS*, Valente M*, Esteves T, Pina MF, Guedes J, Freire A, Quelhas P and Pinto-do-Ó P

*equal contribution

marianavalente@ineb.up.pt

INEB – Instituto de Engenharia Biomédica
Universidade do Porto
Porto, Portugal

XII Congresso Técnico de Anatomia Patológica

Espinho, Portugal, May 22nd, 2011

J . Infarct size evaluation through automatic thresholding segmentation

Several examples of successful infarct size evaluation through the segmentation of tissue performed by automatic thresholding approach. It is visible the segmentation of the normal and infarcted tissue regions and the final result obtained.

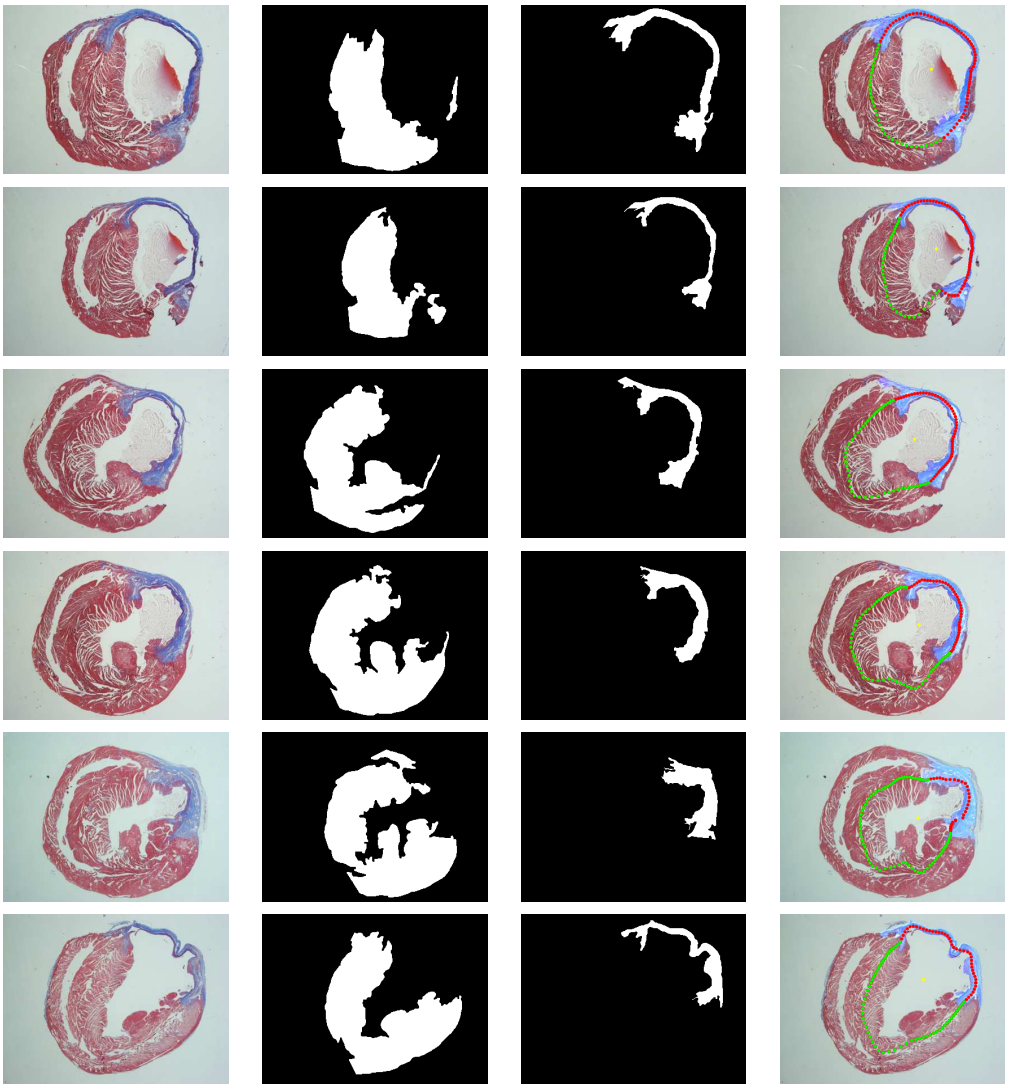

Table J.1 Infarct size evaluation in images of the heart cross section: First column - input images, second column - segmentation result of normal tissue, third column - segmentation result of infarcted tissue, fourth column - infarct size evaluation.

K . Infarct size evaluation through watershed segmentation

Several examples of successful infarct size evaluation through the segmentation of tissue performed by watershed approach. It is visible the watershed segmentation result and the final result obtained with the identification of the infarcted and normal tissue regions.

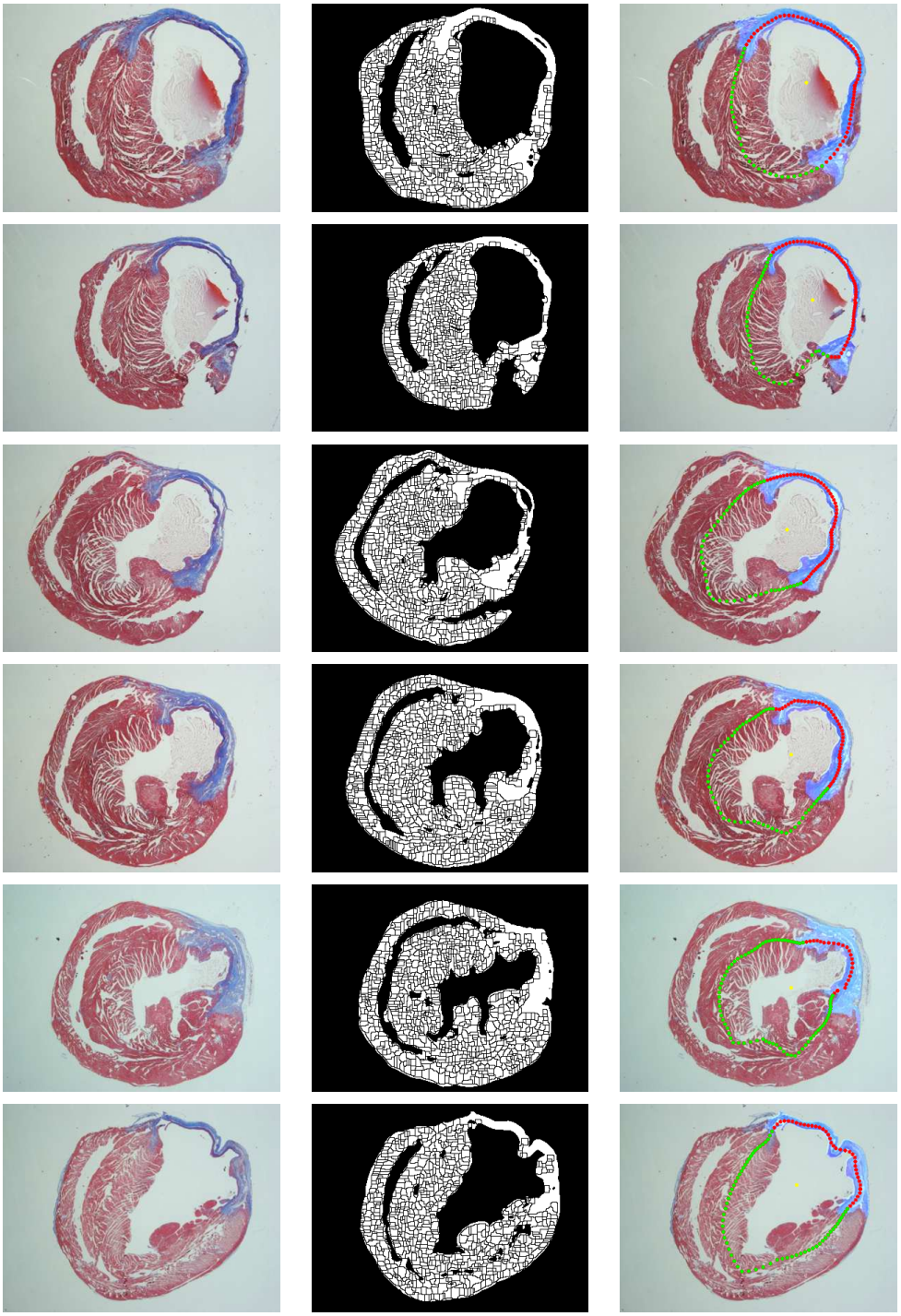

Table K.1 Infarct size evaluation in images of the heart cross section: First column - input images, second column - watershed segmentation result, third column - identification of the infarcted and normal tissue regions and infarct size evaluation.

L . Infarct size evaluation through k-means segmentation

Several examples of successful infarct size evaluation through the segmentation of tissue performed by k-means clustering approach. It is visible the k-means clustering result and the final result obtained with the identification of the infarcted and normal tissue regions.

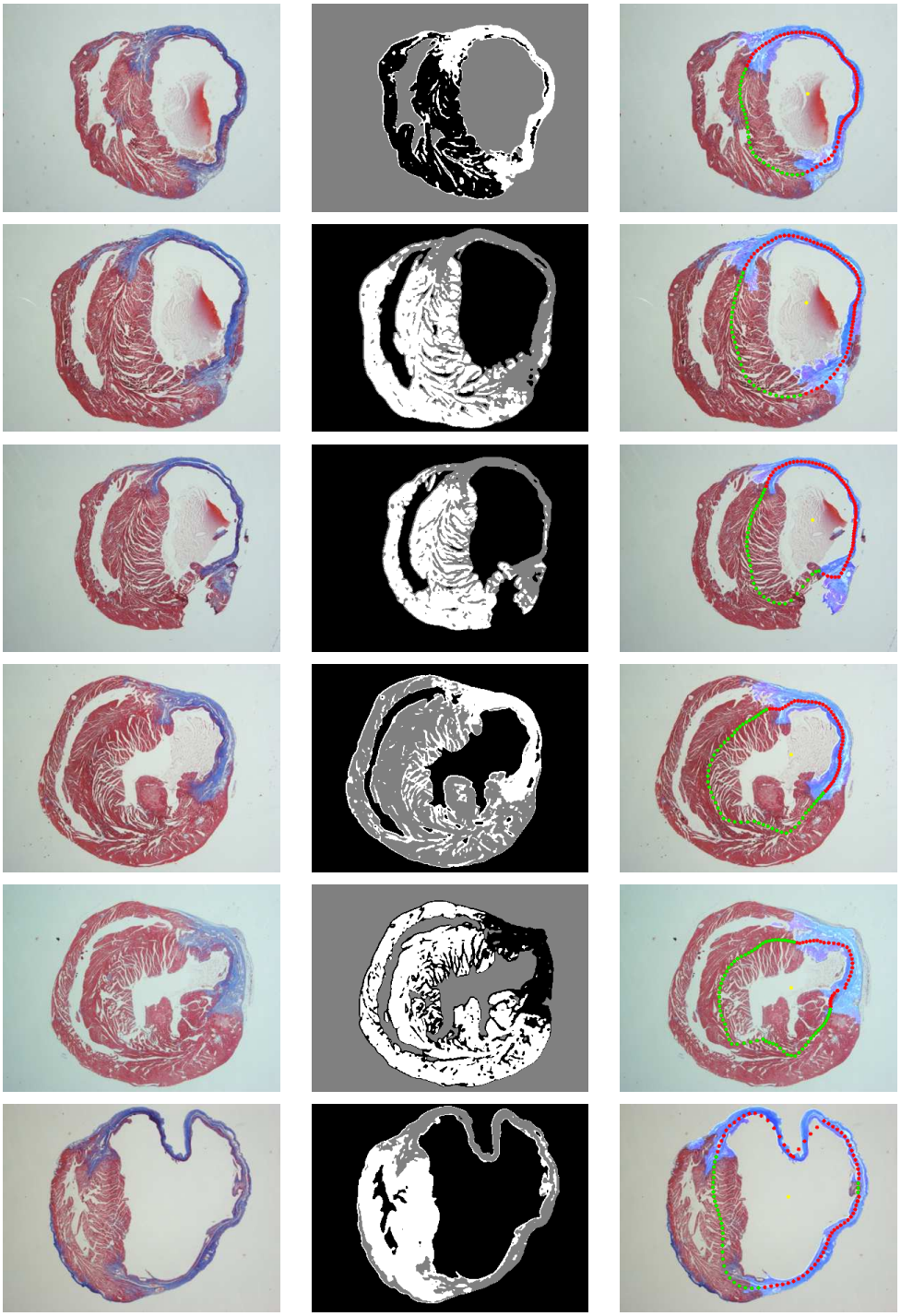

Table L.1 Infarct size evaluation in images of the heart cross section: First column - input images, second column - k-means clustering result, third column - identification of the infarcted and normal tissue regions and infarct size evaluation.

M . Infarct size evaluation through mean-shift segmentation

Several examples of successful infarct size evaluation through the segmentation of tissue performed by mean-shift clustering approach. It is visible the mean-shift clustering result and the final result obtained with the identification of the infarcted and normal tissue regions.

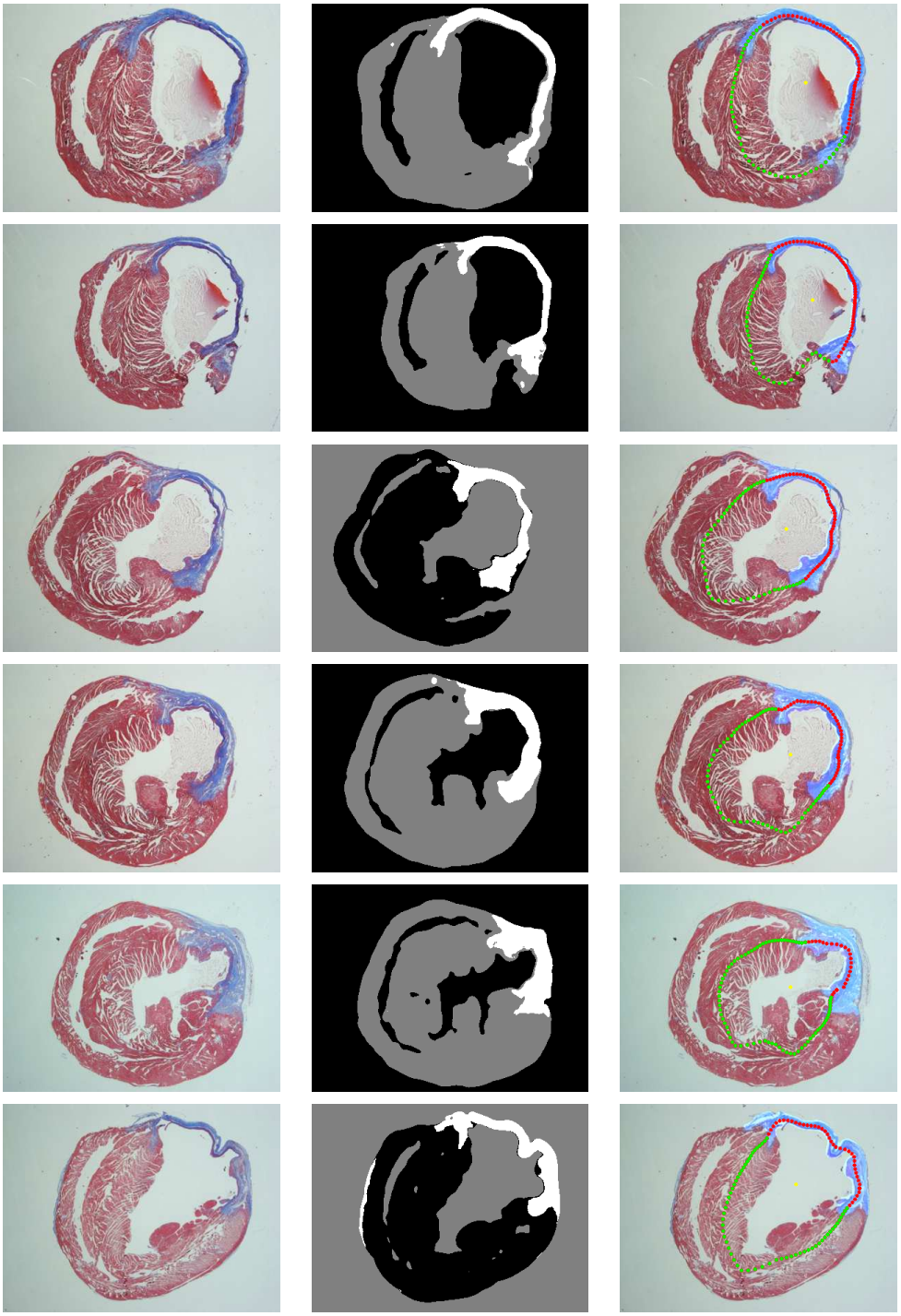

Table M.1 Infarct size evaluation in images of the heart cross section: First column - input images, second column - mean-shift clustering result, third column - identification of the infarcted and normal tissue regions and infarct size evaluation.

N. Infarct size evaluation through anatomical model adaptation

Several examples of successful infarct size evaluation through the segmentation of tissue performed by anatomical model adaptation. It is visible the final adaptation of the anatomical model with the identification of the right and left ventricle lumens of the heart cross section, the estimation of the left ventricle region where the infarct size evaluation is performed and the final result obtained with the identification of the infarcted and normal tissue regions.

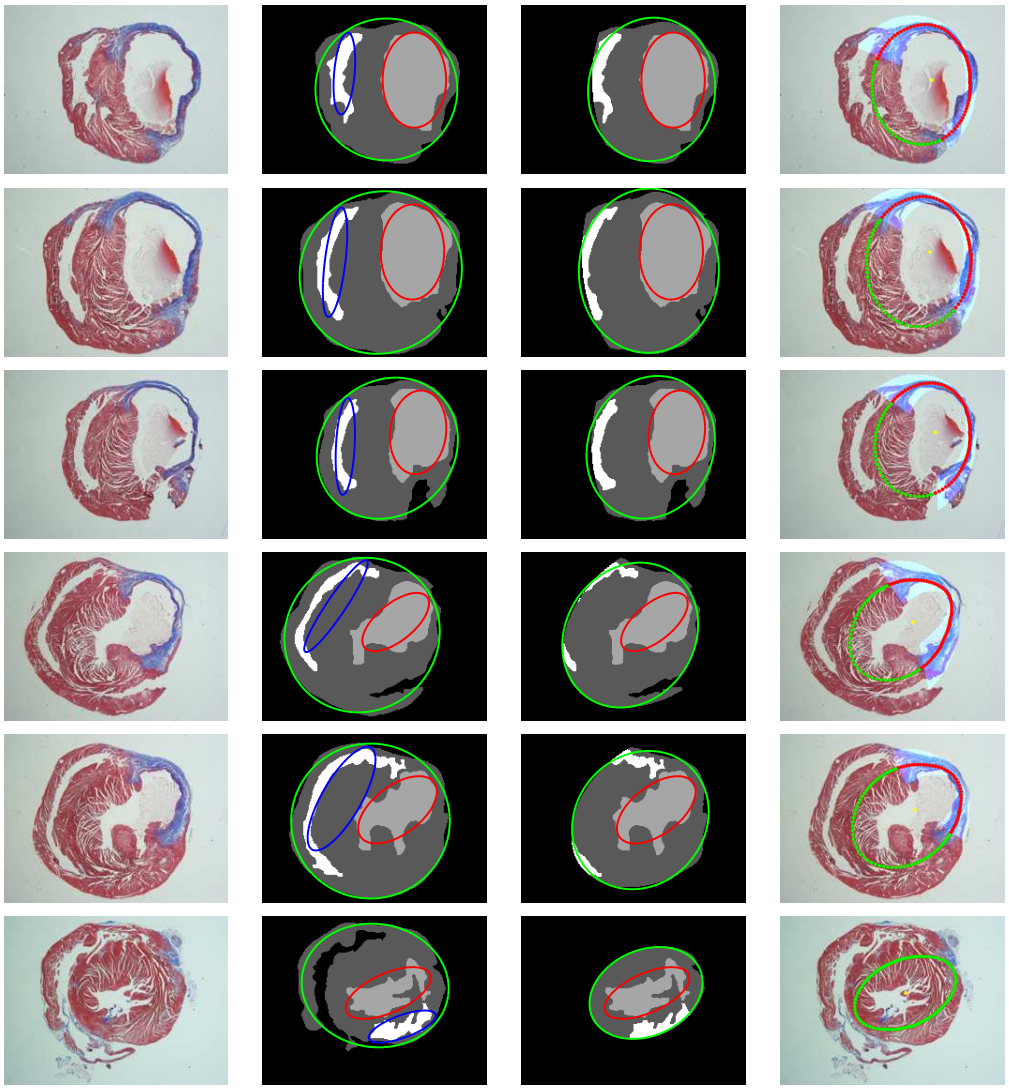

Table N.1 Infarct size evaluation in images of the heart cross section: First column - input images, second column - final adaptation of the anatomical model, third column - estimation of the left ventricle region, fourth column - infarct size evaluation.

Bibliography

[1] M. Alattar, N. Osman, and A. Fahmy. Myocardial segmentation using constrained multi-seeded region growing. *Image Analysis and Recognition (ICIAR)*, 6112:99–107, 2010.

[2] A. Blasiak. *A Comparasion of Image Segmentation Methods*. PhD thesis, Middlebury College, 2007.

[3] A. Bleau and J. Leon. Watershed-based segmentation and region merging. *Computer Vision and Image Understanding*, 77(3):317–370, 2000.

[4] S. Borman. The expectation maximization algorithm: A short tutorial. *Journal of Electronic Imaging*, 12:1–9, 2004.

[5] M. Brown, M. McNitt-Gray, N. Mankovich, and J. Goldin. Method for segmenting chest ct image data using an anatomical model: preliminary results. *IEEE Transactions on Medical Imaging*, 16:1–11, 1997.

[6] D. Comaniciu and P. Meer. Mean shift: A robust approach toward feature space analysis. *IEEE Transactions on Pattern Analysis and Machine Intelligence*, 24:603–619, 2002.

[7] K. Dabov, A. Foi, and V. Katkovnik. Image denoising by sparse 3d transform-domain collaborative filtering. *IEEE Transactions on Image Processing*, 16(8):1–16, 2007.

[8] N. Degabriele, U. Griesenbach, and K. Sato. Critical appraisal of the mouse model of myocardial infarction. *Experimental Physiology*, 89(4):497–505, 2004.

[9] F. Dellaert. The expectation maximization algorithm. *IEEE Signal Processing Magazine*, 13:1–7, 2002.

[10] H. Dietrich. *Mice - general information*. 2006.

[11] T. Esteves, P. Pinto-do Ó, and P. Quelhas. Semi-automatic extraction of the level of infarction in mouse hearts. *RecPad*, pages 1–2, 2010.

[12] T. Esteves, M. Valente, D. Nascimento, P. Pinto-do Ó, and P. Quelhas. Automated myocardial infarction analysis in an experimental model using image segmentation and model adaptation. *Pattern Recognition (Under Revision)*, pages 1–26, 2011.

[13] T. Esteves, M. Valente, D. Nascimento, P. Pinto-do Ó, and P. Quelhas. Automatic and semi-automatic analysis of the extension of myocardial infarction in an experimental murine model. *Proceedings of IbPRIA, LNCS 6669*, pages 151–158, 2011.

[14] R. Gonzalez, R. Woods, and S. Eddins. *Digital Image Processing Using MATLAB*. 2004.

[15] G. Hamarneh and X. Li. Watershed segmentation using prior shape and appearance knowledge. *Image and Vision Computing*, 27:59–68, 2009.

[16] S. Khadir and R. Ahamed. Moving toward region-based image segmentation techniques: A study. *International Journal on Computer Science and Engineering*, 2:59–68, 2009.

[17] D. Kumar, T. Hacker, and J. Buck. Distinct mouse coronary anatomy and myocardial infarction consequent to ligation. *Coronary Artery Disease*, 16(1):41–44, 2005.

[18] S. Lakare. *3D Segmentation Techniques for Medical Volumes*. 2000.

[19] E. Lutgens, M. Daemen, and E. Muinck. Chronic myocardial infarction in the mouse: cardiac structural and functional changes. *Cardiovascular Research*, 41:586–593, 1998.

[20] D Nascimento, M. Valente, T. Esteves, M.F. Pina, J.G. Guedes, Freire A., P. Quelhas, and P. Pinto-do Ó. Miquant - semi-automation of infarct size assessment in models of cardiac ischemic injury. *Plos One (Under Revision)*, pages 1–23, 2011.

[21] N. Otsu. A threshold selection method from gray-level histograms. *EEE Transactions on Systems Man and Cybernetics*, 9:62–66, 1979.

[22] M. Pfeffer, J. Pfeffer, and M. Fishbein. Myocardial infarct size and ventricular function in rats. *Circulation Research*, 44:503–512, 1979.

[23] D. Pham and C. Xu. A survey of current methods in medical image segmentation. *IEEE Transactions on Medical Imaging*, 17:1–14, 1998.

[24] S. Pizer, E. Amburn, and J. Austin. Adaptive histogram equalization and its variations. *Computer Vision, Graphics, and Image Processing*, 39(3):355–368, 1987.

[25] R. Rodriguez and P. Castillo. Two robust techniques for segmentation of biomedical images. *Journal of Intelligent and Robotic System*, 9:355–369, 2006.

[26] J. Russ. *The Image Processing Handbook*. 2006.

[27] M. Sezgin. Survey over image thresholding techniques and quantitative performance evaluation. *Journal of Electronic Imaging*, 13(1):146–165, 2004.

[28] N. Sharma and L. Aggarwal. Automated medical image segmentation techniques. *Journal of Medical Physics*, 35:3–14, 2010.

[29] J. Takagawa, Y. Zhang, and M. Wong. Myocardial infarct size measurement in the mouse chronic infarction model: comparison of area- and length-based approaches. *Journal of Applied Physiology*, 102:2104–2111, 2007.

[30] M. Tellez, L. Sing, and R. Oakley. Myocardial infarction in the c57bl/6j mouse - a quantifiable and highly reproducible experimental model. *Cardiovascular Pathology*, 13:91–97, 2004.

[31] E. Trucco. *Deformable/Active Contours (or Snakes)*. 2005.

[32] J. Vorlicek and J. Rusz. Automatic human body segmentation using mean-shift clustering as assistence in the hyperthermia treatment planning. *Journal of Molecular Spectroscopy*, 256:1–6, 2009.

[33] A. Wessels and D. Sedmera. Development anatomy of the heart: a tale of mice and man. *Physiology Genomics*, 15:165–176, 2003.

[34] K. Wu, D. Gauthier, and M. Levine. Live cell image segmentation. *IEEE Transactions on Biomedical Engineering*, 42:1–12, 1995.

[35] Q. Wu, F. Merchant, and K. Castleman. *Microscope Image Processing*, chapter 7. Elsevier, 1996.

[36] C. Xu and J. Prince. Gradient vector flow: A new external force for snakes. *IEEE Proceedings Conference on Computer Vision and Pattern Recognition*, 3:1–14, 1997.

[37] C. Xu and J. Prince. Snakes, shapes, and gradient vector flow. *IEEE Transactions, Image Processing*, 7:1–14, 1998.